UNIVERSIDADE DE LISBOA
FACULDADE DE CIÊNCIAS
DEPARTAMENTO DE ESTATÍSTICA E INVESTIGAÇÃO OPERACIONAL

Estimation of bowhead whale (*Balaena mysticetus*) population density using spatially explicit capture-recapture (SECR) methods

Gisela Vitória Cheoo

Mestrado em Bioestatística

Dissertação orientada por:
Doutor Tiago Marques
Doutor Len Thomas

2019

Acknowledgements

To Len Thomas, my deep appreciation for welcoming me to CREEM (and its cake rituals) and enduring every stupid question I've put up. Thank you for being a mentor and taking the necessary time to teach me, although your calendar always looked like a train wreck of a puzzle. I'll always hear your 'sheesh' and remember your inability to resist cake time.

No words can describe the joy that is working with Tiago Marques. He was the first person to guide me through the statistical ecology world. For your words of support and guidance, I am sincerely grateful! Among many occasions, thanks for the particular event of dragging a 26 kg bag with broken wheels from St Andrews to Edinburgh's airport.

To the DEBACA team: Aaron Thode, Alexender Conrad, Cornelia Oedekoven, Danielle Harris, Katherine Kim, and Susanna Blackwell (also Tiago, and Len), for providing the data hereby analysed and giving insight about it. This jolly group of eight has introduced me to new concepts about statistical approaches to estimate densities (and many other concepts I still don't quite understand!).

To Paul Conn, for discussing a way to implement his superpopulation concept into this thesis. To David Borchers, for the input after the seminar I gave. Thanks also to Richard Glennie for his help building the likelihood formulation.

To every single person that turned my Scottish experience into something I dearly remember: Amaia Diaz, Carolina Barata, Charles Paxton, Claúdia Faustino, Cornelia Oedekoven, Guilherme Bortolotto, Jessica King, Valentin Popov, Virginia Pujol. Thanks to the St Andrews floorball team. A special thanks to Sean Heath for being a great flatmate, and to Marlene Matthews for being a lovely host during my last week in Scotland.

To Rhona Rodger, and Phil Le Feuvre, always available to help and provide everything needed to properly work at the office.

To all staff involved into making the ISEC 2018 a five star conference, and Len again for letting me attend it.

To Filipe Ribeiro, for also being a mentor – I miss working in the field with "boga-de-boca-arqueada" team.

To all professors and colleagues that somehow helped me through my academic path. A special thanks to Marília Antunes.

To all my dearest friends, the ones that I had the pleasure to share lots of moments

and always made any place feel like home – I am thankful for your friendship.

To Nuno Maia, for your unconditional support and care, and for making my days always brighter! A special thanks to his family too.

To my sister, Mariana Cheoo, for always being there, for your moral support and typically nagging me as older sisters tend to do so. To grandma, Sui Kwong, for being a character of courage and strength (and mostly stubbornness). To mom and dad, Liliana Cheoo, and Calisto Cheoo, for your love and support. Without your invaluable encouragement and sacrifice I could not have done it. Esta tese é para vocês.

Lastly, to the ERASMUS+ programme that allowed me to do part of this thesis in an exceptional research centre, meet new people, and experience life in the country of bagpipes, haggis and cèilidh.

Contents

List of Figures

List of Tables

Resumo

Na área da ecologia, o estudo de populações naturais é feito através de métodos que têm de ser fundamentalmente precisos e eficazes no que toca à estimação do tamanho e densidade populacional. É importante atualizar e fornecer dados que refletem a realidade do problema em questão. As estimativas resultantes destes métodos são ferramentas que levam à diferença entre uma estratégia de ação que viabiliza a gestão e conservação invertendo o processo de declínio das populações e uma estratégia de conservação falhada. Dada a sua relevância, é importante otimizar os métodos existentes e garantir a eficácia das suas previsões. Se os métodos permitirem a monitorização com a mínima intervenção humana, estaremos a reduzir o esforço, o tempo e os custos necessários, e por essa mesma razão, estes métodos são considerados uma via alternativa preferencial.

A baleia-da-Gronelândia (*Balaena mysticetus*) pertence à família Balaenidae e é também conhecida como baleia-da-Gronelândia ou baleia polar. Esta espécie vive em regiões associadas ao Oceano Ártico e subártico, não ocorrendo no hemisfério Sul. A baleia-da-Gronelândia está classificada na Lista Vermelha de Espécies Ameaçadas (IUCN Red List) como Pouco Preocupante (LC – Least Concern). São facilmente identificadas devido ao seu corpo largo, forma arrendonda e por não possuírem barbatana dorsal. Estas baleias apresentam uma tonalidade escura em todo o corpo, exceto os padrões brancos na zona inferior dos maxilares, em partes do corpo da zona ventral e ao redor das suas barbatanas caudais. Os seus padrões brancos aumentam com a idade. Têm uma cabeça triangular quando vista de perfil e um "pescoço" resultante de uma indentação entre a cabeça e a zona dorsal (Rugh & Shelden, 2009). O seu nome comum em inglês, "bowhead whale", surge pela aparência curvada ("bowed") da boca. Além disso, estas baleias são conhecidas pela sua longevidade, tendo sido registado um indivíduo com 211 anos de idade (George et al., 1999). Na região do Alasca, as baleias-da-Gronelândia migram do mar de Bering através do mar de Chukchi para o mar de Beaufort durante o período de migração da primavera/verão, e retornam em meados do final do verão e outono do mar de Beaufort para o mar de Bearing. Apesar das rotas de migração serem bem conhecidas, esta espécie é difícil de ser avistada por passar a maioria do tempo debaixo de água, levando a uma baixa probabilidade de deteção/avistamento. Quando ignorada, esta baixa probabilidade leva à subestimação do tamanho das populações. Contudo, esta espécie é conhecida por emitir vocalizações que são essenciais para encontrar parceiros durante a época de acasalamento e para ajudar a navegação através do gelo marinho. As vocalizações são de baixa frequência, entre 50 a 500 Hz, mas muito intensas, propensas a serem detetadas a grandes distâncias (Abadi et al., 2014). A produção destes sons distintos faz destas baleias um ótimo exemplo para a aplicação de monitorização acústica passiva.

O objetivo deste projeto é estimar a densidade populacional das baleias-da-Gronelândia da região de Bearing-Chukchi-Beaufort através da análise de captura-recaptura espacialmente explícita (SECR). Contudo, a densidade calculada pode ser referente a: (i) animais (i.e., indivíduos); (ii) grupos de animais e (iii) sons. O nosso alvo é estimar inicialmente a densidade (iii) sonora ($\hat{D}_s$), sendo posteriormente convertida para uma densidade populacional ($\hat{D}$). A conversão é feita através da divisão da densidade sonora por dois fatores: (i) taxa de vocalização ($\hat{r}$) e (ii) período de tempo considerado da amostra (T):

$$\hat{D} = \frac{\hat{D}_s}{\hat{r}T}.$$

Os dados analisados nesta tese pertencem a um projeto de nome DEBACA (Density Estimation of Bowhead's off the Arctic Coast of Alaska), e resultam da colaboração entre a companhia americana Greeneridge Sciences Inc e duas instituições académicas – Scripps Institution of Oceanography e a Universidade de St Andrews. O conjunto de dados resulta da colocação de cinco conjuntos de sensors acústicos ao longo da costa do Alasca no mar de Beaufort durante a migração de verão/outono das baleias-da-Gronelândia. Cada um dos conjuntos contém 3 a 13 "DASARs" (Directional Autonomous Seafloor Acoustic Recorders) que gravaram continuamente os sons emitidos pelas baleias. A disposição dos sensores, mais precisamente hidrofones, permitiu a recolha de uma base de dados de acústica passiva durante oito anos (2007–2014) em 5 locais.

Os dados foram divididos segundo a sua análise: os sons foram explorados através de análise manual ou automática. Na análise manual, uma equipa altamente especializada classificou os sons registados, ouvindo as gravações de aúdio e examinando os seus respetivos espetrogramas ao mesmo tempo. Na análise automática, os dados foram processados através de um algoritmo composto por sete passos, incluindo a classificação e localização dos sons. Contudo, os dados manuais e automáticos apresentam problemas distintos. Nos dados manuais ocorre a não-independência entre os sensores causada por intervenção humana. A não-independência não é consistente com o processo de deteção ao longo dos DASARs, resultando num excesso de sons detetados na totalidade dos DASARs. A independência deverá resultar num padrão decrescente no número de deteções em função do número de DASARs nos quais os sons foram detetados. Os dados automáticos ultrapassam o problema da não-independência, contudo apresentam uma quantidade excessiva de sons "singulares" ("singletons") em relação aos dados manuais (aproximadamente mais de 15 vezes). Os sons "singulares" são detetados apenas e somente uma única vez no conjunto de hidrofones. Assume-se que grande parte dos sons "singulares" são, na realidade, falsos positivos. Os falsos positivos são sons classificados como sons "biológicos" da espécie de interesse, mas na realidade são provenientes de outra fonte irrelevante para o estudo.

Nesta tese, optámos pela análise de dados automáticos uma vez que excluem o problema da não-independência, além de não ser possível, geralmente, obter dados manualmente em registos de longa duração. Resta-nos então resolver o problema apresentado pela deteção excessiva de sons "singulares", que por sua vez assume-se que contêm falsos positivos. O problema dos sons "singulares" pode ser abordado das seguintes formas:

1. Analisar todos os dados através de uma análise de captura-recaptura espacialmente explícita (SECR), ou seja, ignorando o problema dos "singulares";

2. Analisar os dados excluindo os sons "singulares";

3. Ajustar um modelo linear com decaimento exponencial aos sons detetados em 2, 3, ..., todos os DASARs de modo a prever o número de sons "singulares". Gerar uma proporção p dividindo o número previsto de "singulares" pelo número original de "singulares". Descartar $1 - p$ de falsos positivos dos sons "singulares";

4. Introduzir uma função de verosimilhança de SECR desenvolvida nesta dissertação que incorpora a truncatura de sons "singulares".

Os pontos 1 a 3 foram analisados através de métodos de SECR com o package *secr* em R. As estimativas de densidade populacional são validadas através da comparação com dados simulados. O método ad hoc número 3 é considerado o mais fidedigno entre os três, uma vez que resolve parcialmente o problema dos falsos positivos nos sons "singulares". O ponto 1 leva à sobrestimação das densidades, dado que todos os falsos positivos contidos nos "singulares" estão incluídos nos dados analisados. No ponto 2 corremos o risco de subestimar a densidade, uma vez que os sons "singulares" provenientes de baleias são totalmente descartados. No ponto 3 as estimativas correm o risco de serem enviesadas, dado que não é possível saber qual a proporção p de sons "singulares" vindos das baleias-da-Gronelândia. O ponto 4 não foi implementado, no entanto estabelecemos as bases para a análise deste conjunto de dados. No caso de implementação da verosimilhança com truncatura de sons "singulares", as estimativas resultantes deste método são apenas referentes a sons detetados em pelo menos dois DASARs. Para trabalho futuro, sugerimos a inclusão de informação adicional na formulação de SECR, tais como os níveis recebidos dos sons e os ângulos dos sons provenientes da fonte sonora.

Palavras-chave: baleia-da-Gronelândia, estimação de densidade, captura-recaptura espacialmente explícita, sensores fixos, acústica passiva

Abstract

Management and conservation of wildlife populations is a major concern. Population density is a key ecological variable when making adequate decisions about them. A variety of methods can be used for estimating density. Capture-recapture (CR, also known as mark-recapture) methods are a popular choice, but ignoring the spatial component of captures has historically led to problems with resulting inferences on abundance. Spatially explicit capture-recapture (SECR) methods use the spatial information to solve two key problems of classical CR: defining a precise study area where captures occur over and reducing unmodeled heterogeneity in capture probabilities.

Arrays of Directional Autonomous Seafloor Acoustic Recorders (DASARs) recorded calls from the Bearing-Chukchi-Beaufort (BCB) population of bowhead whales during the autumn migration. The available passive acoustic dataset was collected over 5 sites (with 3–13 sensors per site) and 8 years (2007–2014), and then processed via both automated and manual procedures. The automated procedure involved computer-processing by a multi-stage detection, classification and localisation algorithm. In the manual procedure, calls were detected and classified by trained staff who manually listened to the recordings and examined spectrograms. The resulting manual data presents some pitfalls for density estimation, including non-independence among sensors caused by human intervention. The non-independence leads to an excess of calls being detected in all DASARs on a site. Data from the automated procedure does not suffer the non-independence issue, but the amount of 'singletons' is approximately 15 times higher than in the manual data. 'Singletons' are calls detected exclusively in one sensor and we assume they mostly comprise false positives. False positives are sounds classified as coming from the species of interest, but in reality are something else.

Considering only automated data from 2013 and 2014, several approaches were performed to solve the excess of singletons. Density estimation with a standard SECR analysis was conducted according to the following approaches: i) ignoring the singletons problem and analysing all calls; ii) removing the singletons; and iii) discarding a proportion of $1 - p$ false positives from the singletons. Simulated results were compared to verify the best approach. We also discuss a new approach by developing a SECR likelihood function that accommodates truncation of certain acoustic cues, specifically singletons.

We have laid foundations for the analysis of this dataset, but there are other possible research avenues to explore. Our next steps would include embedding additional information (like received levels and bearing angle) in the SECR formulation.

Keywords: Bowhead whales, density estimation, spatially explicit capture-recapture, fixed sensor, passive acoustic

Chapter 1

Introduction

1.1 Context of the Problem

The establishment and assessment of management practices concerning wildlife populations must be supported and justified by reliable population estimates. However, population change occurs over time, and it is important to know how it increases or decreases and how many animals of interest are there. One could think population size is enough to support effective management and conservation, but much of the theory and methodology concerning population size is to assume populations are well-defined so that one could randomly sample animals in an area and uniquely identify them (Royle, 2011). A popular way to study natural populations is applying *in situ* monitoring methods. One could resort to traditional abundance estimation methods, such as distance sampling. Bowhead whales are difficult to see as they spend most of their time under the water's surface. Because a portion of bowhead whales is undetected, this will result in biased abundance estimates. In the concept of population size, animals in a population typically live and move in territories or home ranges – they are spatially distributed – and the territories or home ranges are, naturally, not accounted in traditional estimation methods. This project seeks to estimate the population density of bowhead whales. This can be achieved with a spatially-explicit capture recapture (SECR) method by juxtaposing in a precisely delineated area an array of sensors capable of detecting the presence of the animals. Compared to the traditional abundance estimation methods, this will lead to different implications concerning estimation and interpretation of data. A traditional method, such as capture-recapture, will produce an underestimated population size when there is heterogeneity in capture probability. One of the major sources of heterogeneity is due to the location of the animal's centre of movement relative to the sensor. The problem of heterogeneity is taken into account in SECR, even though the home range centre is unknown.

The fact that bowheads produce distinctive sounds makes them a suitable candidate for Passive Acoustic Monitoring (PAM) (Cummings & Holliday, 1985). Additionally, the deployment of an array of hydrophones is chosen accordingly to the known migratory routes of bowhead whales (Braham et al., 1980). There is a lot of potential for fixed PAM in studies of cetaceans (whales and dolphins) concerning their ecology, conservation, and movement.

The present case study focuses on PAM to detect the acoustic cues produced by bowhead whales – their sounds – and analyses them with spatially explicit capture-recapture (SECR) methods to estimate population density of bowhead whales in the Arctic Coast of Alaska, specifically in the Bearing-Chukchi-Beaufort (BCB), during the autumn migration.

1.2 Study Species

1.2.1 Characteristics, Taxonomy and Life History

The bowhead whale (*Balaena mysticetus*) is a cetacean and belongs to the Balaenidae family. Also called Arctic right whale, Greenland right whale or great polar whale, it lives mostly in northern latitudes associated with sea ice, never occurring in the Southern Hemisphere. Bowheads have a classification of least concern (LC), by the IUCN Red List of Threatened

Species. This species is easy to identify due to their large size, rotund shape and lack of a dorsal fin (figure 1.1). Other unique features such as their triangular head (viewed in profile), and neck (existence of an indentation between the head and back). Their name comes from the bowed appearance of the mouth. Bowheads are black with white patterns on their chins, undersides, around their tail stocks, and on their flukes. Being unique to each individual, these white patterns, mainly around the tail and on the flukes, expand with age (Rugh & Shelden, 2009).

Figure 1.1: Cluster of bowhead whales (*Balaena mysticetus*).
Photo by Julie Mocklin

These cetaceans reach a mean length of 18m and a weight of 45,000 to 73,000 kg (Brownell & Ralls, 1986) and females are larger then males, as in all baleen whale species (Burns et al., 1993). Length of bowhead whales at birth is estimated to be 4-4.5m, length at one year to be 8.2m, length at sexual maturity to be 14m in females, and maximum length to be 20m. The duration of gestation is estimated to be 13-14 months and their sexual activity has been observed in March through May (Nerini et al., 1984). The head of these marine mammals correspond over a third of the bulk of the body with 230 to 360 baleen plates on each side of the mouth, instead of teeth. In order to insulate them, bowheads are protected in blubber 5.5-28 cm thick covered by an epidermis up to 2.5 cm thick (Rugh & Shelden, 2009).

During the mating season, bowheads are vocally active and can hear each other 5-10 km away. Breaching (leaping completely out of the water) and fluke slapping (tail smashes down on the water surface) are usual movements of the mating season that may play a role in attracting a mate or asserting dominance, but the role of these behaviours is not well understood (Rugh & Shelden, 2009).

This species is one of the longest living animals, reaching ages exceeding 100 years, and the oldest individual on record was an astonishing 211 years old (George et al., 1999).

1.2.2 Distribution

There are currently four or five recognized stocks of bowheads which are defined by geographically distinct segments of the species' total population: the Western Arctic (or Bering-Chukchi-Beaufort stock), Okhotsk Sea in eastern Russia, Davis Strait and Hudson Bay in north-

eastern Canada (occasionally considered separate stocks) and Spitsbergen in the North Atlantic (figure 1.2) (Heide-Jørgensen et al., 2006; Rugh et al., 2003).

In the Alaskan region, bowhead whales migrate from their Bering Sea wintering grounds through the Chukchi Sea to the Beaufort Sea during spring/summer. The return migration occurs during late spring (April-June) and autumn (September-October) (Moore, 1993). Bowhead whales travel from their eastern Beaufort Sea summering grounds, westward along the coast, and into the Chukchi Sea.

Whales follow open-water leads far from the shore during spring migration. Conversely, the autumn migration is generally near shore and mostly in water depths of 20 to 50 m (Würsig & Clark, 1993).

Figure 1.2: Distribution map of *Balaena mysticetus*. From East to West: Okhotsk Sea, Spitsbergen Sea, Davis Strait, Hudson Bay, and Bering-Chukchi-Beaufort Sea.
Source: http://uk.whales.org/species-guide/bowhead-whale

1.2.3 Ecology, Behaviour and Physiology

Bowhead whales are planktivorous – planktonic crustaceans, especially copepods and euphausiids, were the most important food items found in bowhead whale diet studies, plus mysids and gammarid amphipods (Lowry et al., 2004). Killers whales (*Orcinus orca*) are the only predators of bowheads besides humans.

Bowhead whales are skimmers, as they feed on the surface, and sometimes at or near the seafloor. They are capable of engulfing large volumes of water, and swim forward keeping their mouths continuously open when feeding. When closing their mouths, the water is pushed out, trapping prey inside. Their massive tongue sweeps the food off the baleen into a narrow digestive tract (Perrin et al., 2009).

Being air-breathing mammals, their diving abilities are remarkable – bowheads likely exceed an hour underwater – and they can withstand breaking through ice up to 60 cm thick. During the autumn migration, there is a record for shorter dives (8.65 ± 2.73 min, n=88) compared to dive duration during spring (1.7 to > 28 min) (Würsig et al., 1984). Their vocalisations (very-low frequency and very loud calls) are essential to help them find mates or assist in following each other when navigating through sea ice. Although extremely vocal, they are solitary animals often travelling alone or in small pods of up to six whales (Rugh & Shelden, 2009).

1.2.4 Interaction with Humans

Bowheads were extremely valuable due to their large size, long baleen and thick blubber. Commercial whalers from the 17th to 19th centuries depleted most stocks of these mammals. In the mid-1970s the International Whaling Commission (IWC) concluded that the harvest by Alaskan Eskimos threatened the existence of the bowhead whale, which was still recovering from a period of open-access exploitation (1848-1914) (Conrad, 1989).

Currently, native Alaskans kill around 40 whales per year through quotas set by the IWC and the Chukotka Natives of Siberia allotted five bowheads per year from the Alaska quota. Independent of this quota, the Canadian government allows a limited hunt of these mammals from the Western Arctic stock and from Davis Strait and Hudson Bay (Rugh & Shelden, 2009).

1.3 Introduction to Density Estimation

Ideally, we would count all the animals of a species of interest from a population in a defined area, resulting in the animal's density. Suppose we wanted to count all European honey bees in Europe. The exercise of such counting is impossible, as animals move around, and the areas involved are large. So we have to find solutions on sampling approaches and be able to draw inferences about the total population. For instance, imagine a wildlife survey taking place in a study area of size A. A team of investigators randomly deploy a large number of sample plots with total area a, and detect and count n animals. Assuming all animals within the sample plots are counted, then density D is estimated by:

$$\hat{D} = \frac{n}{a}, \tag{1.1}$$

with the estimated abundance being simply density times the size of the study area

$$\hat{N} = \hat{D}A. \tag{1.2}$$

Frequently, when surveying wild animals, not all animals in the covered areas are detected. If we can estimate the probability p of detecting an animal within a, then density can be estimated as

$$\hat{D} = \frac{n}{\hat{p}a}. \tag{1.3}$$

1.3.1 Existing Methods to Estimate Animal Abundance and Density

This section will guide the reader through the existing methods to estimate animal population size, in particular animal abundance and density. The primary goal is to give an outline of the key existing approaches and explain how one obtains abundance/density estimates.

Animal abundance was traditionally obtained through visual observations. As a result, most methodologies were focused on visually acquired data. Abundance and density estimates based on visual data were built almost exclusively on one of two inferential methods: capture-recapture/mark-recapture (CR/MR) and distance sampling (DS). The methods applied in this dissertation are a combination of the previous two methods, resulting in spatially explicit capture-recapture (SECR) methods.

The generic term 'detectors' is used interchangeably throughout this dissertation with the more specific terms 'traps', 'sensors', and more specifically 'DASARs' in further sections. The same happens with the term 'detections' being described as 'captures' or 'encounters'. Moreover, 'cue', 'acoustic cue', 'sound' and 'vocalisation' have the same meaning in this context.

Plot Sampling or Strip Transects

Estimating the size of biological populations can be accomplished with counting. In plot sampling (also known as strip transects), one performs a count of the population of interest over randomly chosen plots. These plots (or strip transects) are usually long, narrow plots or quadrats (Burnham & Anderson, 1984).

Frequently, plot sampling leads to incomplete counts, because these methods are being applied to situations where the key assumption, that all animals in a given area are detected, is false. This results in an underestimation of density. In this method, one searches a plot/strip of area $2L\omega$ (L is the length of the transect and ω is one-half the width of the strip transect) and it is assumed all individuals of interest are detected and counted. These plots may be traversed by an observer on foot, on terrestrial vehicle, on airplane or helicopter, etc. Under the assumption that all individuals are detected and counted, then density D is estimated as

$$\hat{D} = \frac{n}{2L\omega}. \tag{1.4}$$

However, if some individuals are not detected, i.e., the total number of individuals N_ω in the strip of total width 2ω is bigger than the count of detected individuals n ($N_\omega > n$), the density estimate is naturally biased low. Note this is just estimator 1.1 where the area size is explicit.

Bias derived from incomplete counts are usually due to:

1. probability of detecting individuals decreasing with distance, x, from the centerline of the strip transect;

2. other factors influencing the detection probability. These variables may include: size, shape, coloration and habits of individuals of interest; level of experience/training of observer;

variables related to physical setting (e.g., habitat type, time of day, sun angle, among others).

Distance Sampling (DS)

Distance sampling uses the recorded distances to objects of interest obtained by surveying lines or points to estimate detectability and hence correct detected counts. If line transects are used, then the perpendicular distances to detected individuals are recorded (figure 1.3); otherwise, in the case of point transects, the radial distances from the point to detected individuals are recorded. A point transect may be considered as a line transect of zero length, i.e., a point. The probability of observing an animal decreases as its distance from the observer increases, being the observer a human operator or a sensor. The area effectively searched in distance sampling is calculated by: $A^{'} = 2\mu$ L, with L being the kms of transect (or other units of distance), and μ as a definition for the effective strip width (distance for which unseen animals located closer to the line than μ equals the number of animals seen at distances greater than μ). Then, density in the area effectively searched is $D = n/A^{'}$ (Buckland et al., 2012).

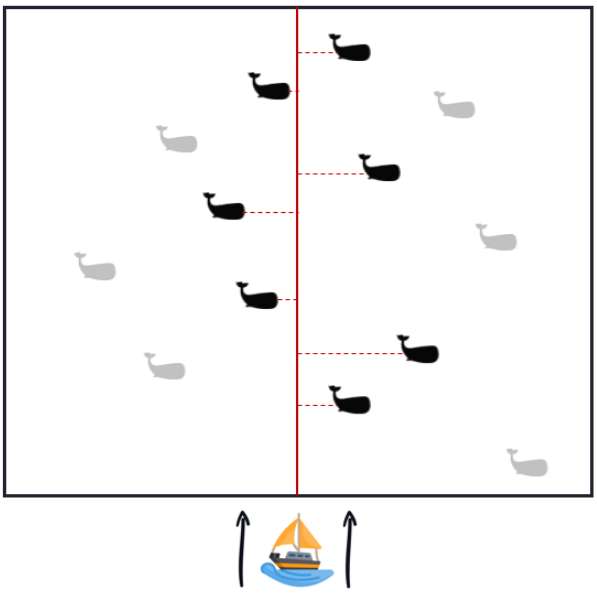

Figure 1.3: Example of distance sampling performed in a line transect survey of a certain whale species: a single observer or a team of observers sail in a specified line transect (centred red line) and record the distances (perpendicular red dashed lines) to detected whales. Black whales indicate detected individuals and therefore recorded distances. Grey whales indicate the presence of animals of interest but observers were unable to detect them.

Distance sampling estimates the area effectively searched, or equivalently the average probability of detection within some fixed truncation distance (Marques et al., 2013). It is important to randomly place a sufficiently large number of line or point transects over the area of interest, so there is a good coverage of the entire area. The recorded distances obtained are then used to model a detection function: $g(y)$, represents the probability of detecting an animal given it is at distance y from the transect. Therefore, the average probability p of detecting an

animal in the survey area is

$$p = \int_0^{\omega} g(y)\pi(y)\, dy, \tag{1.5}$$

where ω is the truncated distance from which it is assumed no more detections occur; $\pi(y)$ is the distribution of distances to all animals (either detected or not) (Buckland et al., 2012). It is assumed that the distribution of animals $\pi(y)$ is known: uniform for line transects, and triangular for point transects. This is a consequence of a suitable random design. However, in poorly designed surveys, transects may be placed along existing landscape features (e.g., roads, rivers, shorelines, etc). This results in $\pi(y)$ having an unknown form as animals might present a density gradient due to those features. This will then lead to biased estimates (Marques, 2007).

Cue counting is a special kind of distance sampling (Hiby, 1985) – one detects cues produced by animals, instead of counting them directly. Cue counting is a form of distance sampling with a temporal component (Borchers et al., 2010). In this case, it is not possible to determine which individuals produced which cue, therefore the density of cues is estimated alternatively, e.g., whale vocalisations per unit area or per unit of time. This cue estimate is then divided by an independent estimate of the average cue production rate (cue rate – number of sounds per unit of time).

As an example, a survey for songbirds comparing point and line transect sampling was performed in Buckland (2006). Three methods are compared and implemented in both point and line sampling: 1) an observer records birds detected from a point for several minutes; 2) an observer records locations of detected birds 'frozen' at a single location; and 3) an observer records distances to detected cues (songbursts), rather than birds. The line transect sampling method was more efficient than the point method. Also, the second method was found to be the most efficient of the point sampling methods. Another particular type of distance sampling is suggested in Marques et al. (2013) when animals occur in clusters, hence becoming the object of analysis. The aim here is to obtain a density of animal clusters and then multiply it by an estimate of the mean cluster size in the population. A potential problem arises when large clusters are easier to detect than smaller ones, leading to a potential bias when determining population mean cluster size.

Based on a set of randomly allocated transects over the study area of interest, unbiased density estimates require the following assumptions:

1. animals on the line or at the point are detected with probability 1, i.e., $g(0) = 1$;
2. animals do not move during the observation process, or the observation process is considered a snapshot, i.e., instantaneous in time;
3. distances are measured without errors;
4. detections are statistically independent events.

Regarding assumption 2), the observation process might happen in a period of time of negligible length, in such a way that animal movement is negligible within the time interval. If

an observer is faster than the animals themselves, it is safe to assure that existing bias from this source can be ignored. In fact, a simulation study revealed that bias was negligible if mean animal speed was one quarter of that of the observer, but not if animal speed was one half that of the observer (Glennie et al., 2015), although the ratio of animal speed to observer speed for low bias depends on the detection function. In the presence of highly mobile animals, we could face considerable overestimation of density. Moreover, the focus can be directed to unobserved responsive movement, resulting in the overestimation of density if animals are attracted to the observer, and underestimation of density if animals avoid the observers.

In assumption 3), the consequence of measurement errors in estimated distances is similar to the error in animal movement (Marques, 2004). When distances are underestimated and overestimated, the densities will be overestimated and underestimated, respectively. In Marques (2004), it is reported that random errors will typically lead to an overestimation of density.

Finally, assumption 4) is strictly required to estimate the parameters of the detection function model, $g(y)$, by maximum likelihood. Reassuringly, methods are known to be robust to the failure of the independence assumption (e.g. Buckland (2006)).

Capture-recapture (CR) or mark-recapture (MR)

Capture-recapture (also designated mark-recapture) is another approach to estimate abundance. This indirect method involves repeatedly sampling a population of interest over time. CR is performed by marking individuals so they can be recognised in later recaptures. One collects a sample of n individuals, marks and returns them to their habitat. The goal is to obtain their capture history data (also known as individual encounter history data), i.e., a sequence of binary random variables that indicates whether an individual was captured or not during one of these sampling occasions (also named trapping occasions) (table 1.1) (Pradel, 1996).

Table 1.1: Example of a capture history data with n successfully captured individuals in a population with N unknown total animals and 10 sampling occasions. '1' represents presence or successful detection in a given sampling occasion; '0' means absence or unsuccessful capture.

	Occasion									
Id	**1**	**2**	**3**	**4**	**5**	**6**	**7**	**8**	**9**	**10**
1	1	0	0	0	1	1	0	0	0	0
2	0	0	1	0	1	0	0	0	0	0
3	0	0	0	0	0	0	0	0	1	0
...	...	...	...	...	...	...	...	...	...	...
...	...	...	...	...	...	...	...	...	...	...
M	0	0	1	0	0	0	0	0	0	1

Depending on what is best suited for each taxon, the recognition from marking can be achieved by photo identification, genetic markers, among others, although many species (e.g.,

tigers, zebras, some cetaceans) possess individually distinctive natural markings that can be used as markers. The recognition from marking results in an unknown fraction n/N of marked animals, since N is unknown. n is the total number of animals successfully captured (from individual 1 to M). A second sample is drawn. This leads to a proportion p of marked animals for the new sample, which is an estimate of the proportion of marked animals in the population. Hence, we can use the Lincoln-Petersen estimator, one of the oldest and simplest methods based on a single recapture occasion, so an estimate of population size could be given by $\hat{N} = n/p$ (Krebs et al., 1989). However, one needs to meet multiple unrealistic assumptions to obtain reliable estimates, such as: (i) individuals do not loose marks, (ii) capture does not affect future capture probability, (iii) the population is closed (i.e., no births, deaths, immigration and emigration occur between samples) and (iv) all individuals are equally catchable (equal probability of being detected). This latter assumption has an immense importance, as its failure will produce biased low estimates caused by heterogeneous capture probabilities. The unmodelled heterogeneity in detection probabilities is explained by the tendency of sampled animals being more detectable than others (the opposite of the required iv) assumption), resulting in the overestimation of animal detection probability and underestimation of abundance. The violation of this assumption can lead to lower precision, but also substantial bias (Link, 2003).

Estimates derived from CR cannot readily be converted into density estimates, because there is not a well-defined sampling area. This CR limitation of a non-explicit spatial context leads to an inadequate conversion to density estimation, because animals move freely through space and the area containing the animals exposed to the sampling effort is bigger than the area immediately surrounding the sampling devices. Hence, CR will tend to estimate the size of the population that would at any one time be potentially detectable from the set of traps used, which is most often ill defined.

CR presents other limitations, such as the variation of individual exposure to capture according to the location to their home-range centre and to the location of the sampling devices. The use of CR to estimate population density does not account for: (i) the location of detectors/traps; (ii) the location of detections/encounters and (iii) the spatial pattern of individual encounters (or capture history data) (Efford & Fewster, 2013). All this extra information could boost the accuracy and/or precision of the density estimates. This will be discussed in the following sub-section with respect to spatially explicit capture-recapture methods.

Spatially Explicit Capture-Recapture (SECR)

Spatially explicit capture-recapture (SECR) methods represent a natural extension of the CR general framework. The primary goal is to estimate the population density of free-ranging animals and obtain statistical inferences about spatial structure of populations from observed detections of a sample of individuals. These methods are aimed to model animal CR data collected with an array of traps (Efford, 2018).

SECR methods overcome some issues presented by conventional CR, in particular the unmodelled heterogeneity in detected animals and an ill-defined population. In SECR, the spatial location of the location of traps that detected an individual are known, reducing the effect of unmodelled heterogeneity (since part of it is modelled) and making the effective survey area

estimable.

The primary data for a conventional SECR analysis is (i) the location of traps, and (ii) capture histories, i.e., detections of known individuals on one or more trapping occasions (Efford, 2018). The following table subtly differs from the CR table, since we know the location of the specific traps where the detections occurred (figure 1.2). Depending on the survey design, researchers may need to divide the data into discrete trapping occasions. For example, camera traps sample continuously, so these occasions can be divided in periods of 24 hours (corresponding to the duration of each occasion (1 to S occasions) exhibited in table 1.3).

Table 1.2: Example of SECR capture histories. Each row corresponds to an object of interest (for example, animals) and each column a trap. '0' indicates no detection at a certain trap, and '1' otherwise. Each trap has an associated x-y coordinates. Our data presents this matrix format.

	Traps									
Id	**1**	**2**	**3**	**4**	**5**	**6**	**7**	**8**	**9**	**10**
1	1	0	0	0	1	1	0	0	0	0
2	0	0	1	0	1	0	0	0	0	0
3	0	0	0	0	0	0	0	0	1	0
...	...	...	...	...	...	...	...	...	...	...
...	...	...	...	...	...	...	...	...	...	...
M	0	0	0	0	0	0	1	0	0	1

Table 1.3: Example of SECR capture histories with trapping occasions (1 to S), and traps (1 to 10). Each row corresponds to an object of interest (for example, animals) and each column a trap. '0' indicates no detection at a certain trap, and '1' otherwise. Each trap has an associated x-y coordinates.

	Occasion 1									
Id	**Trap 1**	**Trap 2**	**Trap 3**	**Trap 4**	**Trap 5**	**Trap 6**	**Trap 7**	**Trap 8**	**Trap 9**	**Trap 10**
1	1	0	0	0	1	1	0	0	0	0
2	0	0	1	0	1	0	0	0	0	0
3	0	0	0	0	0	0	0	0	1	0
...	...	...	...	...	...	...	...	...	...	...
...	...	...	...	...	...	...	...	...	...	...
M	0	0	0	0	0	0	1	0	0	1
	Occasion S									
Id	**Trap 1**	**Trap 2**	**Trap 3**	**Trap 4**	**Trap 5**	**Trap 6**	**Trap 7**	**Trap 8**	**Trap 9**	**Trap 10**
1	1	0	1	0	0	1	0	0	0	0
2	0	1	0	0	1	0	0	0	0	1
3	0	0	1	0	0	0	1	0	0	0
...	...	...	...	...	...	...	...	...	...	...
...	...	...	...	...	...	...	...	...	...	...
M	1	0	0	1	0	0	1	0	0	0

Types of Traps

SECR data can be collected with different types of detectors, in addition to physical traps. Efford et al. (2009) describe three categories (figure 1.4):

a) Multi-catch traps: these hold any number of animals and they stay trapped for the whole

duration of a sampling occasion. Therefore, animals are only captured in one trap on any occasion (e.g., mist-nets);

b) Single-trap: these traps hold solely one animal and it stays unavailable to catch other animals once it caught one (e.g., cage-traps);

c) Proximity detectors: technological development opened new possibilities to study species that were historically impossible to study as they were extremely difficult to physically capture. Proximity detectors are 'traps' that record the presence of an animal and leave it free to be detected in other traps on any occasion (e.g., hair snares, camera traps, microphones, and hydrophones).

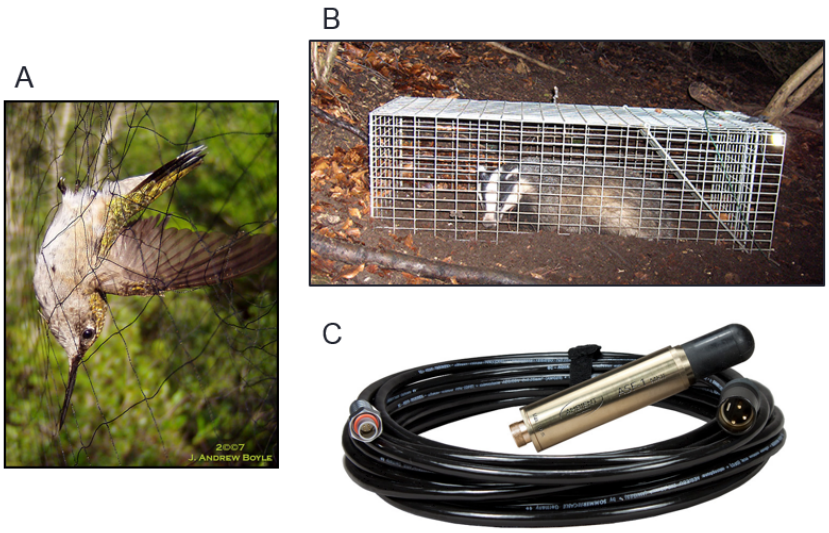

Figure 1.4: Example of three different types of traps: A) Mist-net representing a multi-catch trap. B) Cage-trap exemplifying a single-trap. C) Hydrophone (underwater microphone) is an example of a proximity detector.
Source A: J. Andrew Boyle. Source B: Julian Drewe.
Source C: http://ambient.de/en/product/ambient-sound-fish-asf-1-mkii-hydrophone/

Proximity detectors are a non-invasive type of sampling since they do not physically capture an animal. As described further in the sub-section 1.5, we performed acoustic sampling with proximity detectors in this dissertation.

1.4 Estimating Cetacean Density from Passive Acoustic Data

There are two major ways to collect data for wildlife abundance estimation: visual observations and trapping. The latter is usually achieved by physically capturing or by photo-ID. The most common survey method is visually based distance sampling and alternatively, mark-recapture by trapping. Both methods are explained in detail in the following section. The problem arises when these methods present limitations in terms of cost, effort and danger to the observers. Taking that into account, PAM offers an alternative survey mode capable of producing high-quality data when other methods fail. Consider the following example: the density estimation of cetaceans. This can be achieved through traditional visual survey methods. Only a portion of the animals present is detected as a result of visual surveys dependence on daylight hours and in relatively good weather. Also the survey observers can only see the animals

during a very short period when they are at the surface. Visual surveys are performed using a small number of observation platforms with one or a few vessels with a variable survey duration – a few weeks to a few months of the year (Mellinger et al., 2007).

Visual survey results have an additional problem as they may vary dramatically due to clumping of cetaceans into large groups and to their limited spatial and temporal scales. The need for more reliable and effective methods led to the development of alternatives to estimate abundance and/or density. Passive acoustics surpasses those restrictions as many species are also visually cryptic and not amenable to trapping. Nevertheless, many species have detectable and unique sounds that can be used to estimate abundance/density.

In recent years, passive acoustic methods have risen and became increasingly widespread for not only cetacean observation, but also for several other sound producing animals, since:

a) sound propagation in water is more efficient than in air, as energy from light is absorbed more than that from sound as it passes through water.

b) visual surveys can be very expensive, usually requiring large investments of ship time and teams of trained observers;

c) many deep-diving cetaceans forage at depths where light does not penetrate well and have to resort to echolocation for foraging, hence becoming detectable for PAM.

Passive acoustic density estimation relies on the sounds (also referred as cues) naturally produced by animals that are detected by sensors and used as a tool to estimate animal abundance. In passive acoustic observation, a certain instrument captures cues from the surrounding environment. It is an alternative survey modality that overcomes constraints imposed by visual surveys or physical trapping as the information can be gathered in environments challenging for human observers to work (e.g. deep or polar oceans, presence of fog, recording at night time, among others). Moreover, many species are visually cryptic, others are not amenable to trapping due to lack of effective methods (particularly for recapture in traps) or welfare concerns.

A cue is any identifiable sound, such as calls, whistles, echolocation clicks or feeding buzzes. Acoustic cues are used to identify and/or locate primates (Kalan et al., 2015), birds (Bardeli et al., 2010), bats (Adams et al., 2012), amphibians (Acevedo & Villanueva-Rivera, 2006), fishes (Rountree et al., 2006), and cetaceans (Mellinger et al., 2007). Ultimately, being amenable to automated data collection, passive acoustics is also capable of generating large amounts of data ready to be analysed (Marques et al., 2013).

In passive acoustic monitoring, the object of interest, cue, is used as an indicator of a presence of an animal. In case of 'no detection', it is not equivalent to an animal being absent, but it suggests that the animal did not necessarily produce a sound, or a sound was produced but not detected. A 'no detection' may occur if a human operator is not properly listening; if there is a miscalibration of the sensors detecting the cues, if such instruments are used; among others. Usually it is not possible to count the number of individuals directly. Instead, we count the number of vocalisations, although not knowing how many individuals produced them. By using cue rates (estimated number of cues by the duration of the survey) as an indicator, we need to consider these 'multipliers' in the construction of density estimators. These are factors that convert an indirect estimate into an actual animal density estimate (Marques et al., 2013).

In passive acoustic surveys, the n in equation 1.3 is the number of detected cues, producing an estimate of density of sounds. The estimator can be divided by an estimate of cue rate to produce an estimate of animal density. Another common multiplier is used to account for 'false positives' detections, i.e., sounds classified as coming from the species of interest, but in reality are something else. Both multipliers (cue rate and false positives) are incorporated in the density estimator as follows:

$$\hat{D} = \frac{n(1-\hat{f})}{\hat{p_c} a \hat{r} T}, \tag{1.6}$$

where n is the number of detected sounds during time period T, f is the proportion of detections that are false positives, p_c is the probability of detecting a cue in area a, and r is the cue rate that converts density of sounds to animal density.

Obtaining density estimates from passive acoustic data requires: (i) identifying sounds (those being the object of interest) that relate to animal density; (ii) collecting a sample of sounds, n, generated by a well-designed survey protocol; (iii) estimating the rate of false positives, f; (iv) determining the probability of detection of a cue, p_c; (v) obtaining an estimate of the multiplier r that translates sound density into animal density (Marques et al., 2013).

In this thesis, the population density estimate will be achieved by first acquiring a density estimate of sounds ($\hat{D_s}$ – number of sounds divided by a study area) and then will be divided by two multipliers: (i) cue rate ($\hat{r}$) and (ii) time period over which monitoring took place (T):

$$\hat{D} = \frac{\hat{D_s}}{\hat{r} T}. \tag{1.7}$$

1.4.1 Applications and Considerations

Defining the object detected

Depending on the acoustic survey, it is possible to consider different objects of interest:

1. animals (i.e., unique individuals);
2. groups of animals or
3. individual sounds.

The target must be chosen according to what is best suited to the species of interest and, naturally, the available resources to collect data. Ultimately we are interested in estimating the density of the first. Note that to transform the second density estimate above (groups) into the first, one needs to obtain a multiplier (mean group size) from acoustically detected groups

of animals. Similar to the formula 1.7, we would have:

$$\hat{D} = \frac{\hat{D_g}\hat{s}}{T}, \tag{1.8}$$

with $\hat{D_g}$ being the density estimate of groups of animals, the multiplier $\hat{s}$ representing a mean group size estimate, and T the considered time period.

Species-specific Factors

Several species-specific factors can influence the performance of acoustic surveys. These factors include:

a) Frequency of the sounds of interest. Bowhead whales frequency ranges from 50 to 500 Hz (Abadi et al., 2014). Sounds below 1 kHz have significantly less seawater absorption loss than sounds above 10 kHz (Francois & Garrison, 1982).

b) Vocal behaviour. Not only vocal behaviour varies with age, gender and season, but also some cetaceans vocalise more frequently or more consistently than others, e.g., male baleen whale species during the breeding season (Mellinger et al., 2007).

c) Sound source level. Larger cetaceans, such as mysticete whales, produce intense vocalisations prone to be detected at longer distances. These can be detected at distances of several tens of kilometers regardless of the arrangement of the hydrophones: on a single hydrophone (Barlow & Taylor, 2005) and much farther – hundreds of kilometers – on hydrophone arrays (Širović et al. (2007), Samaran et al. (2010)). It is important to note that the distance at which a sound is detected is a function of the sound source intensity and also the frequency, because higher frequency sounds suffer much greater transmission loss than low frequency sounds. For example, blue whale calls can be detected hundreds of km away, because they are loud and have low frequency. Sperm whale clicks are also loud, but they are high frequency, so can only be heard at most tens of km away.

d) Sound directionality. Directionality in acoustic signals is best suited for animals using echolocation, such as toothed whales. Bowheads (being a baleen whale) do not use echolocation, but a study suggests the existence of directionality of two types of calls (upcalls and downcalls) during the spring migration off Barrow, Alaska (Blackwell et al., 2012). This study indicates calls were slightly stronger ahead of the animals.

1.4.2 Instrumentation Used in Passive Acoustics

There are three types of passive acoustic survey methods:

a) towed acoustic sensors – hydrophones may be attached to a mobile platform (e.g. a ship) to sample a large area. These include a large areal coverage and are simpler to combine acoustic detection with other types of detection, in particular visual;

b) fixed acoustic sensors – hydrophones are fixed to the bottom for long time periods. These are

less expensive and allow longer periods of observation;

c) gliders and drifting sensors are an intermediate between the previous two sensors. Gliders are free-floating autonomous devices that complete a designed line transect survey (Harris & Gillespie, 2014). They can be equipped with a digital acoustic monitoring instrument to record and process *in situ* frequency audio to characterize marine mammal occurrence (Baumgartner et al., 2014). These underwater gliders do not require towing (a)) or mooring (b)) and may act as fixed sensors if they move slowly compared with animal speed (Marques et al., 2013). Drifting sensors are buoys equipped with acoustic sensing arrays. The drifting buoys measure ambient noise and detect passive acoustic signals (Pecknold & Heard, 2015).

There are two types of equipment applied in fixed passive acoustic surveys (Mellinger et al., 2007):

a) cabled hydrophones – normally deployed in permanent or semi-permanent installations, providing a constant supply of data in near-real time (Bacon, 1982);

b) autonomous recorders – a hydrophone and a battery-powered data-recording system. These are deployed semi-permanently underwater by mooring, via a buoy or attached to the seafloor. The recorders can operate up to two years and are typically deployed in arrays of 3 to 10 recorders to improve areal coverage and allow the localisation of sound sources. Autonomous recorders must be later retrieved since they store acoustic data internally (Sousa-Lima et al., 2013).

1.5 The Data

1.5.1 Arrays of DASARs

The Shell Exploration and Production Company (SEPCO) commissioned Greeneridge Sciences, Inc. to deploy arrays of fixed 'Directional Autonomous Seafloor Acoustic Recorders' (DASARs, see figure 1.5) (Greene Jr et al., 2004) to assess the potential Exploration & Production activities, including the impact of airgun sounds on bowhead whales during their westward autumn migration. From 2007 until 2014, Greeneridge Sciences, Inc. deployed, collected, and analysed an extensive acoustic dataset. More than 13 million bowhead calls were detected and localised on up to 40 DASARs. The enormous set of high-quality detected calls analysed in this dissertation was collected by the same autonomous recorders, but only a subset of the recorded vocalisations were considered (years 2013 and 2014).

Arrays of DASARs were deployed at five sites along the Alaskan Beaufort Sea during the late summer/autumn migration route of bowhead whales. The shore distance from the easternmost site to the westernmost was about 280 km – this corresponded from northeast of Kaktovik to northeast of Harrison Bay. Each site was composed of 3 to 13 DASARs (a normal configuration considered 7 DASARs) placed at the vertices of the triangles with 7 km sides and labeled A to G from south to north (up until M if site had 13 DASARs), respectively (figure 1.6). The southernmost DASARs distanced 15-33 km north from the coast and at a water depth of 22-39 m, whereas the northernmost DASAR at each site was 21 km of the southernmost and at a depth of 15-54 m. More information can be found in table 1.4. The installation was executed on

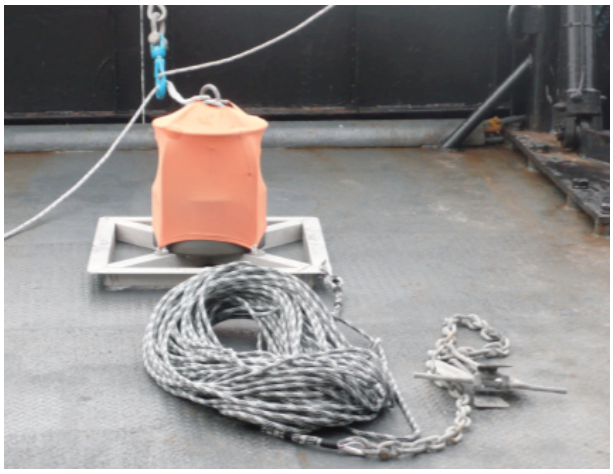

Figure 1.5: Example of one Directional Autonomous Seafloor Acoustic Recorder (DASAR).
Source: https://www.greeneridge.com/en/

the seafloor with no surface buoy attached and DASARs were retrieved by grappling. DASARs recorded sound continuously at 1 kHz (1000 samples/s). This sampling rate allowed for 115 days of continuous recording of sounds in the interval 10–450 Hz frequency band (Blackwell et al., 2013). Each DASAR's clock and orientation had to be calibrated to a certain source level and frequency range, because the orientation of the DASARs on the seafloor was random relative to true north, and each DASAR's clock contained a small and constant time drift, although the drift would become significant over several weeks of deployment. Each site had to be calibrated two times per season: firstly following DASAR deployments and finally just preceding their retrieval (Blackwell et al., 2013) (see figure 1.6 for calibration locations).

Table 1.4: Additional DASARs information.

Site, Year	**Time range of detections [total days]**	**Number of DASARs in operation**	**Other information**
1, 2013	Aug. 08 – Oct. 01 [55]	3 (D–F)	Site 1 was reduced to three of the original seven DASARs
2, 2013	Aug. 09 – Oct. 02 [55]	7 (A–G)	
3, 2013	Aug. 07 – Oct. 01 [56]	7 (A–G)	DASARs A,B and E had some bad bearings
4, 2013	Aug. 06 – Sept. 29 [55]	13 (A–M)	DASARs K and M had some bad bearings
5, 2013	Aug. 06 – Sept. 28 [54]	7 (A–G)	DASARs C,D and E had some bad bearings
1, 2014	Aug. 11 – Sept. 27 [48]	3 (D–F)	Site 1 was reduced to three of the original seven DASARs
2, 2014	Aug. 11 – Sept. 28 [49]	7 (A–G)	
3, 2014	Aug. 12 – Sept. 29 [49]	7 (A–G)	
4, 2014	Aug. 14 – Oct. 02 [50]	13 (A–M)	DASARs K and M had some bad bearings
5, 2014	Aug. 16 – Oct. 01 [47]	7 (A–G)	DASAR F had some bad bearings

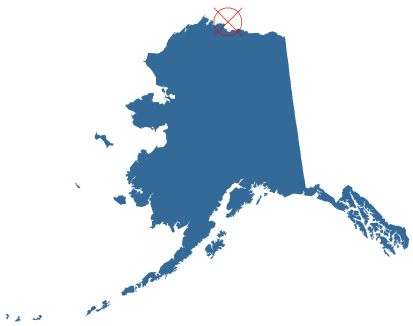

(a)

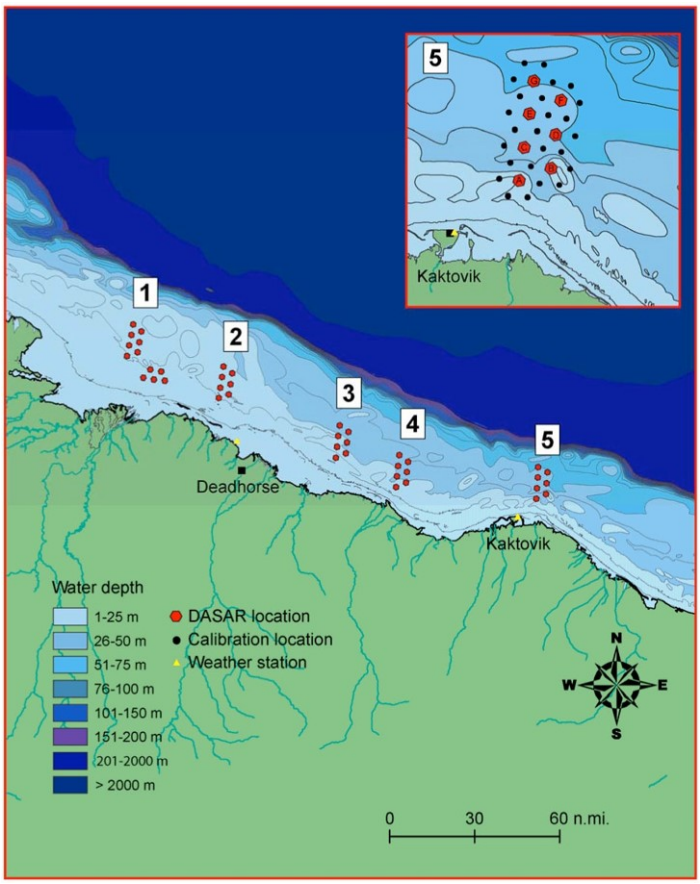

(b)

Figure 1.6: (a) Alaska State map. Red cross with a circle indicates approximate location of DASARs deployment. (b) Distribution of DASARs' deployment locations in 2007-2014 field seasons in northern Alaska coast. There are five main sites with seven-DASAR arrays (red circles), labeled 1 to 5 from west to east. DASARs were labeled A to G from south to north. In 2008, five extra recorders were deployed south of site 1: DASAR locations 1H, 1I, 1J, 1K and 1L (red circles). Inset (5) shows calibration locations at site 5 (black dots) representing DASARs' locations at single array.
Source: Greeneridge Sciences Inc.

1.5.2 DCL – Detection, Classification, Localisation

Detection and Classification

After DASARs retrieval the data was transferred to computers. Vocalisations can be detected either **manually** or **automatically**, and both approaches will present different methodologies. When **manual** analysis was performed, the analysis and classification of the whale calls was done manually by trained staff: specialists listened to recorded calls and looked at spectrograms to find occurrences of the target species' vocalisations. Spectrograms of the acoustic data were examined, 1 minute at a time, for all calls or suspected calls. The spectrograms of all seven DASARs belonging to one site were displayed simultaneously and analysed together (Blackwell et al., 2013). For consistency checkup, a lead analyst performed regular checks among analysts. An example of spectrogram of two main anthropogenic noise contributors (vessel traffic and seismic surveys) recorded during the monitoring program can be found in figure 1.7.

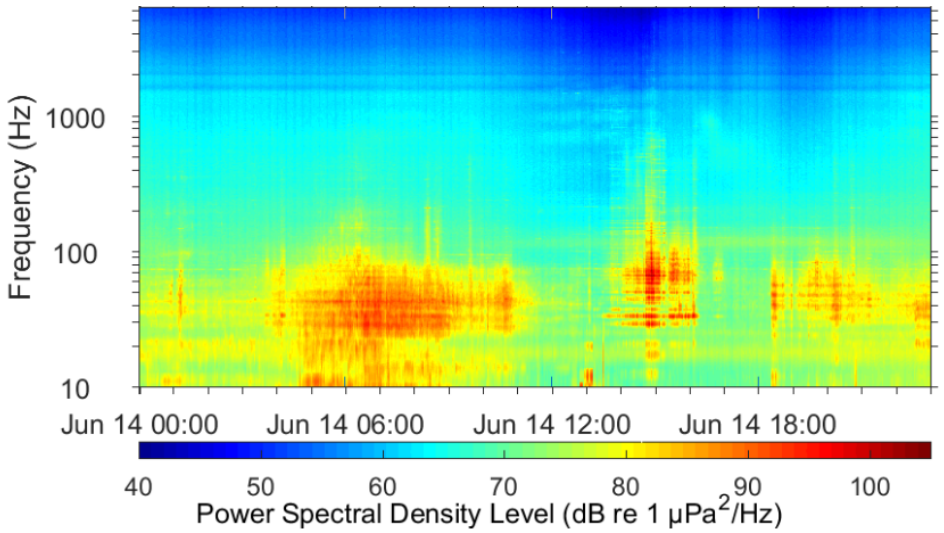

Figure 1.7: Example of spectrogram corresponding to vessel traffic and seismic surveys. Source: https://www.niwa.co.nz/coasts-and-oceans/research-projects/acoustic-monitoring-whales-dolphins-new-zealand-cook-strait-region

The **automated** data was processed through a seven-stage algorithm (figure 1.8) described in detail in Thode et al. (2012). The first four stages were applied independently to each DASAR's data, and consisted of:

1. Energy detection: applying an 'event detector' to flag any potential signal 'events' not considered to be whale calls;

2. Interval detection: applying an 'interval filter' to remove airgun pulses. If an event occurs at regular intervals from a consistent direction, then it is considered to be an airgun pulse. This allows the removal of low-intensity, short-duration, airgun pulses from distant airgun surveys;

3. Feature extraction: creating and equalizing a spectrogram from candidate detections and running an image processor that extracts 25 descriptive features;

4. Neural network: exploiting two cascade multilayer feed-forward neural networks to separate candidate detections based on their feature values. The first network separates 'biologic' vs 'non-biologic' signals, while the second network decides if a call is a 'bowhead' call or 'other biologic' sound.

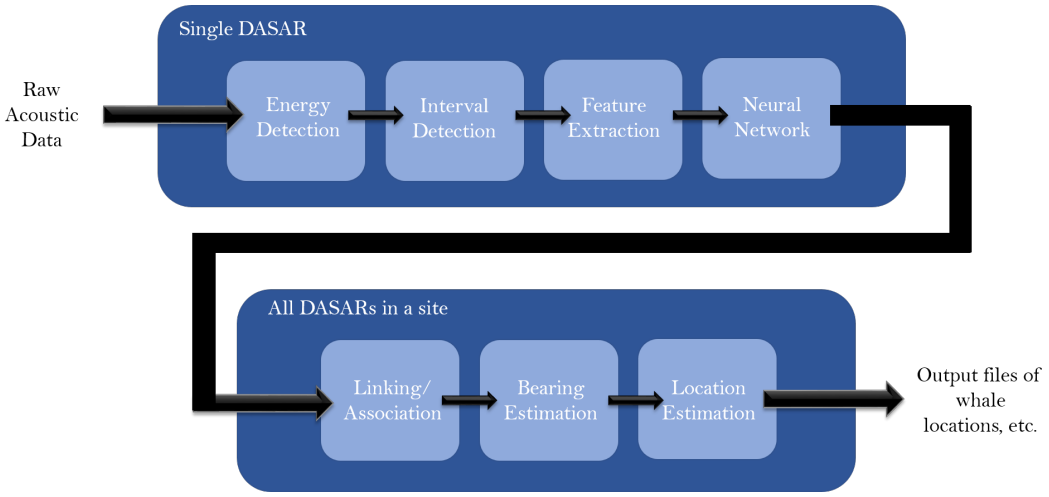

Figure 1.8: Scheme of automated analysis with seven stages. The first four stages require the process over a single DASAR, while the last three produces 'call sets' in order to estimate a call localisation, as well as other features.
Source: Thode et al. (2012)

Until this stage each DASAR was processed independently, but at the fifth stage (linking/association) calls from all DASARs at a site were matched to produce 'call sets' to assess their final localisation. The sixth and seventh stages, bearing and location estimation, estimated a bearing for every call in a given set and quantified the uncertainty of the measurement. Finally, the position of the whale was computed by triangulating the geographic bearings computed previously from matched call sets.

Various methods can be used to detect and classify vocalisations, but the spectrogram correlation is a common choice for studies recognising animal sounds consisting of tones and frequency sweeps (Mellinger & Clark, 2000). Regardless of the method applied, it is important to consider two issues. The first is determining the type(s) of vocalisations to be detected and the amount of variability in those. Secondly, configuring the desired accuracy of detection. The goal is to achieve a trade-off between missed calls (false negatives) and wrong detections (false positives) by configuring the detector's sensitivity or threshold.

Localisation

It is possible to assess the location of a vocalising individual if the used instruments are spaced in a way that two or more can detect it and thus matching time-of-arrival differences. If the hydrophones are deployed far away from one another, they become several single sensors, and matching is not possible. DASARs used in this survey include an omnidirectional pressure sensor and a pair of orthogonal directional sensors. Ultimately, the passive acoustic data collected

can then be used to locate the sources of the recorded calls via two methods: hyperbolic fixing and triangulation. The former involves measuring the time-of-arrival of a sound at the pair of hydrophones with cross-correlation. The latter involves measuring bearings to sound sources from two or more known locations, and then computing the intersections of the bearings. Only the latter is applied in the seven-stage algorithm described in page 19 (Thode et al., 2012). This thesis, however, will not use the localisations assessed by the sensors, but the inclusion of the calls localisations should be considered in future SECR analysis.

1.5.3 Problems Associated with Automated and Manual Data

In the observed automated data, there are a lot of calls detected exclusively in one sensor, i.e., singletons. It is assumed that a large proportion of these singletons are false positives. In the automated data, the amount of singletons is far higher (figure 1.9 a), approximately $\sim$15 times, compared to the manual data. The manual data shares the same problem of having false positives being labeled as true bowhead detections, although to a lesser extent. In addition, the manual data has a second problem concerning the non-independence among sensors caused by human intervention. The non-independence leads to an excess of calls being detected in all DASARs on a site (figure 1.9 b), contrary to the detection pattern in the automated. However, the automated dataset surpasses the problem of non-independence for density estimation and allows big volumes of data. For manual data the proportion of calls detected in 1 to all DASARs is not consistent with the independence of the detection process across DASARs. The independence should result in a decreasing pattern in the number of detections as a function of the number of DASARs in which the detections were made (as shown in figure 1.9 a). On the other hand, the percentage showcased for singletons in 1.9 a) is not assumed to be representative of the decreasing pattern, as the percentage difference from detections made in 1 DASAR to detections made in 2 DASARs is enormous (83.1% to 7.5%). This difference is explained by the large proportion of false positives included in the singletons. The pattern we assume that portrays the reality is best seen in figure 1.10. The visual intuition of this illustrative bar plot, where the singletons are excluded, indicates an exponential decay fitting across the number of calls detected per increasing number of DASARs. It is expected that the number of singletons will be higher than the number of calls detected in 2 DASARs, but not as high as seen in figure 1.9 a). An ad hoc method is tested in the following section 2.5 to assess the model fitting with linear model.

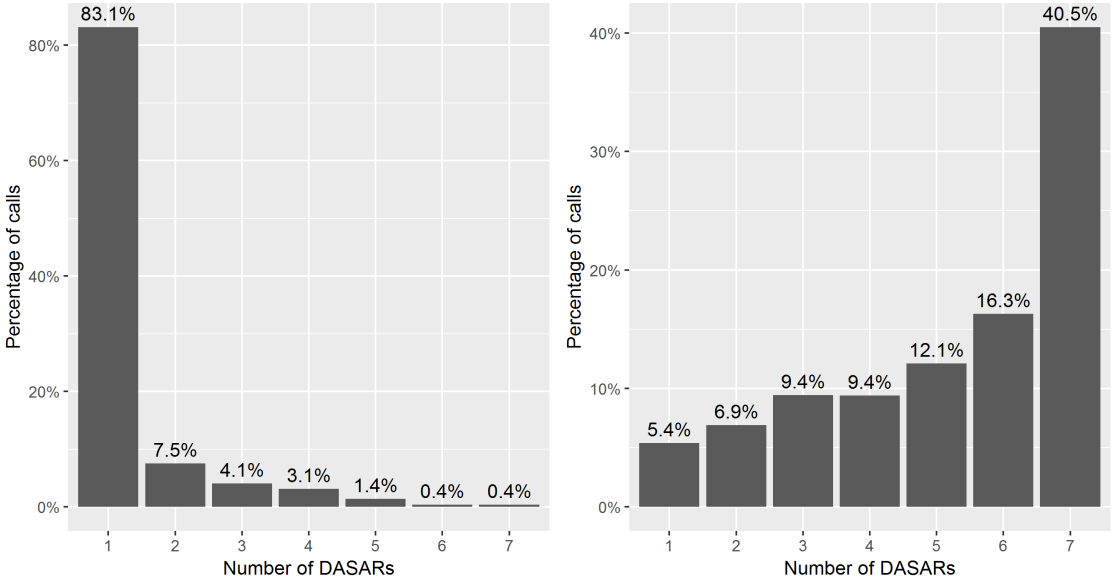

(a) (b)

Figure 1.9: Percentage distribution of calls detected for the modelling dataset, ranging from 1 to 7 DASARs of site 3, year 2013. (a) Proportion of the number of DASARs an automated call was recorded on. (b) Proportion of the number of DASARs a manual call was recorded on. The proportion of singletons for the automated data is 15.389 times higher than the manual data.

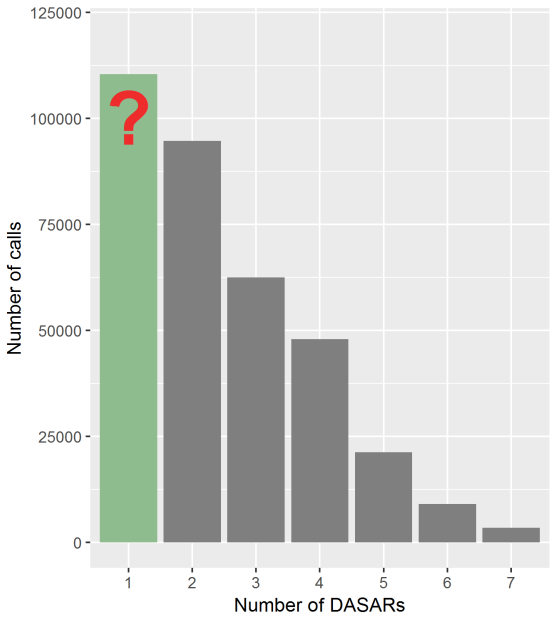

Figure 1.10: Example of the number of calls distribution without the singletons, from 2 to 7 DASARs. The red question mark and green bar indicate a possible higher number of singletons than the one in 2 DASARs according to an exponential decay fitting.

1.6 Main Objectives

An automated dataset will be explored from passive acoustic monitoring composed of five sites and two years (2013 and 2014). This thesis targets the estimation of population density of the BCB bowhead whales with an array of hydrophones recording the detection of bowhead sounds. These detectors operate independently of each other and, being proximity detectors, leave the sound free to be detected by other sensors. The density of sounds (calls/100 km^2) is estimated using a SECR method, and is subsequently converted to a population density (whales/100 km^2 h) using a sound production rate, as explained in equation 1.7.

1.6.1 Solving the Singletons Problem

Induced by the automated detection and classification system used, this data presents an unusually large number of singletons, i.e., detections made in a single hydrophone. Given the hydrophone spacing, and the bowhead call likely sound levels, these are assumed to be mostly false positives, i.e., detections which do not really correspond to bowhead sounds. This leads to severely based density estimates if ignored. This thesis overarching goal is to explore the impact of singletons in SECR density estimates, and to investigate different analysis options that might mitigate their impact on SECR density estimates. Specifically, we propose to:

1. Perform a SECR analysis of every call, including singletons and calls detected more than once, leading to the inclusion of false positives. This should lead to an overestimation of density, as it ignores the underlying problem concerning the singletons;
2. Perform a SECR analysis without singletons, leading to underestimated results, as it removes true bowhead detections;
3. Perform a SECR analysis where a proportion of false positives, $1 - p$, is discarded from the singletons. The expected proportion p of true singletons is obtained by fitting an exponential regression using a linear model to the calls detected in 2, 3, ..., to all DASARs, and predicting the expected number of singletons (only calls detected in a single DASAR). Simply put, the singletons are subsetted with a proportion p. This approach still holds a risk of producing underestimated or overestimated densities;
4. Develop a new likelihood function that accommodates truncation of singletons;
5. Perform a SECR analysis to simulated capture histories. Compare simulated estimates to 'true' estimate to validate which approach (between 1 and 3) is best. Also compare estimates from the observed automated data with estimates from the simulated capture histories, therefore checking for consistency in the estimates produced by our data.

The proposed approaches from 1 to 4 correspond to increasing levels of analysis complexity, but also *a priori* with an increase in the ability to deal with the singletons problem. The last proposed approach involves the simulation of capture histories, which is an important step for the estimates validation method based on the comparison between simulated estimates vs 'true' estimate.

In the next section, the statistical background will address the standard SECR method, the SECR applied to passive acoustics, fitting linear models to the data to execute the 3^{rd} proposed approach, and it will also present the cue rates to convert call densities into population density estimates. The methods will introduce a new SECR likelihood function with truncation of singletons (4^{th} approach), and the data organisation, analysis and estimation of the 1^{st}, 2^{nd}, 3^{rd} and 5^{th} approaches will be thoroughly explained. The estimation of call densities is performed with a standard SECR analysis. Afterwards, the project's results are presented, followed by a discussion and possible ways forward.

Chapter 2

Statistical Background

2.1 Standard SECR Model – Key Notation

A standard SECR likelihood, described in Borchers and Efford (2008), consists of a closed population density being estimated by placing K traps in a region where animals have their home ranges with fixed centres. An animal is then caught in a trap, and remains there until released. Traps are checked in previously chosen time intervals, and trapped animals are marked and released. This is repeated as many times as needed, and after consecutive sampling their complete capture history is known. The period preceding each trap check is named a trapping occasion. It is assumed, initially, that animals are equally at risk of being caught on every trapping occasion.

From a standard survey design, there will be n animals caught in K traps for S trapping occasions. In figure 2.1, there is a single animal i detected in trap k. The k^{th} trap is located at Cartesian coordinates $\mathbf{x}_k$ and traps locations are represented by $\underline{\mathbf{x}} = (\mathbf{x}_1, ..., \mathbf{x}_K)$. $\mathbf{X}$ is the location associated to each animal, and this might be called, for simplicity, as its home range centre.

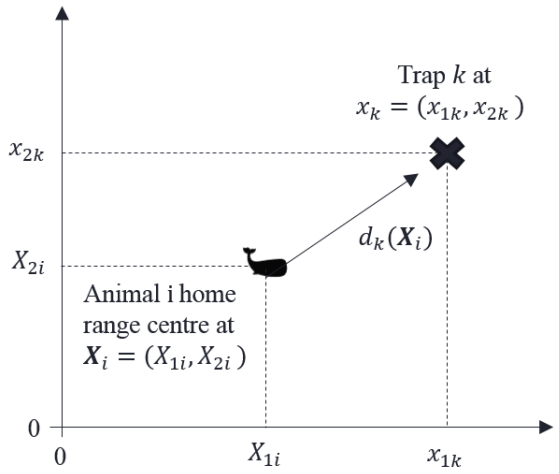

Figure 2.1: Schematic representation of a trap location (black cross), home-range centre location (black whale icon) and distance from trap to centre: $d_k(\mathbf{X}_i)$ is the distance from the i^{th} animal's home range centre at $\mathbf{X}_i$ to the k^{th} trap at x_k.

The capture locations history for the i^{th} animal is $\boldsymbol{\omega}_i = (w_{i1}, ..., w_{is})$. If $w_{is} = k$, then animal i was captured in trap k on occasion s ($s = 1, ..., S$), and $w_{is} = 0$ otherwise. Hence, $w_{i.} = 1$ if animal i was caught on any of the S trapping occasions and $w_{i.} = 0$ otherwise. The probability, $p_{ks}(\mathbf{X};\boldsymbol{\theta})$, represents the probability of detecting an animal with home range centre at $\mathbf{X}$ captured in trap k on occasion s, where $\boldsymbol{\theta}$ is the detection probability parameter vector. As a result, $p_{.s}(\mathbf{X};\boldsymbol{\theta})$ is the probability that an animal is caught in any one of the K traps on occasion s and $p_{.}(\mathbf{X};\boldsymbol{\theta})$ is the probability that is caught at all over the S trapping occasions (see table E.1 in the appendices for a summary of parameters):

$$p_{.}(\mathbf{X}_i;\boldsymbol{\theta}) = P(w_{i.} = 1|\mathbf{X}_i;\boldsymbol{\theta}). \tag{2.1}$$

2.1.1 State and Observation Models

A standard SECR model comprises two submodels: (i) a state model and (ii) an observation model. The state model describes how animal home range centres are distributed in space and the observation model (or spatial detection model) describes how animals are observed in space, conditional on the location of their home range centres. The distances from a particular detector to each home range centre are not observed directly, as the range centres are not known, so DS methods do not apply to this particular data.

The state model (or distribution model) assumes that for the duration of trapping the location of each individual in the population may be summarised by Cartesian x-y coordinates of a point known as home range centre of an animal. The distribution of range centres in the population is usually treated as a homogeneous Poisson point process, where density is the only parameter of interest and is equivalent to the intensity of spatial point process for the home range centres.

The observation model (or capture model) must take into account the properties of each type of detector mentioned in the previous section. The probability that a particular animal i with home range centre $\mathbf{X}_i$ is caught in a trap k, located at $x_k = (x_{1k}, x_{2k})$, is assumed to be a function of the Euclidean distance $d_k(\mathbf{X}_i)$ between animal and trap (Efford et al., 2009).

2.2 SECR Likelihood Formulation

Likelihood with Homogeneous Poisson Density

The likelihood can be simplified when home range centres occur according to a homogeneous Poisson process with rate parameter D. Hence, the likelihood can be written as follows:

$$\begin{aligned}\mathcal{L}(\boldsymbol{\theta}, D|n, \omega_1, ..., \omega_n) &= P(n) \times \binom{n}{n_1, ..., n_C} \prod_{i=1}^{n} \frac{\int_{R^2} P(\omega_i|\mathbf{X};\boldsymbol{\theta}) d\mathbf{X}}{a(\boldsymbol{\theta})} \\ &= \frac{(Da(\boldsymbol{\theta}))^n \exp(-Da(\boldsymbol{\theta}))}{n!} \times \binom{n}{n_1, ..., n_C} \prod_{i=1}^{n} \frac{\int_{R^2} P(\omega_i|\mathbf{X};\boldsymbol{\theta}) d\mathbf{X}}{a(\boldsymbol{\theta})} \end{aligned} \tag{2.2}$$

where the first term $P(n)$ is the probability of observing exactly n capture histories (each animal i with an associated capture history ω_i) that follows a Poisson distribution, $\boldsymbol{\theta}$ is the vector of detection function parameters (described below), and D is the density parameter. As described in Efford et al. (2009), we can define an area a as the effective detection area. This assumes the area presents a uniform distribution of animals:

$$a(\boldsymbol{\theta}) = \int_{R^2} p_{\cdot}(\mathbf{X};\boldsymbol{\theta}) d\mathbf{X}. \tag{2.3}$$

The probability $P(\omega_i|\mathbf{X};\boldsymbol{\theta})$ is the probability of the capture history for an animal i with

home range centre at $\mathbf{X}$ and vector of detection function parameters $\boldsymbol{\theta}$. Therefore, the probability of an animal being captured at least once over S occasions depends on the distances $d_k(\mathbf{X})$ to each of the K traps:

$$p_{\cdot}(\mathbf{X};\boldsymbol{\theta}) = 1 - \prod_{s=1}^{S}\prod_{k=1}^{K}(1 - p_s(d_k(\mathbf{X};\boldsymbol{\theta}))). \tag{2.4}$$

The likelihood with inhomogeneous poisson density is described in the appendices in the section B.

Capture Probability Models – Detection Functions

The vector $\boldsymbol{\theta}$ contains parameters that control the overall efficiency of detection and also its spatial scale. It is believed the efficiency will increase with home range size. There are several suitable detection functions p_c – some examples are shown in table 2.1. These detection functions use the independent parameters g_0 for overall efficiency of detection and σ for spatial scale. The term $P(\omega_i|\mathbf{X};\boldsymbol{\theta})$ is defined by:

$$P(\omega_i|\mathbf{X};\boldsymbol{\theta}) = \prod_{s=1}^{S}\prod_{k=1}^{K} p_{ks}^{\delta_{iks}}(1 - p_{\cdot s})^{1-\delta_{i\cdot s}} \tag{2.5}$$

where $p_{ks} = p_s(d_k(\mathbf{X});\boldsymbol{\theta})$ is the probability of detection at k trap on occasion s, $\delta_{iks} = 1$ if animal i was caught in trap k on occasion s and $\delta_{i\cdot s} = 1$, if $\sum_{k=1}^{K}\delta_{iks} > 0$, and $\delta_{i\cdot s} = 0$ otherwise.

Table 2.1: Example of three candidate detection functions, p_c, for SECR models. The parameter g_0 is common to all functions and represents the intercept, i.e., the probability of detection at a single trap placed in the centre of the home range. d is the distance between an animal home range centre and a trap. σ is the spatial scale parameter and their values are not comparable between functions.

Detection function	p_c	Parameters $\boldsymbol{\theta}$
Half-normal	$p_s = g_0 exp(\frac{-d^2}{2\sigma^2})$	g_0, σ
Hazard rate	$p_s = g_0[1 - exp\{-(\frac{d}{\sigma})^{-b}\}]$	g_0, σ, b
Negative exponential	$p_s = g_0 exp(\frac{-d}{\sigma})$	g_0, σ

2.3 SECR applied to Passive Acoustics

In passive acoustics, the notion of home range disappears, and the notion of animal movement is replaced by sound transmission. Similar to the key notation described previously with a standard SECR, but now with proximity detectors, we have n calls recorded in K sensors. The k^{th} sensor is located at Cartesian coordinates $\mathbf{x}_k$ and sensors locations are represented by $\underline{\mathbf{x}} = (\mathbf{x}_1, ..., \mathbf{x}_k)$. $\mathbf{X}$ is the location associated to each vocalisation. The sensors record the

presence of a vocalisation at or near each sensor (see figure 2.2), leaving the same vocalisation free to be detected in other sensors.

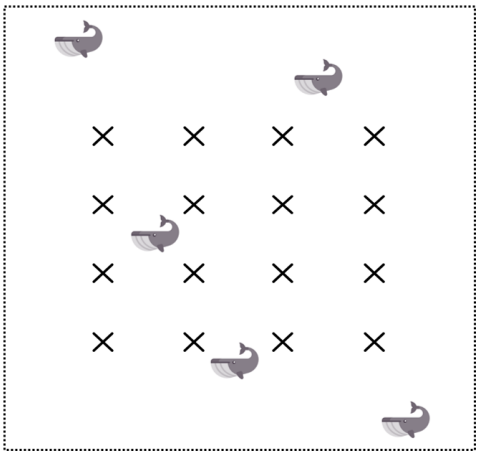

Figure 2.2: Schematic representation of a spatial trapping grid represented by 'X' detectors relative to the location of a whale vocalisation pictured by whale icons.

The probability that a particular vocalisation i with location $\mathbf{X}_i$ is recorded in sensor k, located at $x_k = (x_{1k}, x_{2k})$, is assumed to be a function of the Euclidean distance $d_k(\mathbf{X}_i)$ (Efford et al., 2009) (see example of figure 2.3). Conditional on the whale location, the detection of sounds in each sensor is assumed independent. Each recorded vocalisation is attributed its own capture history from an array of K sensors.

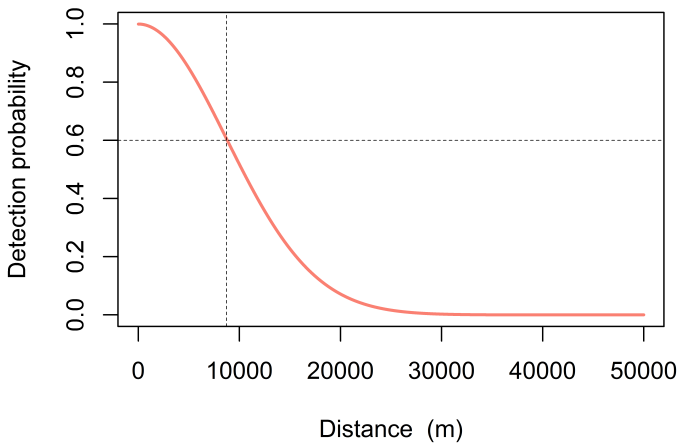

Figure 2.3: Example of a detection function (half-normal distribution). The vertical line indicates σ of the example model (~8.7 km), meaning the probability of a call produced at that distance from a sensor is about 0.6 (horizontal line) and a near zero chance of detection beyond ~30 km.

2.4 Idea behind the Likelihood with Truncation of Singletons

Conn et al. (2011) developed an approach that recognises fundamental differences between individuals of the same population. The 'multi-sample availability' approach claims that in the presence of an open system, a superpopulation is consisted of residents and transients. In a superpopulation, residents are those that used the study area almost exclusively

during the study, and transients are those that passed through the study area but did not remain long. But what defines not remaining long enough? According to the article, it is assumed that transients are present in the study area for only one sampling period. The difficulty comes when ensuring the transients are only available to be detected once. This assumption is difficult to verify, as in some cases transients will likely remain longer in the study area. An estimator exclusively for resident abundance that conditions on individuals observed at least k times is presented below.

A SECR dataset has two types of calls: (i) singletons (calls detected in a single sensor) and (ii) calls detected in more than one sensor. However, singletons contain false positives and detections coming from the animals of interest. Having both detections labeled as singletons imposes a restriction not covered in the SECR likelihood functions described previously in the sub-section 2.2. According to our study, we considered the transients as singletons, and residents as calls detected in more than one sensor (non-singletons). Hence, the probability of the capture history should take into consideration a study design where the singletons are truncated. So by conditioning out calls recorded $k-1$ times (if we want to censor singletons, $k=2$), it becomes less restrictive. Nonetheless, inference is exclusive to resident density, i.e., to the density of calls recorded in more than one sensor. Considering only a capture-recapture approach, the likelihood function for a population censoring singletons is as follows:

$$\mathcal{L} \propto \prod_{i=1}^{M_k} \prod_{t=1}^{T} \frac{(H_{it}P_{it} + (1-H_{it})(1-P_{it}))}{P(\text{call } i \text{ detected at least } k{=}2 \text{ times})}, \tag{2.6}$$

where M_k is the total number of distinct calls encountered at least k times in the CR study; T is the number of sampling periods; H_{it} is the indicator variable which takes on a value of 1 if call i is encountered in sampling period t and 0 otherwise; P_{it} is the probability that call i is detected at time t given that it is available to be detected; and P(call i detected at least $k=2$ times) $= 1 - P_0 - P_1$. P_0 is the probability of recording a call in 0 sensors (in other words, is not recorded at all), and P_1 is the probability of recording a call in only one sensor. P_0 is as follows:

$$\prod_{t=1}^{T}(1-P_{it}) \tag{2.7}$$

and P_1 (probablity of being detected 1 time):

$$P_{i1}\prod_{t=2}^{T}(1-P_{it}) + (1-P_{i1})P_{i2}\prod_{t=3}^{T}(1-P_{it}) + ... + \prod_{t=1}^{T-1}(1-P_{it})P_{iT}. \tag{2.8}$$

2.5 Fitting Linear Models

Fitting a linear model is a solution to fix the problem of having an excessive number of singletons in our data. By fitting an exponential function to the data, we can reduce the amount of singletons according to a proportion. The exponential decay is fitted to the number

of calls recorded in 2, 3, ..., to all DASARs against the number of existing DASARs. A number of calls recorded in just a single DASAR is then predicted from the fitted model. Afterwards, this predicted number of singletons is divided by the original number of singletons in our data. This results in a proportion p of singletons estimated to come from the animal of interest. This proportion will later be used to discard false positives with a proportion of $1 - p$ from the singletons.

A linear model (Rencher & Schaalje, 2008) describes a continuous or categorical dependent variable as a function of one (simple linear model) or more (multiple linear model) discrete or continuous independent variables. Linear models embody both systematic ($\beta_0 + \beta_1 x_1 + \beta_2 x_2 + ... + \beta_k x_k$) and random (error) components (ε), such as the following model of the form:

$$y = \beta_0 + \beta_1 x_1 + \beta_2 x_2 + ... + \beta_k x_k + \varepsilon. \tag{2.9}$$

In the multiple linear model shown in equation 2.9, y is the dependent or response variable and $x_1, x_2, ..., x_k$ are the independent or predictor variables. The constant β_0 represents the intercept; $\beta_j, j = 1, 2, ..., k$, is the regression coefficient and corresponds to the rate of change in y for one unit change in the respective j^{th} regressor, assuming the remaining $k - 1$ regression coefficients are fixed. The random variable ε is the error term, representing random fluctuations, measurement error, or the effect of factors outside of our control.

As stated on the previous section, there is a high proportion of singletons that we assume most are false positives. In order to predict how many singletons should actually be accounted, one can fit an exponential decay to the number of calls recorded in more than one DASAR, which translates to a simple linear regression model. According to our data, a simple linear regression model can be written as:

$$y_i = \beta_0 + \beta_1 x_i + \varepsilon_i, \tag{2.10}$$

with x being the number of DASARs, y the number of calls detected, and $i = 1, 2, ..., n$, n being the total number of DASARs in operation. Site 4 has $n = 13$ DASARs, and sites 2, 3 and 5 have $n = 7$. The term 'linear' indicates the model 2.10 is linear in terms of the expected value of y_i (which is addressed in the assumptions below). It is assumed that y_i and ε_i are random variables and the values of x_i are known constants. The residuals are assumed to follow a normal distribution.

The model has the following assumptions:

1. $E(\varepsilon_i) = 0$ for all $i = 1, 2, ..., n$, or, equivalently, $E(y_i) = \beta_0 + \beta_1 x_i$;
2. $var(\varepsilon_i) = \sigma^2$ for all $i = 1, 2, ..., n$, or, equivalently, $var(y_i) = E[y_i - E(y_i)]^2 = E(y_i - \beta_0 - \beta_1 x_i)^2 = E(\varepsilon_i^2) = \sigma^2$;
3. $cov(\varepsilon_i, \varepsilon_j) = 0$ for all $i \neq j$, or, equivalently, $cov(y_i, j_i) = 0$.

Under these assumptions, the first implies that y_i depends only on x_i and that all other variation in y_i is random; assumption 2 that the variance of ε (or y) does not depend on the

values of x_i (number of DASARs), i.e., there is homoscedasticity or, in other words, it has a constant variance (σ^2) at every value of x_i. Under assumption 3, the y variables are uncorrelated with each other, i.e., there is no auto-correlation between the number of calls recorded.

2.6 Cue Rates to Achieve Population Density Estimates

A call estimate needs to be divided by a cue rate in order to obtain a density estimate, as explained in sub-section 1.4.1. This matter is significantly harder as there are no known bowhead cue rates, neither in the BCB, our geographic interest. The used cue rates are the output of Susanna Blackwell's work (unpublished). The cue rates are presented in table 2.2 and are used later to convert density of cues to density of animals. Because the survey did not cover the entire migration season, a solution is to assume three different scenarios: that 25%, 35%, and 45% of the BCB population was missed.

Table 2.2: Cue rates (calls/h) for sites 2, 3, 4 and 5 of year 2013 and 2014 considering a speed of 4–5 km/h.

		Sites			
Year	Missing percentage of migrating whales	2	3	4	5
2013	25%	4.9	2.5	6.2	2.1
	35%	6.0	3.1	7.6	2.5
	45%	7.7	4.0	9.8	3.2
2014	25%	2.1	1.8	2.7	2.9
	35%	2.5	2.2	3.4	3.5
	45%	3.2	2.8	4.3	4.5

Chapter 3

Methods

3.1 SECR Likelihood with Truncation of Singletons – Homogeneous Poisson process

The development hereby described is largely based on Efford et al. (2009) already presented in section 2.2. By incorporating a spatial context, it is assumed calls are distributed in 2-D space according to a homogeneous Poisson process where they are potentially detected on K sensors. Detection probability is a function of distance between call and sensor, and is denoted $p(d_k(\mathbf{X};\boldsymbol{\theta}))$ (equivalently $p(d_k(\mathbf{X})|\boldsymbol{\theta})$) where $d_k(\mathbf{X})$ is the distance between the k^{th} sensor and the call located at position X, and $\boldsymbol{\theta}$ is a vector of parameters.

In this thesis, we will only retain calls that are recorded in more than one sensor (i.e., $k = 2$, analogous to the notation from Conn et al. (2011)). Contrary to the conventional SECR likelihood of Efford et al. (2009) that had S multiple trapping occasions, in this particular study a single occasion ($S = 1$) is considered. Let K be the number of DASARs recording on $S = 1$ single occasion, n^* be the number of calls recorded in more than one sensor, so that ω^* is defined as the capture history matrix, which has one row for each i call that is recorded in more than one sensor and one column for each sensor; each cell is a '1' if the sensor recorded the call, and a '0' otherwise. ω^* has n^* rows and K columns. Let $\omega_i = \sum_{k=1}^{K} \omega_{ik}^*$, i.e., the number of sensors in which a call is detected.

The likelihood is given by:

$$\begin{aligned} \mathcal{L}(\boldsymbol{\theta}, D|n^*, \omega^*) &= P(n^*|\boldsymbol{\theta})P(\omega^*|n^*, \boldsymbol{\theta}) \\ \equiv \mathcal{L}(\boldsymbol{\theta}, D|n^*, \omega_1^* > 1, ..., \omega_{n^*}^* > 1) &\equiv P(n^*|\boldsymbol{\theta})P(\omega_1^*, ..., \omega_{n^*}^*|\omega_1 > 1, ..., \omega_{n^*} > 1, \boldsymbol{\theta}). \end{aligned} \tag{3.1}$$

The first term in (3.1) is defined as:

$$\frac{(Da^*(\boldsymbol{\theta}))^{n^*} \exp(-Da^*(\boldsymbol{\theta}))}{n^*!}, \tag{3.2}$$

where the effective sampling area, $a^*(\boldsymbol{\theta})$, is large enough that no detections can occur outside of it, and is as follows:

$$a^*(\boldsymbol{\theta}) = \int_{R^2} p^*(\mathbf{X};\boldsymbol{\theta}) d\mathbf{X}, \tag{3.3}$$

with

$$p^*(\mathbf{X};\boldsymbol{\theta}) = 1 - P_0 - P_1 = 1 - P(\omega_i = 0|\mathbf{X};\boldsymbol{\theta}) - P(\omega_i = 1|\mathbf{X};\boldsymbol{\theta}), \tag{3.4}$$

where $p^*(\mathbf{X};\boldsymbol{\theta})$ is the probability of recording a call in at least 2 sensors, i.e., recording a non-

singleton. P_0 is described as:

$$P_0 = \prod_{k=1}^{K} \left(1 - p(d_k(\mathbf{X};\boldsymbol{\theta}))\right). \tag{3.5}$$

The probability of recording a call in one sensor corresponds to the sum of the probabilities of it being recorded in the first sensor, but not in the remaining sensors, plus the probability of it being recorded in the second sensor, but not in the others, and so on until all K sensors are taken into account:

$$\begin{aligned} P_1 = p(d_1(\mathbf{X};\boldsymbol{\theta})) \prod_{k=2}^{K} (1 - p(d_k(\mathbf{X};\boldsymbol{\theta}))) + (1 - p(d_1(\mathbf{X};\boldsymbol{\theta})))p(d_2(\mathbf{X};\boldsymbol{\theta})) \prod_{k=3}^{K} (1 - p(d_k(\mathbf{X};\boldsymbol{\theta}))) \\ +(1 - p(d_1(\mathbf{X};\boldsymbol{\theta})))(1 - p(d_2(\mathbf{X};\boldsymbol{\theta})))p(d_3(\mathbf{X};\boldsymbol{\theta})) \prod_{k=4}^{K} (1 - p(d_k(\mathbf{X};\boldsymbol{\theta}))) \\ +... + \prod_{k=1}^{K-1} (1 - p(d_k(\mathbf{X};\boldsymbol{\theta})))p(d_K(\mathbf{X};\boldsymbol{\theta})). \end{aligned} \tag{3.6}$$

The previous development of the probability can be summarised as:

$$P_1 = P(\omega = 1|\mathbf{X};\boldsymbol{\theta}) = \sum_{k=1}^{K} \left[p(d_k(\mathbf{X};\boldsymbol{\theta})) \prod_{m=1}^{K} \left\{ I(m \neq k) \left(1 - p(d_m(\mathbf{X};\boldsymbol{\theta}))\right) \right\} \right] \tag{3.7}$$

where $I(m \neq k)$ is an indicator function that has value '1' if $m \neq k$, and '0' otherwise.

The second term in (3.1) is defined as:

$$\binom{n^*}{n_1, ..., n_{C^*}} \prod_{i=1}^{n^*} \frac{\int_{R^2} P(\omega_i^*|\omega_i^* > 1; \mathbf{X};\boldsymbol{\theta}) d\mathbf{X}}{a^*(\boldsymbol{\theta})}, \tag{3.8}$$

the observed capture histories ω_i for calls $i = 1, ..., n^*$; $n_1, ..., n_{C^*}$ are the frequencies in which each of the unique recorded calls in at least 2 sensors were detected. Thus, $P(\omega_i^*|\omega_i^* > 1; \mathbf{X};\boldsymbol{\theta})$ is the probability of occurring a capture history ω_i^* conditional on recording a call i in at least 2 sensors, regarding a location in the habitat mask, X, and also $\boldsymbol{\theta}$, a vector of parameters of interest. $\binom{n^*}{n_1,...,n_{C^*}}$ is the associated multinomial coefficient; C^* represents the number of unique capture histories and accounts for the frequencies of each $1, ..., C^*$ capture histories. As an example, consider a survey with 3 sensors (A, B and C). For each recorded call there are seven possible capture histories:

Table 3.1: Example of a survey with 3 sensors (A, B and C), resulting in seven possible types of capture history.

ID of capture history (Type of capture history)	A	B	C
1 (Singleton)	1	0	0
2 (Singleton)	0	1	0
3 (Singleton)	0	0	1
4 (Non-singleton)	1	1	0
5 (Non-singleton)	0	1	1
6 (Non-singleton)	1	0	1
7 (Non-singleton)	1	1	1

In this particular case, $C^* = 4$ (includes the capture history ID number 4, 5, 6 and 7), where n_1, n_2, n_3, and n_{C^*} are the number of recorded calls in more than one sensor with the fourth, fifth, sixth, and seventh type of capture history, respectively. From the equation 3.8, it is also defined:

$$P(\omega_i^*|\omega_i^* > 1; \mathbf{X}; \boldsymbol{\theta}) = \frac{\prod_{k=1}^{K} p(d_k(\mathbf{X}; \boldsymbol{\theta}))^{\omega_{ik}} (1 - p(d_k(\mathbf{X}; \boldsymbol{\theta})))^{(1-\omega_{ik})}}{p^*(\mathbf{X}; \boldsymbol{\theta})}, \tag{3.9}$$

where ω_{ik} is '1' if call i was detected in k sensor, and '0' otherwise. Since hydrophones operate independently, we can calculate those probabilities as shown in the numerator. Note once again that we only have one occasion in the product terms of the equations listed above (3.5,3.7 and 3.9), because we are not segmenting our sampling periods and the PAM survey is continuous from the day of deployment until the sensors retrieval. Here we truncated singletons, but this could be made more general. The equations 3.4, 3.5 and 3.7 would change if we truncated differently – e.g., keeping only recorded calls on more than 2 sensors, 3 sensors, and so forth. Disregarding calls recorded in increasing number of sensors will reduce the precision on parameter estimates, because true detections are eliminated from the data.

The likelihood 3.1, although expressed in terms of integrals over a plane, is in practice approximated by summing over a habitat mask. Each grid cell contained in the habitat mask has a known area A. The mask has a buffer of 100 km created with the R package *secr*, and is constrained at south corresponding to the Alaskan coastline (see figures F.5 and F.6 in the appendices). The habitat mask corresponds to a grid that extends 'buffer' metres north, south, east and west of the detectors (Efford, 2017). For simplicity, it is assumed D as homogeneous, meaning each cell has the same weight in the calculation of the likelihood.

The density D and vector of parameters $\boldsymbol{\theta}$ can be estimated by numerically maximising the full likelihood 3.1 with respect to the parameters. Because D is assumed homogeneous, an alternative described in Borchers and Efford (2008) is to maximize the conditional likelihood:

$$\mathcal{L}(\boldsymbol{\theta}|n^*,\omega^*) \propto a^*(\boldsymbol{\theta})^{-1} \prod_{i=1}^{n^*} \int_{R^2} P(\omega_i^*|\omega_i^* > 1; \mathbf{X}; \boldsymbol{\theta}) d\mathbf{X} \tag{3.10}$$

to obtain estimates $\boldsymbol{\theta}$, and therefore $\hat{a} = a(\hat{\boldsymbol{\theta}})$. D is then estimated using the Horvitz-Thompson-like estimator $\hat{D} = \frac{n}{\hat{a}}$ (Horvitz & Thompson, 1952).

The likelihood with truncation of singletons with an inhomogeneous Poisson process is described in the appendices section C. A log-likelihood function with truncation of singletons was also developed in section D.1 in the appendices.

3.2 Density Estimation with Different Approaches

The estimation of call densities is performed with a standard SECR analysis, assuming the detection function has a half-normal distribution. Call density, $\hat{D}_s$, from the observed automated data will be estimated according to three different approaches (terms in bold along this section are approaches):

1. **'All calls included'** approach, i.e., ignores the singletons problem and evaluates all calls;
2. **'No singletons'** approach, removes all singletons from the data;
3. **'Proportion of singletons'** approach, where a proportion of false positives, $1 - p$, is discarded from the singletons.

These three approaches correspond to the 1^{st}, 2^{nd} and 3^{rd} points listed in the 'Main Objectives' sub-section 1.6. The automated data was resampled 50 times for each approach.

The dilemma with the first approach is that it completely ignores the singletons problem, as false positives are included in the analysed data. Looking at figure 1.9 a), singletons represent the majority of the recorded calls (83.1%). Based on the assumption that the majority of singletons are false positives, the existence of such high percentage of singletons will certainly give us inaccurate and overestimated call densities, and consequently produce overestimated population densities.

The second approach removes most false positives, but at the cost of also removing good detections – the singletons that really correspond to bowhead sounds. By doing so, we expect an underestimation of density.

The third approach is a heuristic way of uncovering how many true singletons exist. After fitting an exponential decay to the number of calls recorded in 2, 3, ..., to all DASARs against the number of existing DASARs, we can extrapolate the number of calls recorded in just a single DASAR. Thereafter, it is calculated the proportion of expected singletons by dividing its predicted value (revealed in the linear model) by the existing number of singletons. This proportion will be used to randomly discard $1 - p$ false positives from the singletons without replacement.

The first, second and third approaches will be tested and analysed with the function *secr.fit* from the R package *secr* according to the likelihood function in 2.2. The resulting estimates will be in units of number of calls/100 km^2. Sites 2, 3, 4 and 5 were assessed, except site 1 that only had three DASARs. Site 1 was not subjected to the same analysis, as it was not possible to fit an exponential decay model to predict singletons, because we would only have two data points per year, as explained in the following section 4. Between these three approaches, the ad hoc analysis of the third approach is assumed to be the most reliable.

The fourth approach in the 'Main Objectives' sub-section 1.6 was not implemented with the automated data, and therefore no population densities with **truncation of singletons** are presented. In case of successful implementation, the resulting population densities would be the most accurate considering the perils of all approaches previously described. However, the population densities from truncation of singletons would only reflect the non-singletons density. A draft R script was compiled and requires some improvement (see sub-section G in the appendices).

The goal of the fifth and last point in the listed objectives is to compare simulated density estimates according to different approaches, and assess the percentage bias from the 'true' estimate. The approach that resulted in an estimate with a lower percentage bias serves as a means to validate which approach is best. Validation means that a model is acceptable for its intended use (Rykiel Jr, 1996). Validation under this thesis ecological problem is deciding if the SECR model according to a certain approach is acceptable to produce reliable call densities that are later used to convert to population densities, i.e., whether the model mimics the 'real world' well enough and produces density estimates closer to 'reality', although 'reality' is unknown. Fifty simulation runs were completed for each one of the three approaches, as well for the 'true' scenario. The 'true' density estimate is set to D = 100 animals/100 km ^{2}, and the parameter values are set to $g_0 = 1$, $\sigma = 8766.5$ m (mean value of the median values in table 4.3 and 4.4 for all sites and years), and 100 km of buffer. Besides the simulations for validation purposes, a hundred simulated capture histories were also generated for consistency checks between estimated densities from the automated data and from simulated data. The simulated capture histories are generated with the *sim.capt* function from the R package *secr*, with the intercept, g_0 set as 1. The σ for each site is set to be equivalent to the estimated $\hat{\sigma}$ from the automated data with the 'proportion of singletons' approach.

For comparison purposes, there are two types of simulated data:

(a) data with a large number of singletons and

(b) data without forcing a large number of singletons.

The a) simulated data aims to mimic the detection process across DASARs from our data that is responsible for the large number of singletons. The b) simulated data aims to produce 'free-of-predefined-constraints' capture histories, i.e., without forcing an excessive number of singletons. Besides the two previous approaches ('no singletons' and 'proportion of singletons'), a new approach is applied to the simulated data: **'no transformation'**. Type a) will be subjected to the first two approaches, and only type b) to the 'no transformation'. This latter approach indicates no subset or transformation performed to the simulated data.

The 'no transformation' performed to the simulated data can be seen as equivalent to the 'all calls included' approach applied to the automated data, since no data manipulation is executed. However, the approaches are named differently to mark a clear distinction between the type of data they are applied to. Specifically, the 'no transformation' is only applied to data free of limitations (i.e., without forcing the singletons problem), and the 'all calls included' is applied to data with an excessive number of singletons.

The process of consistency check relies on the comparison of the mean population density values from the automated vs simulated data. If the automated data estimates fall between the upper and lower bound of the simulated confidence interval, then the density estimates are consistent. The a) type of simulated data is subsetted according to the 'no singletons' approach and a 95% confidence interval is constructed. It is verified if the mean from the automated data with the same approach is contained within the CI. The same procedure is executed to the 'proportion of singletons' approach. Furthermore, a general comparison can be made regarding the absolute differences between densities of the automated and simulated data for all approaches. This general comparison is helpful to provide us some insights into the data. The only consistency check points can be made as seen in table 3.2.

Table 3.2: Types of data and approaches that are directly compared for consistency purposes are marked as 'Check for consistency'. Blank spaces are for general comparisons.

		Automated data		
Simulated data	Approach	All calls	No singletons	Proportion of singletons
Type a) simulated data	No singletons		Check for consistency	
	Proportion of singletons			Check for consistency
Type b) simulated data	No transformation			

The call densities are, afterwards, converted to population densities, $\hat{D}$, with the help of cue rates of the BCB population of bowhead whales.

3.3 Some Considerations on Data Organisation and Analysis

The raw automated data from site 2, 3, 4 and 5 for each year (2013 and 2014) were organised in a TSV (tab-separated format) file format. Site 1, with only three DASARs, was not subjected to the same analysis, as explained in the previous sub-section.

The TSV files were rearranged in matrix tables in a configuration explained in section A in the appendices. The aim is to organise the raw data into a matrix with each recorded call per row and three columns associated to it: DASAR ID, x coordinate, and y coordinate. Only calls recorded in more than one DASAR had the x-y coordinates information. It is not relevant that the singletons do not have x-y coordinates information, as for the SECR analysis the only necessary information are the DASAR IDs to construct the capture history for each call. This matrix is an object named *data*. The matrix was created and then dissected through a developed function *func_ resample* (see section D in the appendices) to provide us insightful information about the calls recorded in each site/year. The input for this function is described in the same section D. The output is as follows:

1. Integer object *count* with the number of calls detected in 1, 2, 3, ..., to all DASARs from the original automated data (prior to resampling);
2. List with n *data* objects (n equals the number of resamples the user requested) for the 'all calls included' approach;
3. List with n *data* objects for the 'no singletons' approach;
4. List with n *data* objects for the 'proportion of singletons' approach;
5. Data frame with the mean values, lower CI, and upper CI with the number of calls detected in 1, 2, 3, ..., to all DASARs for each approach;
6. Data frame with the mean values, lower CI, and upper CI with the number of calls detected in A, B, C, ..., to all DASARs for each approach;
7. Vector with the total number of recorded calls a resample had. Each vector corresponds to an approach;
8. Numeric object p, as the proportion of true singletons from the linear model;
9. Saves four '.png' graphs in a chosen working directory: linear model to predict the number of singletons; percentage distribution of number of calls detected per number of DASARs without applying any approach; percentage distribution of number of calls detected per number of DASARs with the 'proportion of singletons' approach; and frequency of calls detected per day from one resample.
10. Prints the measured execution time of the function, as well as the execution date.

The resampling was performed 50 times for each approach (totaling 150 *data* objects). Each *data* matrix is subjected to a standard SECR analysis to estimate the call density with a half-normal distribution detection function. Additionally, as explained in the input for this function, only 0.5% of the automated data was analysed for each site/year, since the raw data totaled more than 13 million recorded calls for all sites/years. However, the population densities presented in the results section are converted to reflect 100% of the total calls detected.

Chapter 4

Results

The automated data contained 13,272,624 calls for sites 1 to 5 and for years 2013 and 2014 (table 4.1). Site 1 only had three DASARs; sites 2, 3 and 5 had seven DASARs; and site 4 was composed of thirteen DASARs. In site 4, two of the sensors had bad bearings, and for that reason a call could only be detected in a maximum of 11 DASARs. The spatial distribution of 0.5% of all calls over the Alaskan coast is portrayed in figure 4.1. Only non-singletons are displayed in figure 4.1, as it is required at least two DASARs detecting the same call for localisations to be assessed.

The 95% confidence intervals and mean number of calls detected are presented in tables E.2, E.3, and E.4 in the appendices with three approaches: 'all calls included', 'no singletons', and 'proportion of singletons', respectively. The values exhibited in these tables result from 50 resamples of the automated data where only 0.5% of calls were evaluated.

The following sub-sections will guide the reader through the proposed solution to evaluate how many calls should be considered as true singletons (fitting linear models); the call density estimates and population density estimates resulted from the automated data will be calculated according to three approaches ('all calls included', 'no singletons', and 'proportion of singletons'); and, ultimately, simulated estimates will be compared to validate which approach is best.

Table 4.1: Number of calls recorded in one or multiple DASARs.

		Number of DASARs											
Site	Year	1	2	3	4	5	6	7	8	9	10	11	Total
1	2013	347,069	44,006	32,227	–	–	–	–	–	–	–	–	423,302
2	2013	838,871	57,285	39,606	32,159	24,818	17,160	1,852	–	–	–	–	1,011,751
3	2013	1,271,860	114,693	62,523	47,903	21,201	6,073	5,381	–	–	–	–	1,529,634
4	2013	3,000,810	254,557	90,823	61,055	45,129	36,761	31,382	26,743	19,398	2,564	1,372	3,570,594
5	2013	1,203,756	132,898	68,986	34,823	9,654	4,602	2,716	–	–	–	–	1,457,435
1	2014	181,468	20,878	15,914	–	–	–	–	–	–	–	–	218,260
2	2014	531,312	37,465	25,665	20,735	13,737	9,855	1,641	–	–	–	–	640,410
3	2014	948,215	56,809	38,100	29,889	26,535	25,685	22,670	–	–	–	–	1,147,903
4	2014	1,895,943	168,116	58,407	39,547	27,710	20,746	16,270	13,021	10,768	8,745	4,165	2,263,438
5	2014	837,666	55,348	36,605	28,361	24,248	17,360	10,309	–	–	–	–	1,009,897

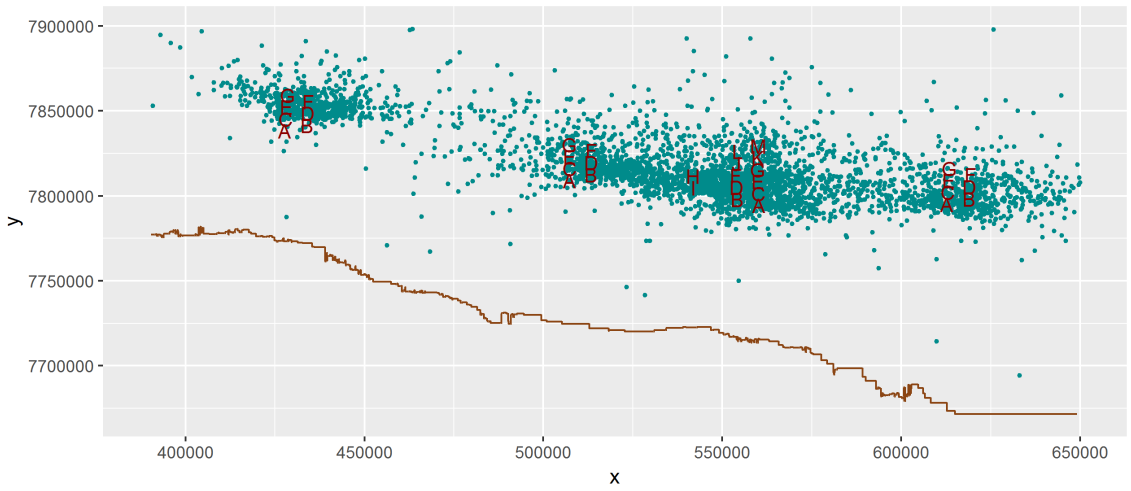

(a)

(b)

Figure 4.1: Spatial distribution of calls recorded in more than one DASAR for each site. Estimated call locations are represented by blue dots (in x-y coordinates), DASARs are represented by red letters (A-G or A-M), and the brown line illustrates the Alaskan coast. (a) Sites 2, 3, 4, 5, year 2013 (left to right). (b) Sites 2, 3, 4, 5, year 2014 (left to right).

4.1 Fitting Linear Models: How Many True Singletons Are There?

The proportion of false positives is higher than one would expect with all sites for both years showing >80% of singletons (see figures 4.2 and 4.3). A reasonable amount of singletons would be less than 50% of the total data, presenting a smooth drop from the number of detected singletons to calls detected in 2 DASARs, much like seen in figure 1.10, with the green bar displayed in the figure being the expected number of singletons. A proposed solution is to analyse the overall trend from this dataset by reducing the amount of singletons according to a proportion. This proportion is generated from a regression analysis fitting an exponential function to our data.

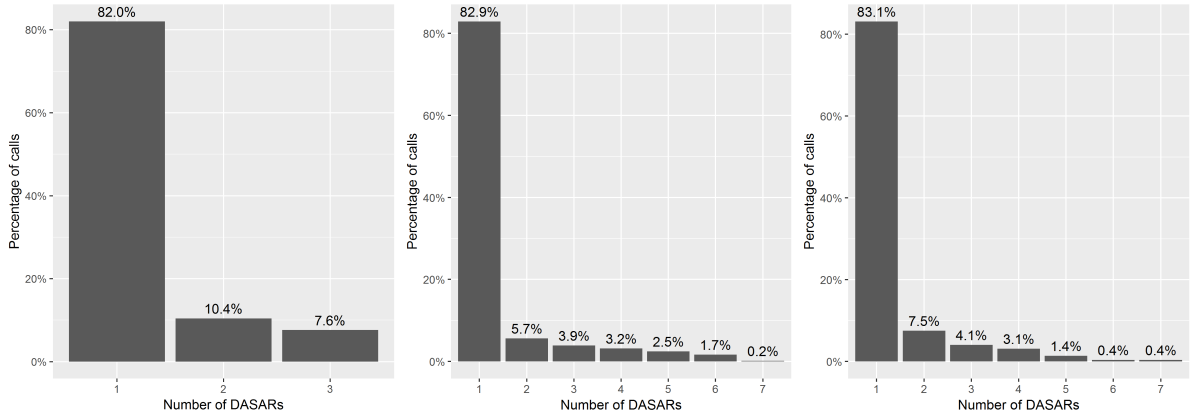

Figure 4.2: Distribution of the number of calls that were detected at exactly k DASARs (k = 1,..., 11) in each site. (a) Site 1, year 2013. (b) Site 2, year 2013. (c) Site 3, year 2013. (d) Site 4, year 2013. (e) Site 5, year 2013.

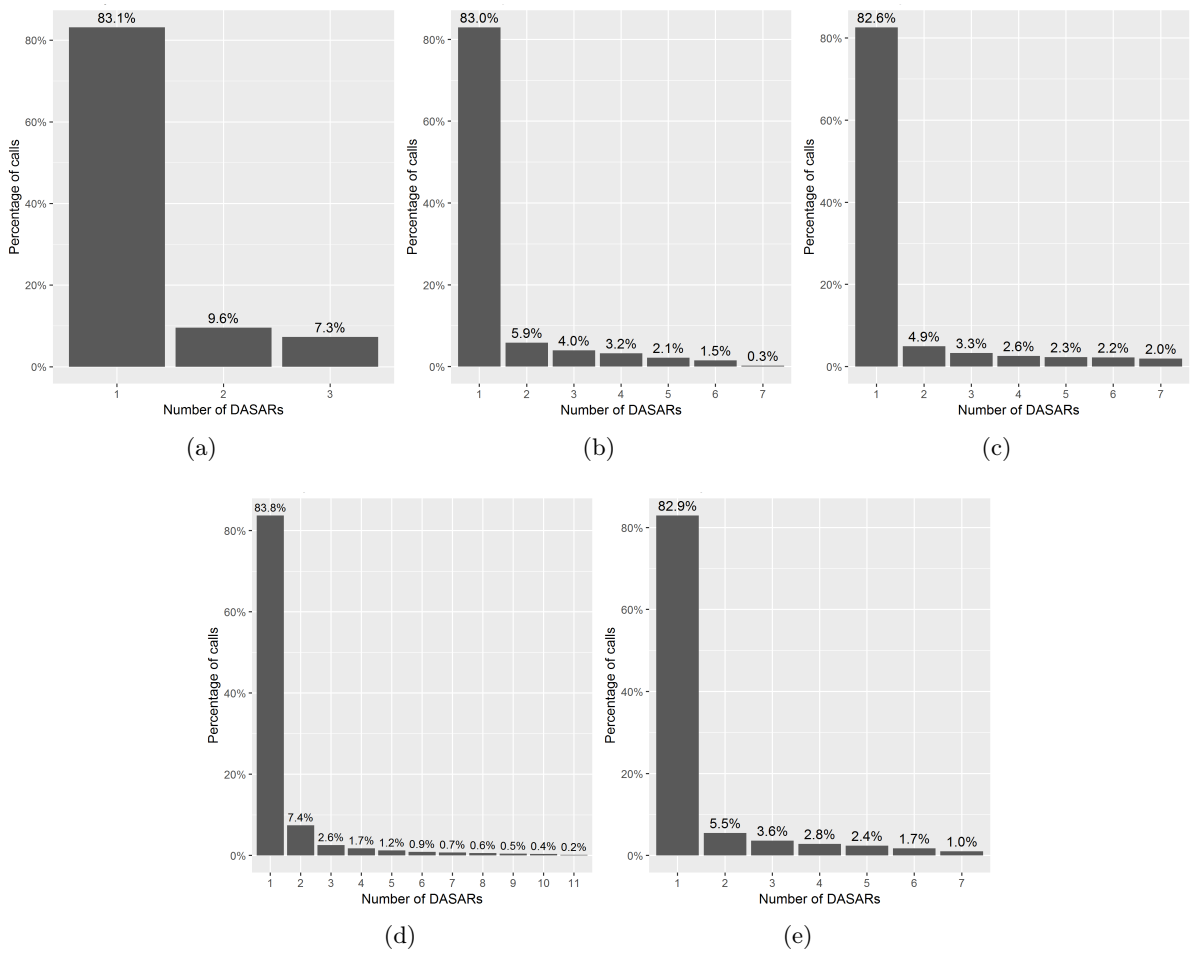

Figure 4.3: Percentage distribution of calls recorded at exactly k DASARs (k = 1,...,11). in each site. (a) Site 1, year 2014. (b) Site 2, year 2014. (c) Site 3, year 2014. (d) Site 4, year 2014. (e) Site 5, year 2014.

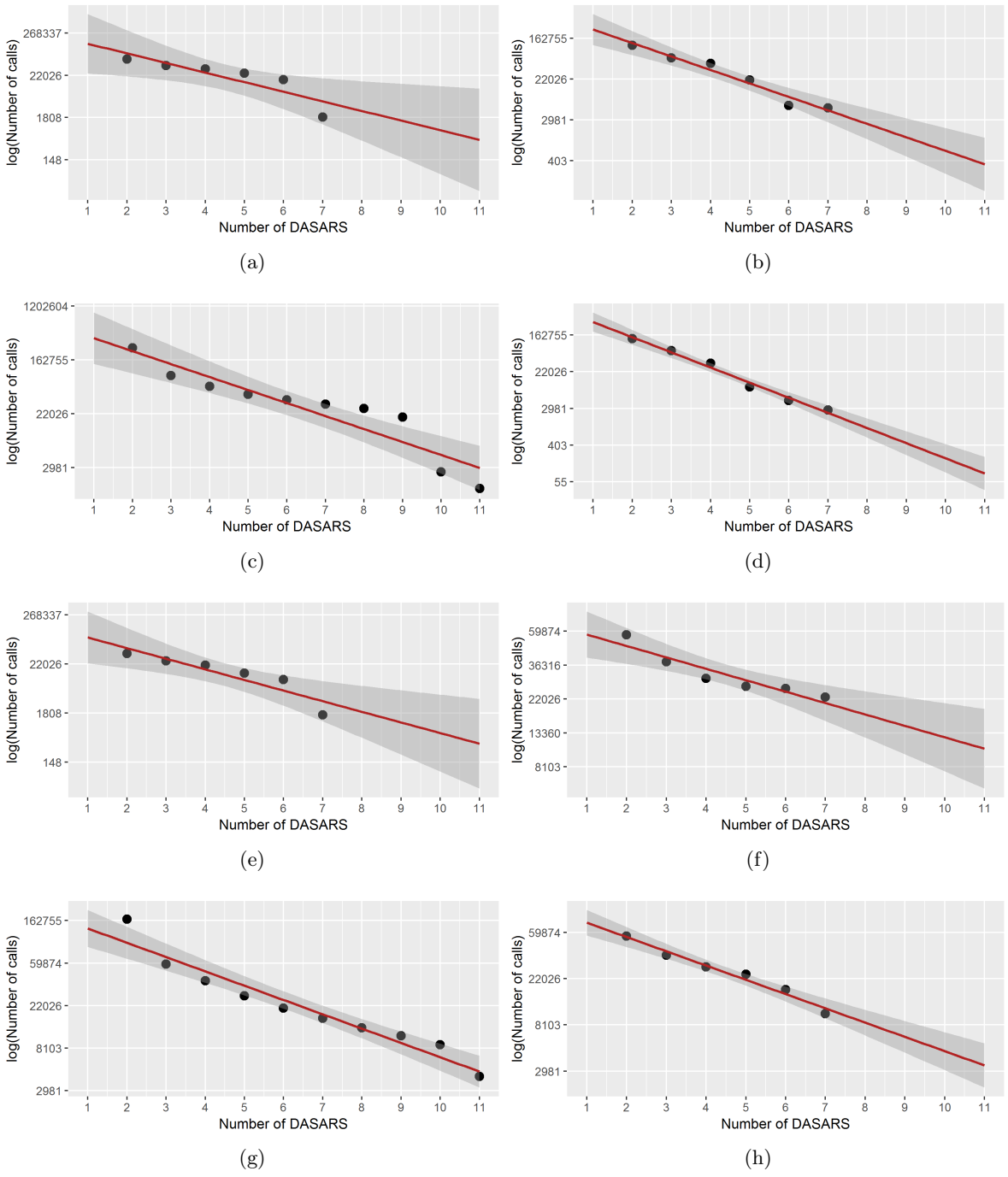

Figure 4.4: Linear regression model of an exponential relationship between explanatory variable, number of DASARs (x-axis) and the response variable, number of calls in the logarithmic scale (y-axis). Each black dot corresponds to an observation and the red line matches the regression line, where the grey band area is the 95% confidence level interval for the predicted values. (a) Site 2, year 2013. (b) Site 3, year 2013. (c) Site 4, year 2013. (d) Site 5, year 2013. (e) Site 2, year 2014. (f) Site 3, year 2014. (g) Site 4, year 2014. (h) Site 5, year 2014.

The hypotheses to consider regarding the linear model are:

H_0: $\beta_1 = 0$ vs H_1: $\beta_1 \neq 0$

The null hypothesis, H_0, is rejected for the usually considered significance values (.1, .05 and .01) for sites 3, 4 and 5 of year 2013 and 2014, i.e., there is a significant relationship between the number of DASARs and the number of calls recorded, assuming the residuals follow a normal distribution. For site 2 of 2013 and 2014, the null hypothesis is rejected at .05 and 0.1 significance levels. More information about these linear models are given in table E.5 in the appendices.

After validating the exponential fitting, it is calculated the proportion of singletons (p, see table 4.2) by dividing the expected amount of singletons by the existing number of singletons contained in the dataset. A random sample without replacement is performed to the automated singletons data with a proportion of p (simply put, $1 - p$ false positives are removed from the singletons data). The percentage distribution of calls after resampling is exhibited in figure 4.5, 4.6, 4.7, and 4.8.

Table 4.2: Proportion of singletons according to predicted values.

Site	Year	Proportion of singletons	Year	Proportion of singletons
2	2013	0.1718	2014	0.1600
3	2013	0.1973	2014	0.0601
4	2013	0.1218	2014	0.0714
5	2013	0.2735	2014	0.0882

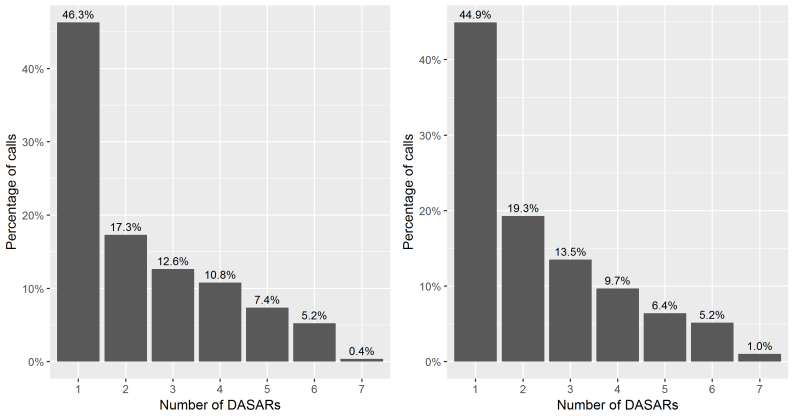

(a) (b)

Figure 4.5: Percentage distribution of calls recorded at exactly k DASARs (k = 1,...,7) in site 2. The percentage distribution results from a single sample after subsetting the number of singletons according to a proportion p. (a) Year 2013. (b) Year 2014.

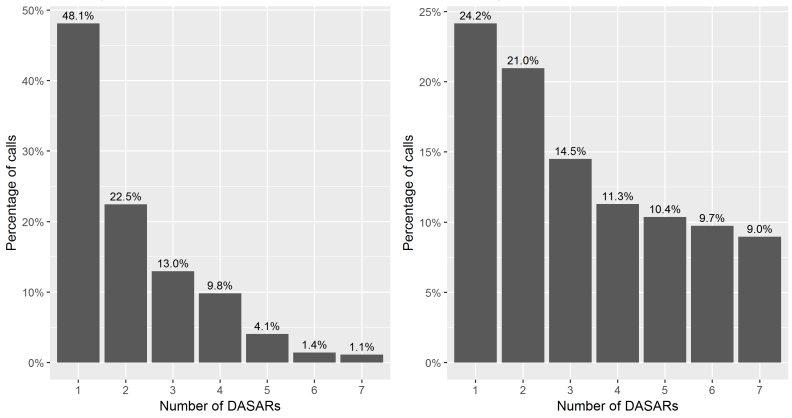

(a) (b)

Figure 4.6: Percentage distribution of calls recorded at exactly k DASARs (k = 1,...,7) in site 3. The percentage distribution results from a single sample after subsetting the number of singletons according to a proportion p. (a) Year 2013. (b) Year 2014.

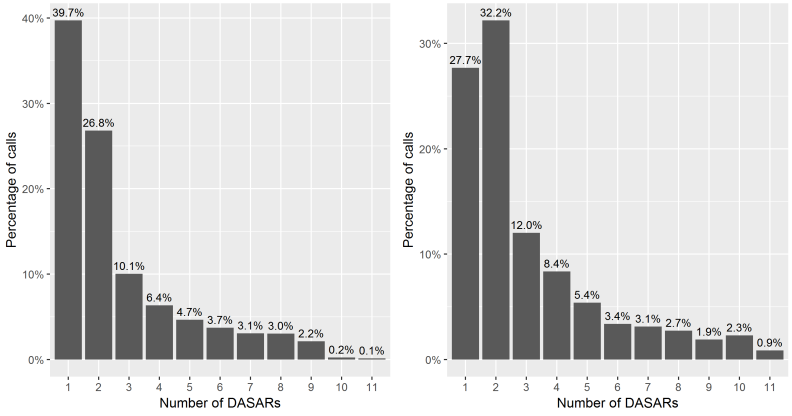

(a) (b)

Figure 4.7: Percentage distribution of calls recorded at exactly k DASARs (k = 1,...,11) in site 4. The percentage distribution results from a single sample after subsetting the number of singletons according to a proportion p. (a) Year 2013. (b) Year 2014.

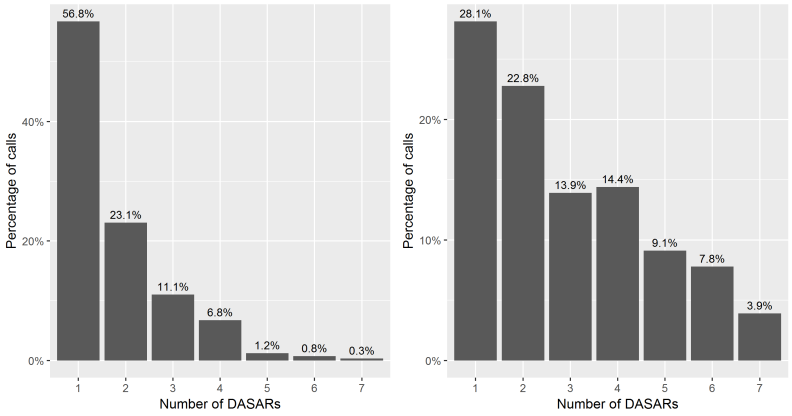

(a) (b)

Figure 4.8: Percentage distribution of calls recorded at exactly k DASARs (k = 1,...,7) in site 5. The percentage distribution results from a single sample after subsetting the number of singletons according to a proportion p. (a) Year 2013. (b) Year 2014.

4.2 Call Density and Population Density Estimates from the Automated Data

The overall call estimates (number of calls/100 km^2), in descending order, were produced according to: i) 'all calls included' approach, a ii) 'proportion of singletons' approach, and iii) 'no singletons' approach. Site 3 in 2014 was the only site that held similar estimates between the second and third approaches (23.2596 calls/100 km^2 and 25.6214 calls/100 km^2, respectively). The call densities are observed in table 4.3 and 4.4, and were generated from 50 resamples for each site, year and approach combined. The overall mean call density value of the i) approach is 715.5068 calls/100 km^2, of the ii) is 103.8139 calls/100 km^2, and of the iii) approach is 53.7926 calls/100 km^2. The estimates from the 'no singletons' approach were mostly around half from the 'proportion of singletons' approach estimates. The mean call density estimate of the 'all calls included' approach was around 15 times higher than the 'no singletons', and 7 times higher than the 'proportion of singletons' approach. In 2013, the mean call density was 375.2225 calls/100 km^2, and in 2014 was 206.8531 calls/100 km^2. The estimates are also illustrated in figure 4.9. All call density estimates correspond to 0.5% of the total calls in the automated data per site/year, as explained previously in section 3.

The parameter estimates, sigma and intercept, are shown in tables 4.3 and 4.4, with the mean and median values of sigma, and the mean values of intercept. Site 2, 2014 (with 'proportion of singletons' approach), and site 5, 2014 (with 'no singletons' and 'proportion of singletons' approaches) presented excessively high sigma estimates, due to a few resamples (out of 50 resamples) presenting a higher amount of calls being detected in more DASARs rather than in less DASARs. For instance, having more calls being detected in 4 to 7 DASARs will produce higher sigma estimates, whereas having more calls being detected in 1 to 3 DASARs in the data will produce lower sigma estimates. For that reason, the median values should be the ones considered for comparison purposes within each site, year and approach. The mean intercept values of the 'all calls included' approach are <0.6, while the intercept estimates for the 'no singletons' and 'proportion of singletons' are >0.6. This is explained, once again, by the

higher number of singletons constituting the samples from the 'all calls included' approach.

The estimated call densities were only assessed with 0.5% of the automated data, but the population density estimates were calculated with call density estimates divided by a factor of 0.005, hence representing 100% of the calls.

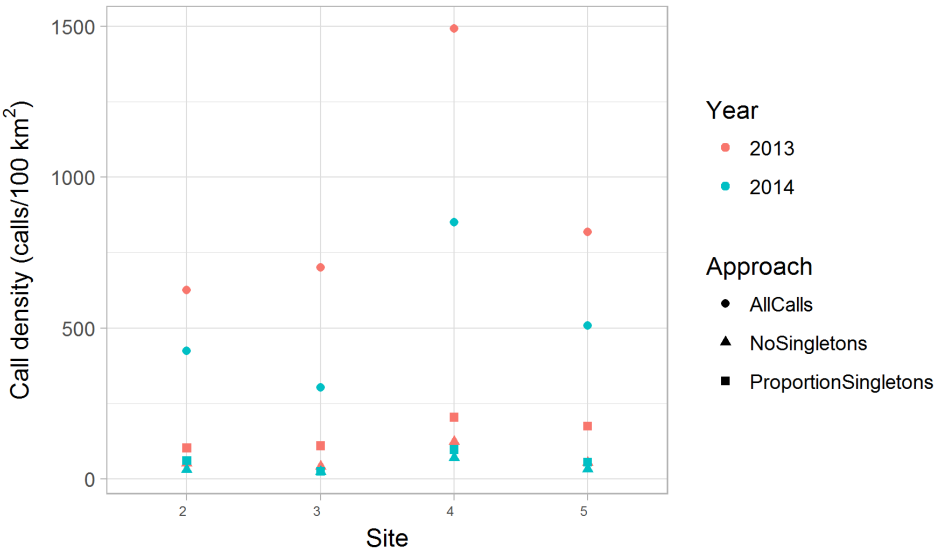

Figure 4.9: Call density estimates (number of calls/100 km^2) from different approaches: all calls included (circle icons), no singletons included in the dataset (triangle icons); and subset singletons according to a proportion (square icons). Estimates from year 2013 (salmon colour), and estimates from year 2014 (blue colour).

The estimated population densities (number of whales/100 km^2h) resulted from an SECR analysis composed of 90,564 recorded calls: 6,696 (site 2, 2013), 11,479 (site 3, 2013), 25,375 (site 4, 2013), 11,469 (site 5, 2013), 4,717 (site 2, 2014), 8,020 (site 3, 2014), 15,668 (site 4, 2014) and 7,140 (site 5, 2014). The call density estimates are the mean values of 50 resamples calculated according to three approaches ('all calls included', 'no singletons', and 'proportion of singletons'), and according to a percentage of missing migrating whales (25%, 35% and 45%). The call densities are then converted to population densities. All population density estimates showcased higher values if the 'proportion of singletons' approach was used compared to the 'no singletons', as one would expect, since the automated data contained a vast majority of singletons. The estimates produced by 'all calls included' approach were far higher compared to the remaining approaches, because all singletons were retained in the data. Combining the estimates from all sites and year, the mean population density of the 'all calls included' approach is as follow: 40.4974 whales/100 km^2h (25% missing whales), 33.2231 whales/100 km^2h (35% missing whales), and 25.9553 whales/100 km^2h (45% missing whales). The mean values of the 'no singletons' are: 2.9598 whales/100 km^2h (25% missing whales), 2.4258 whales/100 km^2h (35% missing whales), and 1.896 whales/100 km^2h (45% missing whales). Finally, the mean population density of the remaining approach is: 5.8971 whales/100 km^2h (25% missing whales), 4.8522 whales/100 km^2h (35% missing whales), and 3.7886 whales/100 km^2h (45% missing whales).

Table 4.3: Mean density estimates of 2013 with four different approaches: 1) all calls included in the data, 2) excluding singletons; 3) subsetting singletons according to a proportion; and 4) truncating singletons. Call density, sigma and intercept estimates are the mean of 50 resamples.

		Site and Year											
Approach	Estimates	2, 2013			3, 2013			4, 2013			5, 2013		
All calls included	Call density	625.5461 [53]			700.2639 [54]			1,493.2780 [54]			819.2810 [51]		
No singletons	estimate	52.2465 [53]			41.9510 [54]			123.7110 [54]			54.4141 [51]		
Proportion of singletons	(calls/100km^2)	102.5924 [53]			110.0455 [54]			204.2116 [54]			175.1285 [51]		
Truncation of singletons	[total days] $^{(a)}$	*			*			*			*		
All calls included		7.6128 (7.6299$^{(+)}$)			10.5351 (10.6149$^{(+)}$)			7.8689 (7.8750$^{(+)}$)			9.9858 (9.9741$^{(+)}$)		
No singletons		9.1334 (9.1447$^{(+)}$)			29.2297 (12.5725$^{(+)}$)			8.5385 (8.5397$^{(+)}$)			11.5080 (11.5196$^{(+)}$)		
Proportion of singletons	Sigma estimate (km)	8.7735 (8.7665$^{(+)}$)			11.7845 (11.8632$^{(+)}$)			8.5042 (8.4953$^{(+)}$)			10.4716 (10.4937$^{(+)}$)		
Truncation of singletons		*			*			*			*		
All calls included		0.471			0.311			0.349			0.272		
No singletons		1.000			0.891			1.000			0.956		
Proportion of singletons	Intercept (g_0) estimate	1.000			0.788			1.000			0.645		
Truncation of singletons		*			*			*			*		
Cue rate [Percentage of missing migrating whales]		4.9 [25%]	6.0 [35%]	7.7 [45%]	2.5 [25%]	3.1 [35%]	4.0 [45%]	6.2 [25%]	7.6 [35%]	9.8 [45%]	2.1 [25%]	2.5 [35%]	3.2 [45%]
All calls included	Population	20.0727	16.3927	12.7735	43.2262	34.8598	27.0164	37.1684	30.3216	23.5147	63.7474	53.5478	41.8342
No singletons	density	1.6765	1.3691	1.0669	2.5896	2.0884	1.6185	3.0792	2.512	1.9481	4.2339	3.5565	2.7785
Proportion of singletons	estimate	3.2920	2.6885	2.0949	6.7929	5.4782	4.2456	5.0829	4.1466	3.2157	13.6266	11.4463	8.9424
Truncation of singletons	(whales/100km^2 h) $^{(b)}$	*	*	*	*	*	*	*	*	*	*	*	*

Table 4.4: Mean density estimates of 2014 with four different approaches: 1) all calls included in the data, 2) excluding singletons; 3) subsetting singletons according to a proportion; and 4) truncating singletons. Call density, sigma and intercept estimates are the mean of 50 resamples.

		Site and Year											
Approach	Estimates	2, 2014			3, 2014			4, 2014			5, 2014		
All calls included	Call density	423.9070 [40]			302.4377 [47]			850.4499 [48]			508.8908 [44]		
No singletons	estimate	31.8346 [40]			23.2596 [47]			70.8910 [48]			32.0332 [44]		
Proportion of singletons	(calls/100km^2)	60.5376 [40]			25.6214 [47]			97.3585 [48]			55.0158 [44]		
Truncation of singletons	[total days] $^{(a)}$	*			*			*			*		
All calls included		7.3149 (7.3124$^{(+)}$)			11.5375 (11.4969$^{(+)}$)			8.3148 (8.3094$^{(+)}$)			8.5044 (8.5112$^{(+)}$)		
No singletons		13.1153 (9.0729$^{(+)}$)			25.0802 (14.2105$^{(+)}$)			9.2756 (9.2926$^{(+)}$)			4,157.2560 (11.8096$^{(+)}$)		
Proportion of singletons	Sigma estimate (km)	826.4434 (8.5908$^{(+)}$)			25.8420 (14.2742$^{(+)}$)			9.2538 (9.2577$^{(+)}$)			23,762.86 (10.9259$^{(+)}$)		
Truncation of singletons		*			*			*			*		
All calls included		0.472			0.579			0.360			0.484		
No singletons		0.984			0.999			1.000			0.976		
Proportion of singletons	Intercept (g_0) estimate	0.959			1.000			1.000			0.976		
Truncation of singletons		*			*			*			*		
Cue rate [Percentage of missing migrating whales]		2.1 [25%]	2.5 [35%]	3.2 [45%]	1.8 [25%]	2.2 [35%]	2.8 [45%]	2.7 [25%]	3.4 [35%]	4.3 [45%]	2.9 [25%]	3.5 [35%]	4.5 [45%]
All calls included	Population	42.0543	35.3256	27.5981	29.7909	24.3744	19.1513	54.6843	43.4258	34.3366	33.2348	27.5374	21.4180
No singletons	density	3.1582	2.6529	2.0726	2.2911	1.8746	1.4729	4.5583	3.6198	2.8622	2.0920	1.7334	1.3482
Proportion of singletons	estimate	6.0057	5.0448	3.9412	2.5238	2.0649	1.6224	6.2602	4.9713	3.9308	3.593	2.977	2.3155
Truncation of singletons	(whales/100km^2 h) $^{(b)}$	*	*	*	*	*	*	*	*	*	*	*	*

a) Call density estimates of 0.5% of all calls; *b)* Mean swim speed of the whales of 4–5 km/h; * Values to be estimated by computing equation 3.1; *(+)* Median value of 50 resamples.

4.3 Comparison with Simulated Capture Histories

4.3.1 What is the Best Approach?

Comparing the simulated estimates with different approaches (figure 4.10), the approach 'proportion of singletons' is validated as the best approach to produce reliable estimates, since it held the lowest percentage bias to the 'true' density estimate. The presented percentage bias are: 'all calls included' (265.144 %), 'no singletons' (-57.029%), and 'proportion of singletons' (-27.505 %). The 'true' simulated data produced a percentage bias of -3.948 %.

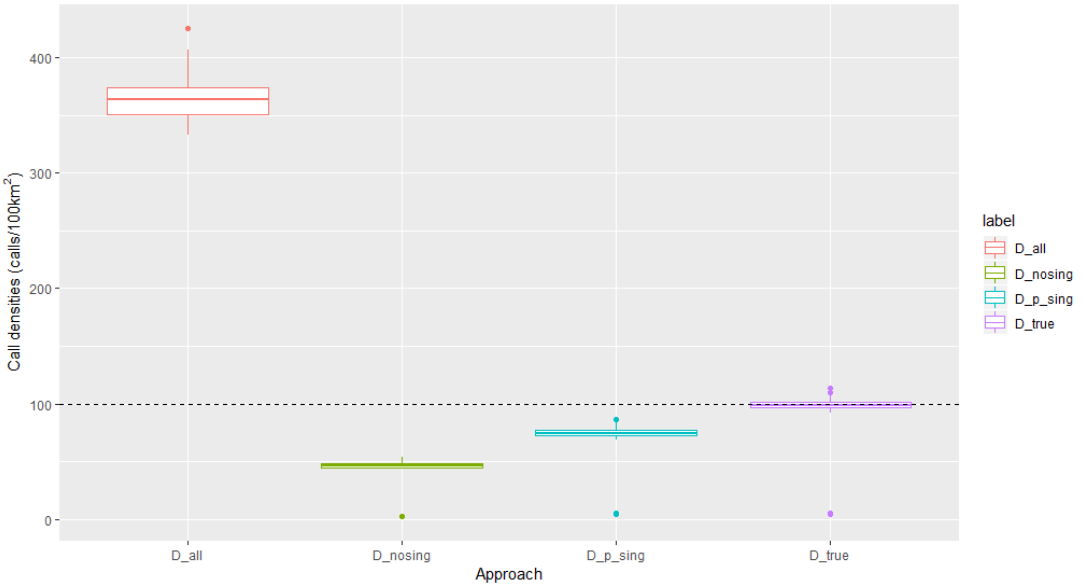

Figure 4.10: Call density estimates (number of calls/100 km^2) from simulated data with different approaches: all calls included (red), no singletons included in the dataset (green); and subset singletons according to a proportion (blue), and set to 'true' estimate (purple). Dashed line represents 'true' density estimate (100 animals/100 km^2).

4.3.2 Consistency Check between Call Density Estimates

In the first type of simulated data, the call density values are estimated under the 'no singletons' and the 'proportion of singletons' approach. The second type of simulated data is performed with the 'no transformation' approach. Table 4.5 shows the simulated call density estimates and their respective coefficients of variation.

After fitting SECR models to the a) and b) simulated data, the produced call densities and sigma estimates are compared to the estimated values from the automated data (table E.6 in the appendices). Figure 4.11 illustrates a boxplot for each one of the four approaches ('all calls included', 'no singletons', 'proportion of singletons', and 'no transformation') and simultaneously for each year (automated data from 2013 and 2014), as well as for the simulated data.

Table 4.6 exhibits the mean values of the call density estimates for each type of data and approach. The mean value of the **b) type of simulated data** (56.050 calls/100 km^2) is compared against the mean values from the **automated data**. The absolute difference between the call densities from the simulated data and from the automated data with 'all calls included'

approach is 659.4571 calls/100 km^2; from the 'no singletons' approach is 2.2571 calls/100 km^2; and from the automated data with the 'proportion of singletons' approach is 47.7642 calls/100 km^2. The 'no singletons' mean difference is within a reasonable range. Opposite to the 'all calls included' approach that had almost 15 times more calls compared to the simulated data, and the 'proportion of singletons' presented almost the double amount of calls.

The absolute difference between the **a) type of simulated data** with the 'no singletons' approach, and the automated data excluding singletons is 28.1893 calls/100 km^2. For the automated data with a 'proportion of singletons' vs a) type of simulated data with the same approach, it reveals a difference of 10.0868 calls/100 km^2. The mean values, standard deviation, minimum and maximum are presented in table 4.6.

Table 4.5: Call density and sigma estimates from simulated capture histories with corresponding coefficient of variation (CV).

		Site 2		
Approach	Estimates	Simulated data [a)]	Simulated data [b)]	CV(%)
No singletons	Call density estimate	$18.6417^{(*)}$ [$347.21^{(*)}$]	–	34.39
Proportion of singletons	(calls/100km^2)	$80.9259^{(*)}$ [$1359.80^{(*)}$]	–	35.68
No transformation [c)]	[N calls]	–	$45.2740^{(*)}$ [$1277.5^{(*)}$]	44.72
No singletons		$9.638^{(+)}$	–	876.99
Proportion of singletons	Sigma estimate (km)	$9.322^{(+)}$	–	851.01
No transformation [c)]		–	$11.860^{(+)}$	212.77
		Site 3		
Approach	Estimates	Simulated data [a)]	Simulated data [b)]	
No singletons	Call density estimate	$21.6501^{(*)}$ [$770.57^{(*)}$]	–	58.99
Proportion of singletons	(calls/100km^2)	$58.1064^{(*)}$ [$2105.74^{(*)}$]	–	72.57
No transformation [c)]	[N calls]	–	$15.4172^{(*)}$ [$1913^{(*)}$]	107.99
No singletons		$14.078^{(+)}$	–	95.13
Proportion of singletons	Sigma estimate (km)	$14.021^{(+)}$	–	72.59
No transformation [c)]		–	$241.444^{(+)}$	63.23
		Site 4		
Approach	Estimates	Simulated data [a)]	Simulated data [b)]	
No singletons	Call density estimate	$37.3398^{(*)}$ [$881.98^{(*)}$]	–	33.05
Proportion of singletons	(calls/100km^2)	$144.3252^{(*)}$ [$3501.34^{(*)}$]	–	42.56
No transformation [c)]	[N calls]	–	$129.0128^{(*)}$ [$3594.5^{(*)}$]	37.48
No singletons		$8.776^{(+)}$	–	5.71
Proportion of singletons	Sigma estimate (km)	$9.532^{(+)}$	–	5.37
No transformation [c)]		–	$9.893^{(+)}$	5.56
		Site 5		
Approach	Estimates	Simulated data [a)]	Simulated data [b)]	
No singletons	Call density estimate	$24.7818^{(*)}$ [$711.75^{(*)}$]	–	46.74
Proportion of singletons	(calls/100km^2)	$91.5510^{(*)}$ [$2167.90^{(*)}$]	–	40.30
No transformation [c)]	[N calls]	–	$34.495^{(*)}$ [$1791.333^{(*)}$]	51.10
No singletons		$12.560^{(+)}$	–	98.03
Proportion of singletons	Sigma estimate (km)	$11.403^{(+)}$	–	5.26
No transformation [c)]		–	$18.993^{(+)}$	173.15

a) Simulated data with a large number of singletons.

b) Simulated data without forcing a large number of singletons.

c) Simulated data with no subset/transformation performed to it.

$^{(*)}$ Mean value of 100 simulations; $^{(+)}$ Median value of 100 simulations.

Table 4.6: Call density estimates statistics for each approach and type of data. The automated data was composed of 400 resamples per approach; the a) and b) simulated data were composed of 400 simulations each per approach.

Mean	Type of data		
Approach	Automated data	Simulated data [a)]	Simulated data [b)]
All calls included	715.507	–	–
No singletons	53.793	25.603	–
Proportion of singletons	103.814	93.727	–
No transformation [c)]	–	–	56.050
Standard deviation	**Type of data**		
Approach	Automated data	Simulated data [a)]	Simulated data [b)]
All calls included	345.114	–	–
No singletons	31.006	57.472	–
Proportion of singletons	13.135	54.074	–
No transformation [c)]	–	–	52.166
Minimum	**Type of data**		
Approach	Automated data	Simulated data [a)]	Simulated data [b)]
All calls included	253.406	–	–
No singletons	1.653	3.076	–
Proportion of singletons	0.807	3.093	–
No transformation [c)]	–	–	2.874
Maximum	**Type of data**		
Approach	Automated data	Simulated data [a)]	Simulated data [b)]
All calls included	1574.256	–	–
No singletons	127.842	209.558	–
Proportion of singletons	54.511	279.247	–
No transformation [c)]	–	–	179.945

a) Simulated data with a large number of singletons.

b) Simulated data without forcing a large number of singletons.

c) Simulated data with no subset/transformation performed to it.

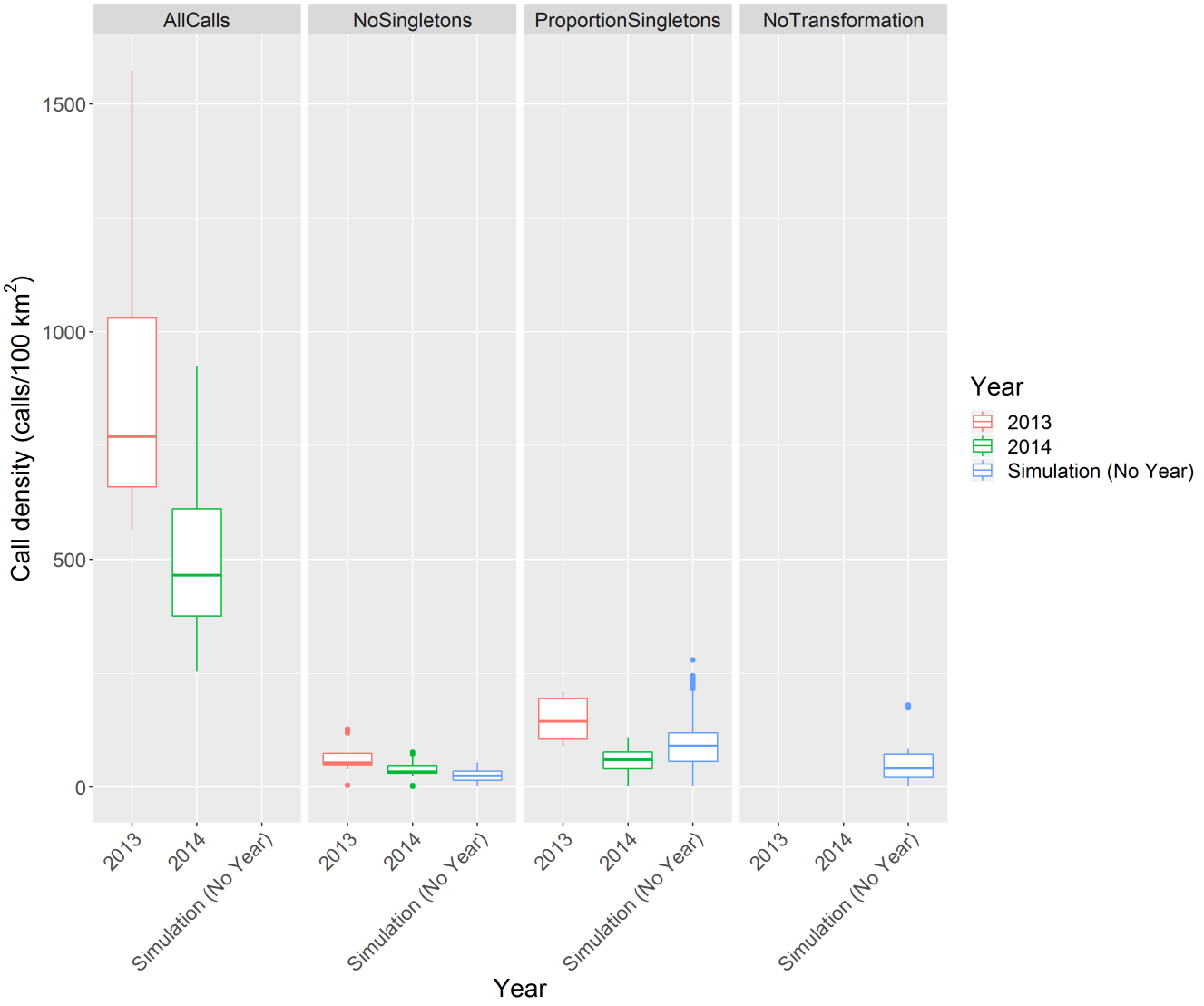

Figure 4.11: Call density estimates (number of calls/100 km^2) from the automated data resulting from 50 resamples for each year (2013 and 2014) and for each one of the four approaches. The estimates from the simulated data results from 100 simulations for each approach (only three are considered: 'no singletons', 'proportion of singletons', and 'no transformation').

4.3.3 Consistency Check between Population Density Estimates

The mean call densities are converted to population densities (whales/100 km^2 h) with the equation 1.7. The population density estimates are presented in figure 4.12, 4.13, and 4.14, displaying the estimates with 25%, 35%, and 45% of missing migrating whales. The corresponding values can be consulted in table 4.7, for the simulated data and the automated data. Table 4.8, 4.9 and 4.10 register the absolute differences between population densities for each approach and year. Some insights can be made by checking the absolute differences, but also by examining the confidence intervals, and verify if the automated data estimates will fall between the simulated upper and lower bound.

The values marked as red (table 4.8, 4.9 and 4.10) reveal absolute differences <1 whales/100 km^2 h, only for the 'no singletons' and 'proportion of singletons' approach. Considering only the density estimates from **a) type of simulated data**, the population densities from the automated data are compared under the **'proportion of singletons'** approach, as the differences were < 1 for all percentages of missing whales. For the **'no singletons'** approach, the difference between automated and simulated data was 1.5521 whales/100 km^2 h (25% of missing whales), and 1.2728 whales/100 km^2 h (35% of missing whales). However, for the 45% of missing whales, the difference was closer to 1 (0.9970 whales/100 km^2 h). Considering only the density estimates from **b) type of simulated data**, the automated data with the 'no proportion' approach held lower differences (< 0.4 whales/100 km^2 h). The automated population densities with 'all calls' approach is overall, and as expected, much higher compared to the estimates of type a) and b) of simulated data.

Another comparison method is examining the CIs of the simulated and automated data and check if the automated mean population densities are contained within the 95% CI of the simulated data. The 95% confidence level interval in table 4.11 reveals that the mean population density values from the automated data with a **'proportion of singletons'** approach falls within the CI of the **a) type of simulated data** with the same approach. Contrary to the **'no singletons'** approach, where the mean population density from the automated data is higher than the CI upper limit. Considering the 95% CI of the **b) type of simulated data**, the only approach from the automated data that falls within the CI belongs to the **'no singletons'**. The **'all calls'** approach estimates are, once again, much higher than the upper limits of the a) and b) type of simulated data.

The automated population densities from the **'no singletons'** and **'proportion of singletons'** approaches are, therefore, consistent with the simulations, as they were contained within the CIs for the **a) simulated data**. The 'proportion of singletons' ad hoc approach is assumed to provide more reliable estimates compared to the 'no singletons' approach, and as validated in the sub-section 4.3.1. For this reason, the final suggested BCB population densities of bowhead whales are: 5.8971 whales/100 km^2 h (with 25% missing whales); 4.8522 whales/100 km^2 h (with 35% missing whales); and 3.7886 whales/100 km^2 h (with 45% missing whales).

Table E.7 in the appendices exhibits the reverse comparison, i.e., the CIs are produced by the automated data and the mean values of the simulated data will/will not fall within their CIs.

Table 4.7: Population density estimates (whales/$100km^2$h) from 50 resamples of the automated data (2013 and 2014) vs from 100 simulated capture histories. The estimates are sorted according to three cue rates and their respective percentages of missing migrating whales (25%, 35% and 45%).

	Site 2								
	Simulated data [a]			2013			2014		
Approaches	3.5 [25%]	4.25 [35%]	5.45 [45%]	4.9 [25%]	6.0 [35%]	7.7 [45%]	2.1 [25%]	2.5 [35%]	3.2 [45%]
All calls included	–	–	–	20.073	16.393	12.774	42.054	35.326	27.598
No singletons	0.890	0.733	0.572	1.677	1.369	1.067	3.158	2.653	2.073
Proportion of singletons	3.863	3.182	2.481	3.292	2.689	2.095	6.006	5.045	3.941
	Simulated data [b]								
No transformation [c]	2.161	1.780	1.388						
	Site 3								
	Simulated data [a]			2013			2014		
Approaches	2.15 [25%]	2.65 [35%]	3.40 [45%]	2.5 [25%]	3.1 [35%]	4.0 [45%]	1.8 [25%]	2.2 [35%]	2.8 [45%]
All calls included	–	–	–	43.226	34.860	27.016	29.791	24.374	19.151
No singletons	1.683	1.365	1.064	2.590	2.088	1.619	2.291	1.875	1.473
Proportion of singletons	4.516	3.664	2.855	6.793	5.478	4.246	2.524	2.065	1.622
	Simulated data [b]								
No transformation [c]	1.198	0.972	0.758						
	Site 4								
	Simulated data [a]			2013			2014		
Approaches	4.45 [25%]	5.50 [35%]	7.05 [45%]	6.2 [25%]	7.6 [35%]	9.8 [45%]	2.7 [25%]	3.4 [35%]	4.3 [45%]
All calls included	–	–	–	37.168	30.322	23.515	54.684	43.426	34.337
No singletons	1.402	1.134	0.885	3.079	2.5120	1.948	4.558	3.620	2.862
Proportion of singletons	5.419	4.384	3.420	5.083	4.147	3.216	6.260	4.971	3.931
	Simulated data [b]								
No transformation [c]	4.844	3.919	3.058						
	Site 5								
	Simulated data [a]			2013			2014		
Approaches	2.50 [25%]	3.00 [35%]	3.85 [45%]	2.1 [25%]	2.5 [35%]	3.2 [45%]	2.9 [25%]	3.5 [35%]	4.5 [45%]
All calls included	–	–	–	63.747	53.548	41.834	33.235	27.537	21.418
No singletons	1.656	1.380	1.075	4.234	3.557	2.779	2.092	1.733	1.348
Proportion of singletons	6.119	5.099	3.973	13.627	11.446	8.942	3.593	2.977	2.316
	Simulated data [b]								
No transformation [c]	2.305	1.921	1.497						

a) Simulated data with a large number of singletons.

b) Simulated data without forcing a large number of singletons.

c) Simulated data with no subset/transformation performed to it.

Table 4.8: Absolute differences of population density estimates (whales/100 km^2 h) between approaches and years for 25% of missing migrating whales.

	Approach	All calls included	No Singletons	Proportion Singletons	No Singletons	Proportion Singletons	No Transformation
Approach	Year	2013 and 2014	2013 and 2014	2013 and 2014	Simulation (No Year) [a)]	Simulation (No Year) [b)]	Simulation (No Year) [c)]
All calls included	2013 and 2014	–	37.5375	34.6002	39.0896	35.5181	37.8704
No Singletons	2013 and 2014	37.5375	–	2.9373	1.5521	2.0194	0.3328
Proportion Singletons	2013 and 2014	34.6002	2.9373	–	4.4894	0.9179	3.2701
No Singletons	Simulation (No Year) [a)]	39.0896	1.5521	4.4894	–	3.5715	1.2193
Proportion Singletons	Simulation (No Year) [b)]	35.5181	2.0194	0.9179	3.5715	–	2.3522
No Transformation	Simulation (No Year) [c)]	37.8704	0.3328	3.2701	1.2193	2.3522	–

Table 4.9: Absolute differences of population density estimates (whales/100 km^2 h) between approaches and years for 35% of missing migrating whales.

	Approach	All calls included	No Singletons	Proportion Singletons	No Singletons	Proportion Singletons	No Transformation
Approach	Year	2013 and 2014	2013 and 2014	2013 and 2014	Simulation (No Year) [a)]	Simulation (No Year) [b)]	Simulation (No Year) [c)]
All calls included	2013 and 2014	–	30.7973	28.3709	32.0701	29.1409	31.0751
No Singletons	2013 and 2014	30.7973	–	2.4264	1.2728	1.6564	0.2778
Proportion Singletons	2013 and 2014	28.3709	2.4264	–	3.6992	0.7699	2.7042
No Singletons	Simulation (No Year) [a)]	32.0701	1.2728	3.6992	–	2.9293	0.9950
Proportion Singletons	Simulation (No Year) [b)]	29.1409	1.6564	0.7699	2.9293	–	1.9342
No Transformation	Simulation (No Year) [c)]	31.0751	0.2778	2.7042	0.9950	1.9342	–

Table 4.10: Absolute differences of population density estimates (whales/100 km^2 h) between approaches and years for 45% of missing migrating whales.

	Approach	All calls included	No Singletons	Proportion Singletons	No Singletons	Proportion Singletons	No Transformation
Approach	Year	2013 and 2014	2013 and 2014	2013 and 2014	Simulation (No Year) [a)]	Simulation (No Year) [b)]	Simulation (No Year) [c)]
All calls included	2013 and 2014	–	24.0594	22.1668	25.0563	22.7731	24.2801
No Singletons	2013 and 2014	24.0594	–	1.8926	0.9970	1.2863	0.2207
Proportion Singletons	2013 and 2014	22.1668	1.8926	–	2.8896	0.6063	2.1133
No Singletons	Simulation (No Year) [a)]	25.0563	0.9970	2.8896	–	2.2832	0.7762
Proportion Singletons	Simulation (No Year) [b)]	22.7731	1.2863	0.6063	2.2832	–	1.5070
No Transformation	Simulation (No Year) [c)]	24.2801	0.2207	2.1133	0.7762	1.5070	–

a) Simulated data with a large number of singletons.

b) Simulated data without forcing a large number of singletons.

c) Simulated data with no subset/transformation performed to it.

Table 4.11: Confidence interval (95%) of population densities from simulated data and mean values of the automated data.

25% missing migrating whales				Automated data		
	Approach	Lower CI	Upper CI	All calls	No singletons	Proportion of singletons
Simulated data [a)]	No singletons	0.8227	1.9928	40.4974	2.9598	–
	Proportion of singletons	3.4005	6.5580		–	5.8971
Simulated data [b)]	No transformation [c)]	0.1486	5.1054		–	–
35% missing migrating whales				Automated data		
	Approach	Lower CI	Upper CI	All calls	No singletons	Proportion of singletons
Simulated data [a)]	No singletons	0.6728	1.6332	33.2231	2.4258	–
	Proportion of singletons	2.7477	5.4168		–	4.8522
Simulated data [b)]	No transformation [c)]	0.1550	4.1410		–	–
45% missing migrating whales				Automated data		
	Approach	Lower CI	Upper CI	All calls	No singletons	Proportion of singletons
Simulated data [a)]	No singletons	0.5255	1.2725	25.9554	1.8960	–
	Proportion of singletons	2.1426	4.2219		–	3.7886
Simulated data [b)]	No transformation [c)]	0.1195	3.2310		–	–

a) Simulated data with a large number of singletons.

b) Simulated data without forcing a large number of singletons.

c) Simulated data with no subset/transformation performed to it.

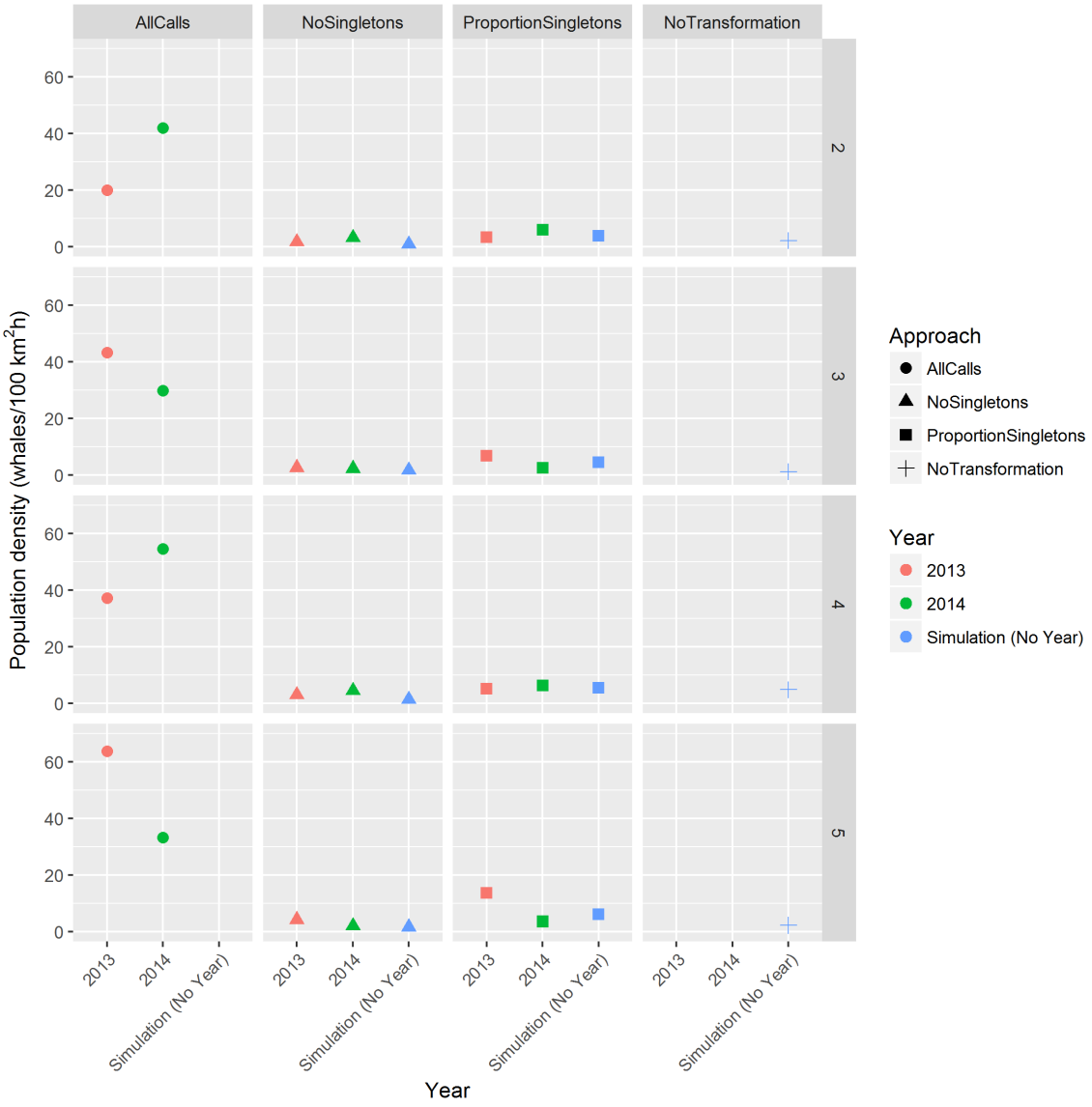

Figure 4.12: Population density estimates (number of whales/100 km^2 h) with 25% of missing migrating whales and from different approaches: all calls included (circle icon); no singletons included in the automated data (triangle icons); subset singletons according to a proportion in the automated data (square icons); and not performing any subset to the simulated data (cross icons). Estimates from 2013 (salmon colour), and estimates from 2014 (green colour). The mean estimates generated from 100 simulations are blue coloured, and have no year associated.

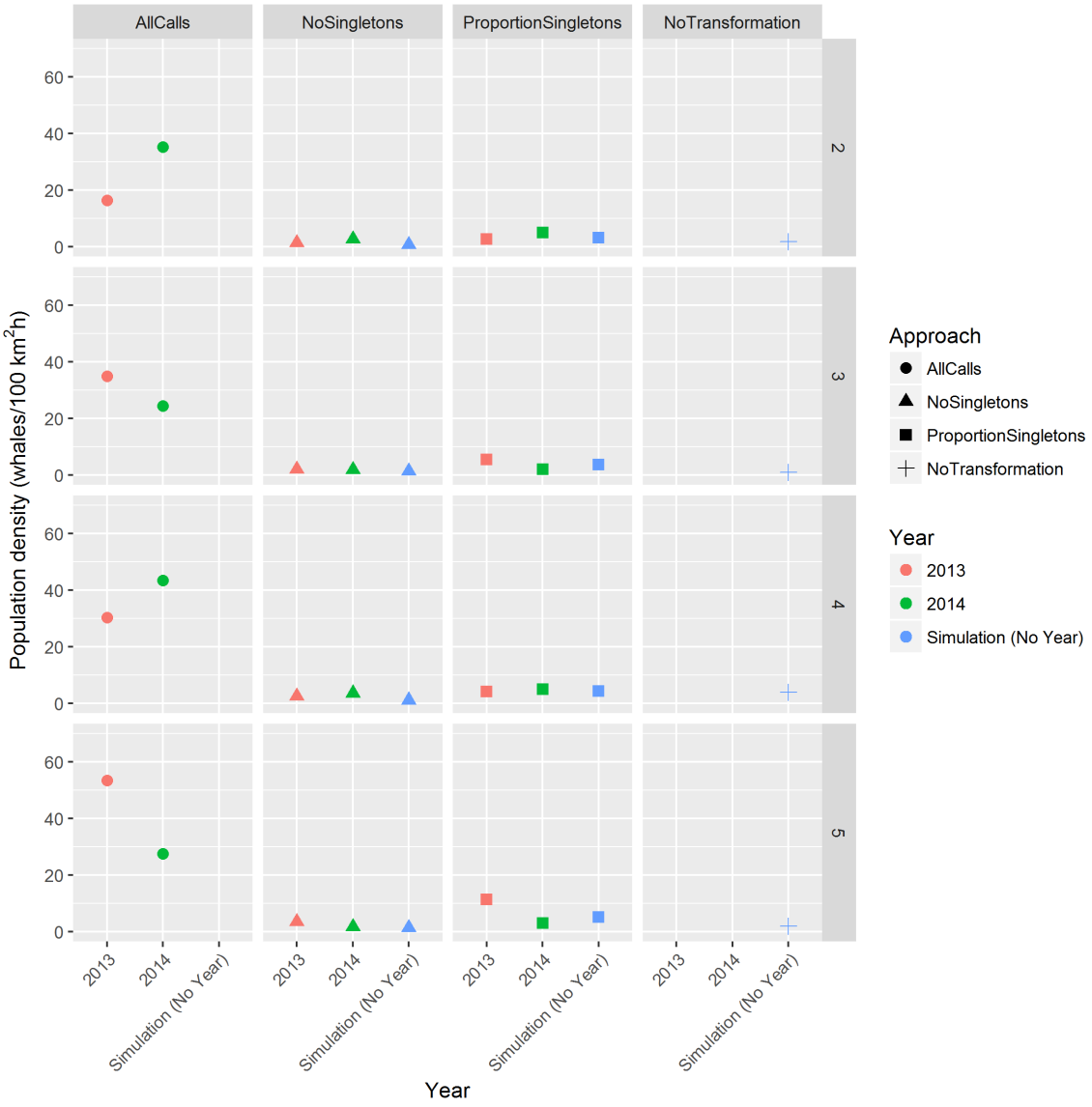

Figure 4.13: Population density estimates (number of whales/100 km^2 h) with 35% of missing migrating whales and from different approaches: all calls included (circle icon); no singletons included in the automated data (triangle icons); subset singletons according to a proportion in the automated data (square icons); and not performing any subset to the simulated data (cross icons). Estimates from 2013 (salmon colour), and estimates from 2014 (green colour). The mean estimates generated from 100 simulations are blue coloured, and have no year associated.

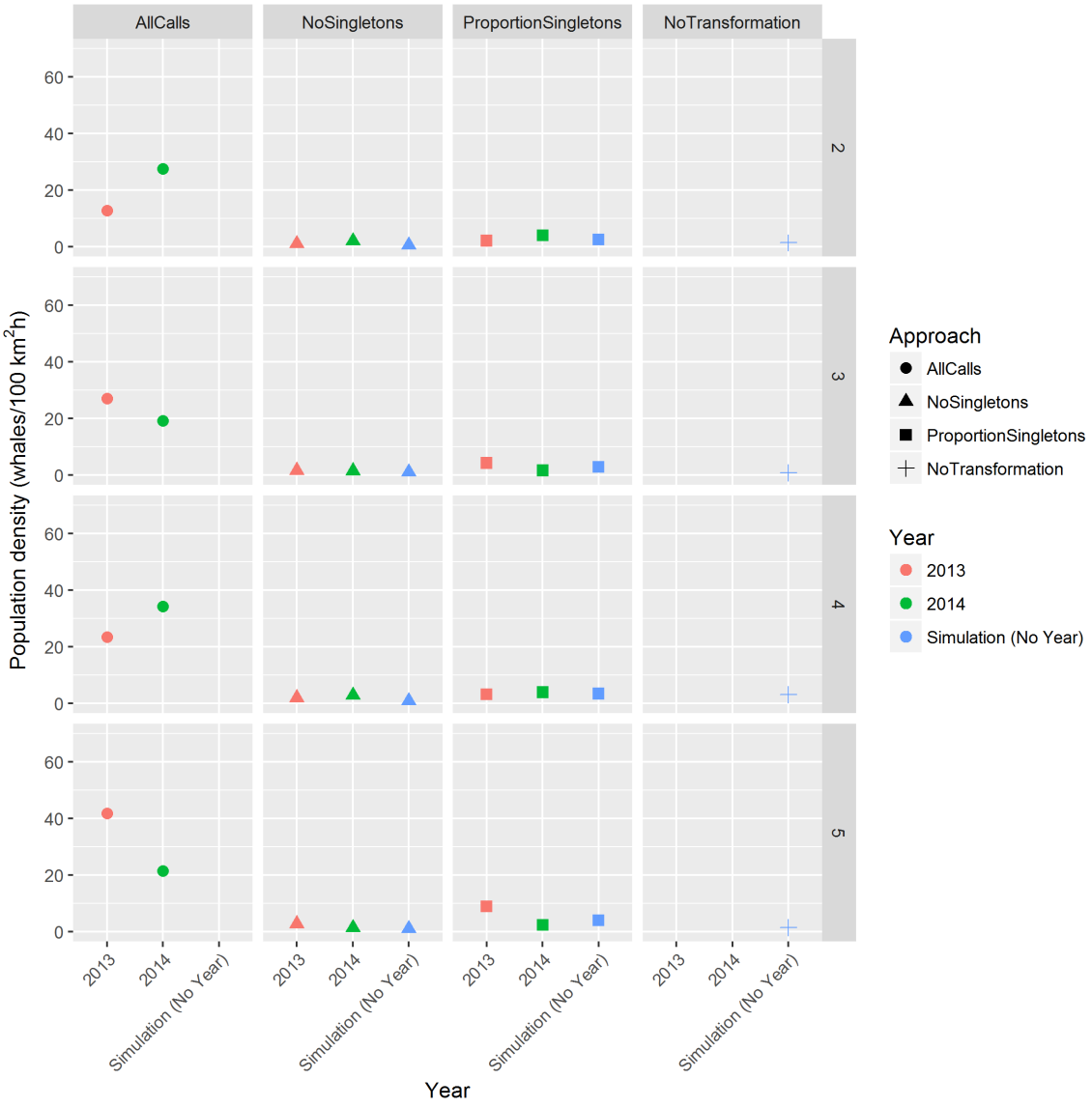

Figure 4.14: Population density estimates (number of whales/100 km^2 h) with 45% of missing migrating whales and from different approaches: all calls included (circle icon); no singletons included in the automated data (triangle icons); subset singletons according to a proportion in the automated data (square icons); and not performing any subset to the simulated data (cross icons). Estimates from 2013 (salmon colour), and estimates from 2014 (green colour). The mean estimates generated from 100 simulations are blue coloured, and have no year associated.

Chapter 5

Discussion

The management of wildlife populations is an extremely difficult mission. The trends of cetaceans populations are alternating, and even dramatically shifting, as they are increasingly affected by human activities. For those reasons, we, as scientists, must gather teams and apply methods capable of complementing the existing information and giving valid results on the trends in population density. Cetacean abundance studies are generally based on visual techniques, such as line transect surveys (Buckland et al., 2012) (for instance, distance sampling). But visual methods are restricted to daylight and good weather, many times underestimating the density values.

Passive Acoustic Monitoring presents itself as a game changer concerning the study of population densities of sound producing animals. Due to its distinctive characteristics, PAM is potentially able to accurately obtain those estimates, since it relies on acoustic cues that vary according to the studied species. Regarding bowhead whales, PAM in the Arctic has been driven by three main issues concerning bowhead whales (Clark et al., 2015): (i) find how many bowheads exist in the Bearing-Chukchi-Beaufort (BCB) population; (ii) understand the potential impacts of offshore oil and gas operations; and (iii) understand how large-scale changes in arctic sea ice conditions might impact the population. This thesis will only focus on the first topic.

The dataset used was collected within a PAM project active for over eight years in the Canadian Beaufort sea with five arrays of hydrophones capable of detecting acoustic cues produced by bowhead whales. The advantage of working with static PAM comes from the sensors characteristics, DASARs, as they are suitable for long-term deployment, besides the ability of acoustically locating the detections of bowhead whales.

The survey considered several sites with multiple sensors at each site. Each site was considered a single SECR array with 7 DASARs for sites 2, 3, and 5; 3 DASARs for site 1; and 13 DASARs for site 4. For many technical and methodological reasons already described in this thesis, we excluded site 1, and examined the last two years of the dataset (2013 and 2014). The present dissertation aims to provide insights on the bowhead whale population density over the Beaufort Canadian sea, more precisely in the BCB. The SECR likelihood functions 3.1 and C.1 were developed based on the SECR methods described in Efford et al. (2009), and combined with the concept of truncation (Conn et al., 2011) of singletons – acoustic cues only detected in a single sensor. The problem arises with the singletons containing a presumably high yet unknown amount of false positives, and for that reason a solution would require the singletons censoring out of the likelihood functions. The ultimate goal is to estimate the density of bowhead whales' vocalisations, and then convert to a density estimate of bowhead whales crossing a migratory corridor in the Alaskan Beaufort sea.

5.1 Underlying Assumptions

It is important to emphasize the automated data hereby analysed was collected in areas that do not cover the entire width of the migration corridor in the Alaskan Beaufort sea during 2007–2014, although only the last two were analysed. In addition, the time periods do not correspond to the entire autumn migration season. Currently, there are no known bowhead cue rates or estimates of population size we could rely on to compare with our estimates. In this work

we assumed no false negatives (missed detections) that could potentially lead to underestimated density values. A multiplier could be included in the likelihood function in order to prevent this phenomenon. More elegant and exhaustive analysis might be conducted to improve our project by incorporating these factors, and increase the current knowledge of the BCB population of bowhead whales.

5.2 Conclusions

This thesis aimed to obtain population density estimates of bowhead whales (whales/100 km^2 h) in the BCB by converting the number of detected vocalisations to number of whales with SECR. This method converts acoustic cues into animal density by accounting for: (i) the proportion of singletons, (ii) the cue rate, and (iii) the probability of detecting cues (in this thesis, it was adopted a half-normal distribution). However, the automated PAM data presented a problem of holding an excess of singletons. We assume a large portion of singletons are, in fact, false positives. The bowhead whale density estimates were calculated according to three approaches, intended to deal with the singletons problem in different ways: a) 'all calls included' in the dataset, i.e., ignoring the singletons problems, and hence overestimating the population densities, as false positives are included in the dataset; b) 'no singletons' approach, where we eliminate all singletons, therefore excluding potential false positives, but leading to underestimated densities as all true singletons were removed; and c) 'proportion of singletons', i.e., excluding singletons according to a $1 - p$ of false positives, in other words, p being the proportion of true singletons, but still risking an underestimation or overestimation of densities. An additional approach, truncating singletons, can be achieved by implementing the likelihood in equation 3.1. In this thesis, the likelihood was not implemented, although a draft R script was developed, and is presented in the appendices. With this last approach, the inferences could only be made regarding cues recorded at least twice, as explained in the section 2 and 3. As expected, the overall BCB population densities from the b) approach were lower compared to the c) approach, and the densities from the a) approach were considerably higher compared to b) and c) approaches. The results from the 'proportion of singletons' are closer to reality, whereas the estimates from the 'no singletons' approach are considered inadequate. The estimates resulting from the 'all calls included' approach are the least adequate of all three, because the problem concerning the amount of singletons is completely ignored. If implemented, the estimates resulting from truncating singletons would be presumable closest to unbiased.

Call density estimates were simulated according to 'all calls included', 'no singletons', and 'proportion of singletons' approaches, and compared to a certain 'true' density estimate. The 'proportion of singletons' presented the lowest percentage bias, therefore proving to be the best approach among all, as expected. Therefore, the suggested 2013 and 2014 BCB population density estimates of bowhead whales with the 'proportion of singletons' approach are: 5.8971 whales/100 km^2 h (with 25% of missing migrating whales), 4.8522 whales/100 km^2 h (with 35% of missing migrating whales), and 3.7886 whales/100 km^2 h (with 45% of missing migrating whales).

Future work on this dataset would include the use of additional parameters, such as the estimated locations of the bowhead whale calls, the measured bearing in degrees, and received

sound levels (Borchers et al., 2015). These parameters could be added to the likelihood developed in this thesis, consequently resulting in more reliable estimates. Other additional parameters are described in the appendices (see section A). Moreover, it would be helpful to gather data from visually confirmed groups of bowhead whales, and compare with our density estimates. If possible, other sensors should be used, for example gliders , as they do not fall short concerning spatial coverage, and they also account for animal movement as well, unlike fixed sensors.

Future investigation on this area should focus on studying the species acoustic ecology, as there are still unanswered questions about the proportion of the population vocalising, and when. This should bring more clarity to the vocalisation rates. Automated detection and classification systems also make mistakes usually ignored with visual surveys and could be improved. At last, more accessible and inexpensive hardware needs to be developed to increase not only the number of surveys performed, but also the accuracy and precision of the population density estimates.

5.3 Acquired Competencies

The MSc in Biostatistics allowed the development of this project dissertation at CREEM (Centre for Research into Ecological & Environmental Modelling) and DEIO – FCUL (Departamento de Estatística e Investigação Operacional – Faculdade de Ciências da Universidade de Lisboa). The traineeship at CREEM occurred between March and July, 2018. The remaining thesis was produced and written in the following months until the delivery in March, 2019.

It is worth to list explicitly what this MSc dissertation allowed me to develop and become more familiar in terms of tools and statistical competencies:

1. Organise and manipulate large datasets;
2. Perform an exploratory data analysis;
3. Compile, run and debug code;
4. Code more efficiently;
5. Work with several R packages: secr, xtable, sp, rgdal, plyr, knitr, ggplot2, tidyr, gmodels, among others;
6. Being able to implement SECR analysis;
7. Deal with different statistical distributions;
8. Create a bespoke log-likelihood function based on the SECR framework;
9. Use *R Markdown* to turn analysis into readable reports to be presented during meetings (in HTML structure);
10. Able to work and compile large documents in LaTeX;
11. Create dynamic reports within the spirit of reproducible research.

5.4 Final Remarks

Statistical procedures were used to obtain practical answers to ecological questions. In this work, we have estimated bowhead whales densities at BCB for their autumn migration season in 2013 and 2014 using hydrophones. By defining our unknowns, and comparing our experimental results (automated data) with simulated data, we have obtained more insight into the estimates produced that are helpful to complement the current lack of knowledge. Additionally, we compared results from different approaches and, ultimately, set the foundations for a new approach by truncating singletons. In the meantime, more follow up questions arose that need further development. Through this thesis, I learnt many valuable tools on how to do science, and enjoyed every step that led to the creation of this thesis.

References

Abadi, S. H., Thode, A. M., Blackwell, S. B. & Dowling, D. R. (2014). Ranging bowhead whale calls in a shallow-water dispersive waveguide. *The Journal of the Acoustical Society of America*, *136*(1), 130–144.

Acevedo, M. A. & Villanueva-Rivera, L. J. (2006). From the field: using automated digital recording systems as effective tools for the monitoring of birds and amphibians. *Wildlife Society Bulletin*, *34*(1), 211–214.

Adams, A. M., Jantzen, M. K., Hamilton, R. M. & Fenton, M. B. (2012). Do you hear what I hear? Implications of detector selection for acoustic monitoring of bats. *Methods in Ecology and Evolution*, *3*(6), 992–998.

Bacon, D. R. (1982). Characteristics of a PVDF membrane hydrophone for use in the range 1-100 MHz. *IEEE transactions on Sonics and Ultrasonics*, *29*(1), 18–25.

Bardeli, R., Wolff, D., Kurth, F., Koch, M., Tauchert, K.-H. & Frommolt, K.-H. (2010). Detecting bird sounds in a complex acoustic environment and application to bioacoustic monitoring. *Pattern Recognition Letters*, *31*(12), 1524–1534.

Barlow, J. & Taylor, B. L. (2005). Estimates of sperm whale abundance in the northeastern temperate Pacific from a combined acoustic and visual survey. *Marine Mammal Science*, *21*(3), 429–445.

Baumgartner, M. F., Stafford, K. M., Winsor, P., Statscewich, H. & Fratantoni, D. M. (2014). Glider-based passive acoustic monitoring in the Arctic. *Marine Technology Society Journal*, *48*(5), 40–51.

Blackwell, S. B., McDonald, T. L., Kim, K. H., Aerts, L. A. M., Richardson, W. J., Greene Jr, C. R. & Streever, B. (2012). Directionality of bowhead whale calls measured with multiple sensors. *Marine Mammal Science*, *28*(1), 200–212.

Blackwell, S. B., Nations, C., McDonald, T., Greene, C., Thode, A., Guerra, M. & Michael Macrander, A. (2013). Effects of airgun sounds on bowhead whale calling rates in the Alaskan Beaufort Sea. *Marine Mammal Science*, *29*(4), E342–E365.

Borchers, D. L. & Efford, M. G. (2008). Spatially explicit maximum likelihood methods for capture–recapture studies. *Biometrics*, *64*(2), 377–385.

Borchers, D. L., Marques, T. A., Gunnlaugsson, T. & Jupp, P. (2010). Estimating distance sampling detection functions when distances are measured with errors. *Journal of Agricultural, Biological, and Environmental Statistics*, *15*(3), 346–361.

Borchers, D. L., Stevenson, B., Kidney, D., Thomas, L. & Marques, T. A. (2015). A unifying model for capture–recapture and distance sampling surveys of wildlife populations. *Journal of the American Statistical Association*, *110*(509), 195–204.

Braham, H. W., Fraker, M. A. & Krogman, B. D. (1980). Spring migration of the Western Arctic population of bowhead whales. *Marine Fisheries Review*, *42*(9), 36–46.

Brownell, R. L. & Ralls, K. (1986). Potential for sperm competition in baleen whales. *Report of the International Whaling Commission*, *8*, 97–112.

Buckland, S. T. (2006). Point-transect surveys for songbirds: robust methodologies. *The Auk*, *123*(2), 345–357.

Buckland, S. T., Anderson, D. R., Burnham, K. P. & Laake, J. L. (2012). *Distance sampling: estimating abundance of biological populations*. Springer Science & Business Media.

Burnham, K. P. & Anderson, D. R. (1984). The need for distance data in transect counts. *The Journal of Wildlife Management*, 1248–1254.

Burns, J. J., Montague, J. J. & Cowles, C. J. (1993). The bowhead whale. *Society for Marine Mammalogy, Special Publication, No. 2*.

Clark, C. W., Berchok, C. L., Blackwell, S. B., Hannay, D. E., Jones, J., Ponirakis, D. & Stafford, K. M. (2015). A year in the acoustic world of bowhead whales in the Bering, Chukchi and Beaufort seas. *Progress in Oceanography*, *136*, 223–240.

Conn, P. B., Gorgone, A. M., Jugovich, A. R., Byrd, B. L. & Hansen, L. J. (2011). Accounting for transients when estimating abundance of bottlenose dolphins in Choctawhatchee Bay, Florida. *The Journal of Wildlife Management*, *75*(3), 569–579.

Conrad, J. M. (1989). Bioeconomics and the bowhead whale. *Journal of Political Economy*, *97*(4), 974–987.

Cummings, W. C. & Holliday, D. V. (1985). Passive acoustic location of bowhead whales in a population census off Point Barrow, Alaska. *The Journal of the Acoustical Society of America*, *78*(4), 1163–1169.

Efford, M. G. (2018). secr 3.1 - spatially explicit capture–recapture in R. Retrieved May 14, 2018, from https://cran.r-project.org/web/packages/secr/vignettes/secr-overview.pdf

Efford, M. G., Borchers, D. L. & Byrom, A. E. (2009). Density estimation by spatially explicit capture–recapture: likelihood-based methods. In *Modeling demographic processes in marked populations* (pp. 255–269). Springer.

Efford, M. G. & Fewster, R. M. (2013). Estimating population size by spatially explicit capture–recapture. *Oikos*, *122*(6), 918–928.

Efford, M. (2017). Habitat masks in the package secr. Retrieved September 12, 2018, from http://www.otago.ac.nz/density/pdfs/secr-habitatmasks.pdf

Francois, R. E. & Garrison, G. R. (1982). Sound absorption based on ocean measurements. Part II: Boric acid contribution and equation for total absorption. *The Journal of the Acoustical Society of America*, *72*(6), 1879–1890.

George, J. C., Bada, J., Zeh, J., Scott, L., Brown, S. E., O'hara, T. & Suydam, R. (1999). Age and growth estimates of bowhead whales (*Balaena mysticetus*) via aspartic acid racemization. *Canadian Journal of Zoology*, *77*(4), 571–580.

Glennie, R., Buckland, S. T. & Thomas, L. (2015). The effect of animal movement on line transect estimates of abundance. *PloS one*, *10*(3), e0121333.

Greene Jr, C. R., McLennan, M. W., Norman, R. G., McDonald, T. L., Jakubczak, R. S. & Richardson, W. J. (2004). Directional frequency and recording (DIFAR) sensors in seafloor recorders to locate calling bowhead whales during their fall migration. *The Journal of the Acoustical Society of America*, *116*(2), 799–813.

Harris, D. & Gillespie, D. (2014). Investigating the potential of a wave glider for cetacean density estimation—A Scottish study. *The Journal of the Acoustical Society of America*, *136*(4), 2277–2277.

Heide-Jørgensen, M. P., Laidre, K. L., Jensen, M. V., Dueck, L. & Postma, L. D. (2006). Dissolving stock discreteness with satellite tracking: bowhead whales in Baffin Bay. *Marine Mammal Science*, *22*(1), 34–45.

Hiby, A. R. (1985). An approach to estimating population densities of great whales from sighting surveys. *Mathematical Medicine and Biology: A Journal of the IMA*, *2*(3), 201–220.

Horvitz, D. G. & Thompson, D. J. (1952). A generalization of sampling without replacement from a finite universe. *Journal of the American statistical Association*, *47*(260), 663–685.

Kalan, A. K., Mundry, R., Wagner, O. J. J., Heinicke, S., Boesch, C. & Kühl, H. S. (2015). Towards the automated detection and occupancy estimation of primates using passive acoustic monitoring. *Ecological Indicators*, *54*, 217–226.

Krebs, C. J. et al. (1989). *Ecological Methodology*. Harper & Row New York.

Link, W. A. (2003). Nonidentifiability of population size from capture-recapture data with heterogeneous detection probabilities. *Biometrics*, *59*(4), 1123–1130.

Lowry, L. F., Sheffield, G. & George, J. (2004). Bowhead whale feeding in the Alaskan Beaufort Sea, based on stomach contents analyses. *Journal of Cetacean Research and Management*, *6*(3), 215–223.

Marques, T. A. (2004). Predicting and correcting bias caused by measurement error in line transect sampling using multiplicative error models. *Biometrics*, *60*(3), 757–763.

Marques, T. A. L. O. (2007). *Incorporating measurement error and density gradients in distance sampling surveys* (Doctoral dissertation, University of St Andrews).

Marques, T. A., Thomas, L., Martin, S. W., Mellinger, D. K., Ward, J. A., Moretti, D. J., ... Tyack, P. L. (2013). Estimating animal population density using passive acoustics. *Biological Reviews*, *88*(2), 287–309.

Mellinger, D. K. & Clark, C. W. (2000). Recognizing transient low-frequency whale sounds by spectrogram correlation. *The Journal of the Acoustical Society of America*, *107*(6), 3518–3529.

Mellinger, D. K., Stafford, K. M., Moore, S. E., Dziak, R. P. & Matsumoto, H. (2007). An overview of fixed passive acoustic observation methods for cetaceans. *Oceanography*, *20*(4), 36–45.

Moore, S. E. (1993). Distribution and movement. *The bowhead whale*, 313–386.

Nerini, M. K., Braham, H. W., Marquette, W. M. & Rugh, D. J. (1984). Life history of the bowhead whale, *Balaena mysticetus* (Mammalia: Cetacea). *Journal of Zoology*, *204*(4), 443–468.

Pecknold, S. & Heard, G. (2015). *Preliminary Modeling of Acoustic Detection Capability for the Drifting Arctic Monitoring System*. DRDC-Atlantic Research Centre Dartmouth NS Canada.

Perrin, W. F., Würsig, B. & Thewissen, J. G. M. (2009). *Encyclopedia of Marine Mammals*. Academic Press.

Pradel, R. (1996). Utilization of capture-mark-recapture for the study of recruitment and population growth rate. *Biometrics*, 703–709.

Rencher, A. C. & Schaalje, G. B. (2008). *Linear Models in Statistics*. John Wiley & Sons.

Rountree, R. A., Gilmore, R. G., Goudey, C. A., Hawkins, A. D., Luczkovich, J. J. & Mann, D. A. (2006). Listening to fish: applications of passive acoustics to fisheries science. *Fisheries*, *31*(9), 433–446.

Royle, J. A. (2011). Hierarchical spatial capture–recapture models for estimating density from trapping arrays. In *Camera Traps in Animal Ecology* (pp. 163–190). Springer.

Rugh, D. J., Demaster, D., Rooney, A., Breiwick, J., Shelden, K. & Moore, S. E. (2003). A review of bowhead whale (*Balaena mysticetus*) stock identity. *Journal of Cetacean Research and Management*, *5*(3), 267–280.

Rugh, D. J. & Shelden, K. E. W. (2009). Bowhead whale: *Balaena mysticetus*. In *Encyclopedia of Marine Mammals (Second Edition)* (pp. 131–133). Elsevier.

Rykiel Jr, E. J. (1996). Testing ecological models: the meaning of validation. *Ecological modelling*, *90*(3), 229–244.

Samaran, F., Adam, O. & Guinet, C. (2010). Detection range modeling of blue whale calls in Southwestern Indian Ocean. *Applied Acoustics*, *71*(11), 1099–1106.

Širović, A., Hildebrand, J. A. & Wiggins, S. M. (2007). Blue and fin whale call source levels and propagation range in the Southern Ocean. *The Journal of the Acoustical Society of America*, *122*(2), 1208–1215.

Sousa-Lima, R. S., Norris, T. F., Oswald, J. N. & Fernandes, D. P. (2013). A review and inventory of fixed autonomous recorders for passive acoustic monitoring of marine mammals. *Aquatic Mammals*, *39*(1).

Thode, A. M., Kim, K. H., Blackwell, S. B., Greene Jr, C. R., Nations, C. S., McDonald, T. L. & Macrander, A. M. (2012). Automated detection and localization of bowhead whale sounds in the presence of seismic airgun surveys. *The Journal of the Acoustical Society of America*, *131*(5), 3726–3747.

Würsig, B. & Clark, C. (1993). Behavior. J. J. Burns, J. J. Montague and C. J. Cowles, eds. The bowhead whale. Special Publication Number 2, The Society for Marine Mammalogy.

Würsig, B., Dorsey, E. M., Fraker, M. A., Payne, R. S., Richardson, W. J. & Wells, R. S. (1984). Behavior of bowhead whales, *Balaena mysticetus*, summering in the Beaufort Sea: surfacing, respiration, and dive characteristics. *Canadian Journal of Zoology*, *62*(10), 1910–1921.

Appendices

Appendix A

Output Files

The raw data was organised in a TSV (tab-separated values) file format. Once systematised and organised, the ouput files resembled the table presented in A.1. The first column presents call IDs in each row in the format of 'sNyYYcWWW' where N is the number representing a site (1,2,3,4 or 5), 'YY' the year (2013 or 2014) and WWW the number of a call. If a call is a singleton, the format will be presented as 'sNyYYcsingWWW'. The following 3 columns exhibited information of the call itself and its location, suchlike:

1. 'atev': Calculated time of the whale call as a conventional date string (YYYY-MM-DD hh:mm:ss);
2. 'utmx': Calculated UTM easting coordinate of the estimated location of the whale call;
3. 'utmy': Calculated UTM northing coordinate of the whale call.

Table A.1: Example of output file structure. The first column A corresponds to the column of individual calls; the second group of columns B aggregates 3 columns related to the call and its location; at last, the third group C aggregates sets of 5 columns, each set associated with information of a single DASAR where the call was detected.

A) Id	**B) 3 columns call related**	**C) 5 columns per DASAR**
Call 1	Columns concerning the call itself and its location	Each column associated to one DASAR where the call was detected
Call 2		
Call 3		
...		

The following group of 5 columns sets per DASAR may include:

1. 'did': DASAR ID;
2. 'bgrid': Measured bearing in degrees of event (whale call) relative to the Northing axis. This includes 'bref', the calibrated orientation of the DASAR. If one noted a consistent offset, one could change 'bref', then recalculate 'bgrid' and the location;
3. 'bref': Reference bearing used for 'bgrid';

4. 'cmt': Measured arrival time in c-format. The estimated precision is about 1 second (equivalent to about 1500 meters distance). The arrival time is not presently used in the location calculation;

5. 'sigdb': Approximate acoustic level at hydrophone in dB re 1 μPa. This is the root-mean-square (rms) level in the band measured for the call averaged over the measured length of the call. The background noise is measured for one second starting two seconds before the call and is subtracted from the call levels. This process is subject to random errors.

In this thesis, the analysed data only included the 'did' column, and the additional information 'utmx' and 'utmy' were used for plotting purposes.

Appendix B

Likelihood with Inhomogeneous Poisson Density

The state model, as described in sub-section 2.2, is a spatial Poisson process for home range centres. This Poisson process returns an expected value of the process (home range centres per unit area) and can be either homogeneous (constant over space) or inhomogeneous (varying over space). If density is homogeneous, $D(\mathbf{X};\phi)$ is a function of location where $\mathbf{X}$ represents a pair of x-y coordinates and its expected value is a flat surface and the parameter ϕ is one number, i.e., the density. However, if density is inhomogeneous, then ϕ is a vector of several parameters.

As described in (Efford et al., 2009), in the event of home range centres occurring independently in a plane according to an inhomogeneous Poisson process with rate parameter $D(\mathbf{X};\phi)$, we will have a likelihood in terms of:

$$\mathcal{L}(\phi,\boldsymbol{\theta}|n,\omega_1,...,\omega_n) = P(n|\phi,\boldsymbol{\theta}) \times P(\omega_1,...,\omega_n|n,\boldsymbol{\theta},\phi). \tag{B.1}$$

Assuming independent detections between calls (i.e., DASARs operate independently), the marginal n is Poisson distributed with rate parameter:

$$\lambda(\phi,\boldsymbol{\theta}) \tag{B.2}$$

that arises from integrating the Poisson process (first term) with the probability of being detected at least once (second term):

$$\lambda(\phi,\boldsymbol{\theta}) = \int_{R^2} D(\mathbf{X};\phi)p_{\cdot}(\mathbf{X};\boldsymbol{\theta})d\mathbf{X}. \tag{B.3}$$

It is sometimes omitted the parameter vectors ϕ and $\boldsymbol{\theta}$ in the development below. Assuming independent detections between detected calls, the conditional distribution for $\omega_i,...,\omega_n$, given n unique capture histories is:

$$P(\omega_i, ..., \omega_n | n, \phi, \boldsymbol{\theta}) \equiv P(\omega_i, ..., \omega_n | \omega_{1.} > 0, ..., \omega_{n.} > 0, \phi, \boldsymbol{\theta})$$
$$= \binom{n}{n_1, ..., n_C} \prod_{i=1}^{n} P(\omega_i | \omega_{i.} > 0, \phi, \boldsymbol{\theta}), \tag{B.4}$$

where $n_1, ..., n_C$ are the frequencies in which each of the C unique detected capture histories were detected, $\binom{n}{n_1,...,n_C}$ is the associated multinomial coefficient, and the following equation is the probability of observing capture history ω_i for call i, given it was detected, i.e., $\omega_{i.} > 0$.

$$P(\omega_i | \omega_{i.} > 0, \phi, \boldsymbol{\theta}) = \int_{R^2} P(\omega_i | \omega_{i.} > 0, \phi, \mathbf{X}) f(\mathbf{X} | \omega_{i.} > 0, \phi, \boldsymbol{\theta}) d\mathbf{X}. \tag{B.5}$$

The terms inside the previous integral can be expressed in terms of the detection probability function $p_{ks}(\mathbf{X}; \boldsymbol{\theta})$ and inhomogeneous Poisson process rate $D(\mathbf{X}; \phi)$. The probability of observing capture history ω_i for call i, given that its home range centre is at $\mathbf{X}$, and that it was detected is:

$$P(\omega_i | \omega_{i.} > 0, \mathbf{X}) = p_{.}(\mathbf{X})^{-1} \prod_{s=1}^{S} \prod_{k=1}^{K} p_{ks}(\mathbf{X})^{\delta_k(\omega_{is})} [1 - p_{.s}(\mathbf{X})]^{1 - \delta_{.}(\omega_{is})}. \tag{B.6}$$

Equally as in the homogeneous Poisson section, $\delta_k(\omega_{is}) = 1$ if $\omega_{is} = k$ and is zero otherwise, $\delta_{.}(\omega_{is}) = 1$, if $\delta_k(\omega_{is}) > 0$ for any $k = 1, ..., K$, and is zero otherwise. Assuming independence of detection between occasions:

$$p_{.}(\mathbf{X}) = 1 - \prod_{s=1}^{S} [1 - p_{.s}(\mathbf{X})]. \tag{B.7}$$

The second term in the integral B.5 is the conditional density function of home range centres $\mathbf{X}$ given a call is recorded, and is expressed as follows:

$$f(\mathbf{X} | \omega_{i.} > 0, \phi, \boldsymbol{\theta}) = \frac{D(\mathbf{X}; \phi) p_{.}(\mathbf{X}; \boldsymbol{\theta})}{\int_{R^2} D(\mathbf{X}; \phi) p_{.}(\mathbf{X}; \boldsymbol{\theta}) d\mathbf{X}}$$
$$= \frac{D(\mathbf{X}; \phi) p_{.}(\mathbf{X}; \boldsymbol{\theta})}{\lambda(\phi, \boldsymbol{\theta})}. \tag{B.8}$$

The parameters ϕ and $\boldsymbol{\theta}$ of the model can be estimated by maximizing the likelihood equation B.1.

$$\hat{N} = \int D(\mathbf{X}; \hat{\phi}) d\mathbf{X} \tag{B.9}$$

Appendix C

SECR likelihood with Truncation of Singletons – Inhomogeneous Poisson process

Considering a inhomogeneous Poisson process, the likelihood is given by:

$$\mathcal{L}(\boldsymbol{\theta}, \phi | n^*, \omega^*) = P(n^* | \boldsymbol{\theta}, \phi) P(\omega^* | n^*, \boldsymbol{\theta}, \phi), \tag{C.1}$$

with ϕ defined previously in the appendices section B, and the remaining terms $\boldsymbol{\theta}$, n^*, and ω^* are explained in section 3.1.

The first term is the Poisson probability mass function

$$P(n^* | \boldsymbol{\theta}, \phi) = \frac{\lambda(\boldsymbol{\theta}, \phi)^{n^*} \exp(-\lambda(\boldsymbol{\theta}, \phi))}{n^*!}, \tag{C.2}$$

where

$$\lambda(\boldsymbol{\theta}, \phi) = \int_{R^2} D(\mathbf{X}; \boldsymbol{\theta}) p^*(\mathbf{X}; \boldsymbol{\theta}) d\mathbf{X}, \tag{C.3}$$

and $p^*(\mathbf{X}; \boldsymbol{\theta})$ is already defined in 3.4.

The second term in the equation C.1 is given by:

$$\begin{aligned} P(\omega^* | n^*, \boldsymbol{\theta}, \phi) &= P(\omega_1^*, \ldots, \omega_{n^*}^* | \omega_1 > 1, \ldots, \omega_{n^*} > 1, \boldsymbol{\theta}, \phi) \\ &= \binom{n^*}{n_1, \ldots, n_{C^*}} P(\omega_i | \omega_i > 1, \boldsymbol{\theta}, \phi), \end{aligned} \tag{C.4}$$

with

$$P(\omega_i | \omega_i > 1, \boldsymbol{\theta}, \phi) = \int_{R^2} P(\omega_i | \omega_i > 1, \boldsymbol{\theta}, \phi, \mathbf{X}) f(\mathbf{X} | \omega_i > 1, \boldsymbol{\theta}, \phi) d\mathbf{X}, \tag{C.5}$$

where

$$P(\omega_i|\omega_i > 1, \boldsymbol{\theta}, \phi, \mathbf{X}) = \frac{\prod_{k=1}^{K} p(d_k(\mathbf{X};\boldsymbol{\theta}))^{\omega_{ik}}(1 - p(d_k(\mathbf{X};\boldsymbol{\theta})))^{(1-\omega_{ik})}}{p^*(\mathbf{X};\boldsymbol{\theta})} \tag{C.6}$$

and where

$$\begin{aligned} f(\mathbf{X}|\omega_i > 1, \boldsymbol{\theta}, \phi) &= \frac{D(\mathbf{X};\phi)p^*(\mathbf{X};\boldsymbol{\theta})}{\int_{R^2} D(\mathbf{X};\phi)p^*(\mathbf{X};\boldsymbol{\theta})d\mathbf{X}} \\ &= \frac{D(\mathbf{X};\phi)p^*(\mathbf{X};\boldsymbol{\theta})}{\lambda(\boldsymbol{\theta},\phi)}. \end{aligned} \tag{C.7}$$

Appendix D

R code development

We needed to develop a system capable of reading and processing the original files with the automated data. For that purpose, the following functions were developed:

1. *func_check_sites*: Checks which site and year were selected and saves in a vector all possible DASARs. For example, if the user chooses to analyse site 2 of year 2013, the elements of the created vector would be: S213A, S213B, S213C, S213D, S213E and S213G.

2. *func_one_row_one_call*: Creates a matrix with one call per row with additional information in other columns, as explained in A section in the appendices.

3. *func_unique_detection_per_row*: Labels each single detection (not call) per row by reorganising the previous matrix. For example, if a call was recorded by DASARs A, B and D, there will be 3 rows, one for each DASAR detecting such call.

4. *func_exp_lm*: Fits an exponential regression using a linear model by accounting the number of DASARs a call was recorded on. The exponential decay is fitted to the number of calls recorded in 2, 3, ..., to all DASARs against the number of existing DASARs. The number of singletons is then extrapolated and divided by the original number of singletons in the automated data, resulting in a proportion p of true singletons. This function returns objects of class 'lm'.

5. *func_ggplotregression*: Saves a *ggplot* image according to the linear model considered previously.

6. *func_prop_sing*: Resamples singletons without replacement according to the proportion p of singletons.

7. *func_fusion_sing_others*: The resampled singletons data is added to the data with calls recorded in more than one DASAR (non-singletons). A subsequent resampling without replacement is performed to the data (with singletons and non-singletons) according to an assigned proportion. The recommended proportion is 0.005 to reduce the CPU usage. Analysing 0.5% of the total data is necessary, as the original automated data holds more than 13 million calls.

8. *func_ organise_ all*: Suchlike function *func_ unique_ detection_ per_ row*, the output will be a matrix with a detection per row.

9. *func_ prop_ final*: Calculates the proportion of DASARs recording each call for a single resample.

10. *func_ plot_ final*: Saves a *ggplot* with the proportions calculated in the previous function for a single resample.

11. *func_ resample*: Combines every function listed from 1 to 10 and prints all objects created.

The *func_ resample* has five arguments: **site**, **y**, **pathtosave**, **nrsimul**, **p_subset**. To start, choose the desired site (**site**) and year (**y**). Sites must be 2, 3, 4, or 5, and year must be equal to 2013 or 2014; choose a directory, for example, "C:/Users/Gisela Cheoo/Desktop" (**pathtosave**) where all images with a ".png" file extension will be saved; **nrsimul** must be an integer number of resamples the user requires; **p_subset** is the proportion chosen to sample all detections and must be a value between 0 and 1 (as previously mentioned, the recommended proportion is 0.005).

D.1 Log-likelihood function with Truncation of Singletons

The function *loglikelihood* was created regarding the calculation of the maximum log-likelihood estimate:

$$n^* log(D) + n^* log(a^*(\boldsymbol{\theta})) - Da^*(\boldsymbol{\theta}) - log(a^*(\boldsymbol{\theta})) + \sum_{i=1}^{n^*} log\left[\int_{R^2} P(\omega_i^* | \omega_i^* > 1; \mathbf{X}; \boldsymbol{\theta}) d\mathbf{X}\right]. \quad \text{(D.1)}$$

Its computation was extremely arduous, and it still needs to be adjusted. We start with three objects when evaluating the log-likelihood: (i) capture histories of calls, (ii) habitat mask, and (iii) DASARs. The object (i) *capthist* is a matrix with each call per row and each DASAR per column where it is registered a positive detection with '1' and no detection with '0' for each call. The object (ii) *mask* includes all points in a habitat mask excluding the areas where one believes there is no detection (such as land areas) and object (iii) *traps*, DASARs with their ID and respective location.

Four arguments are required to implement this log-likelihood: (i) **par**, starting values of a set of parameters (density, D; intercept, g_0; and sigma, σ), (ii) **data.set**, which matches with *capthist* as an object truncated of singletons, (iii) **traps**, and (iv) **mask**. The starting values were set according to the estimates calculated previously with the package *secr* using values resulted from using a proportion of singletons. D is in number of calls/100 km^2 and σ is in km.

The function *optim* was used to calculate the log-likelihood maximum with the R package *stats*. The draft R script of the function *loglikelihood* is presented in section G in the appendices.

Appendix E

Tables

Table E.1: SECR parameters description and corresponding interval.

Description	Variable	Interval	Other information
Number of calls	n	–	–
Calls	i	$i = 1, ..., n$	–
DASARs (traps)	k	$k = (1, ..., K)$	–
Location of traps	$\underline{x}$	$\underline{x} = (x_1, ..., x_K)$	–
Number of trapping occasions	S	–	–
Trapping occasions	s	$s = 1, ..., S$	–
Home range centres of calls	$\mathbf{X}$	x-y coordinates	–
Capture locations history of a call i	$\boldsymbol{\omega}_i$	$\boldsymbol{\omega}_i = (w_{i1}, ..., w_{is})$	$\boldsymbol{\omega}_{i.} = 1$, if call i was detected
–	–	–	on any of the S occasions;
–	–	–	$\boldsymbol{\omega}_{i.} = 0$, otherwise
Capture probability parameter vector	$\boldsymbol{\theta}$	–	–
Probability that a call with home range	$p_{ks}(\mathbf{X};\boldsymbol{\theta})$	–	–
centre $\mathbf{X}$ is detected at DASAR k on occasion s	–	–	–
Probability that a call with home range centre $\mathbf{X}$	$p_{.s}(\mathbf{X};\boldsymbol{\theta})$	–	–
is detected in any one of the K DASARs on occasion s	–	–	–
Probability that a call with home range centre $\mathbf{X}$	$p_{.}(\mathbf{X};\boldsymbol{\theta})$	–	If call was detected: $p_{.}(\mathbf{X};\boldsymbol{\theta}) =$
is caught at all over the S trapping occasions	–	–	$P(\omega_{i.} = 1 \mid X_i;\boldsymbol{\theta})$

Table E.2: Mean and confidence interval of number of calls detected in 1 to 11 DASARs, in 2013 and 2014, from 50 resamples including all calls (singletons and non-singletons).

Site	Year	Nr DASARs	Mean	Lower CI	Upper CI	Year	Mean	Lower CI	Upper CI
2	2013	1	4,197.24	4,189.78	4,204.70	2014	2,660.30	2,653.77	2,666.83
		2	285.96	281.85	290.07		186.06	182.36	189.76
		3	198.42	194.49	202.35		126.16	122.68	129.64
		4	159.56	155.73	163.39		103.48	101.11	105.85
		5	122.36	119.56	125.16		68.74	66.56	70.92
		6	85.08	82.60	87.56		49.42	47.21	51.63
		7	9.38	8.51	10.25		7.84	7.13	8.55
3	2013	1	6,361.06	6,352.52	6,369.60	2014	4,739.94	4,732.26	4,747.62
		2	574.74	568.51	580.97		285.62	282.11	289.13
		3	311.18	306.11	316.25		191.40	187.07	195.73
		4	238.72	234.45	242.99		146.96	143.62	150.30
		5	106.30	103.13	109.47		130.58	126.87	134.29
		6	29.34	27.72	30.96		128.06	125.30	130.82
		7	26.66	25.12	28.20		116.44	113.41	119.47
4	2013	1	15,008.74	14,995.89	15,021.59	2014	9,476.30	9,466.35	9,486.25
		2	1,269.82	1,259.94	1,279.70		836.60	829.05	844.15
		3	455.60	449.39	461.81		293.84	289.08	298.60
		4	300.56	296.23	304.89		200.06	196.24	203.88
		5	229.20	224.34	234.06		140.20	137.58	142.82
		6	182.84	178.80	186.88		105.16	102.47	107.85
		7	158.26	154.91	161.61		79.32	76.93	81.71
		8	130.26	127.16	133.36		65.80	63.70	67.90
		9	96.96	94.16	99.76		55.10	53.24	56.96
		10	12.82	11.83	13.81		44.56	42.69	46.43
		11	6.94	6.25	7.63		20.06	18.95	21.17
5	2013	1	6,018.32	6,010.61	6,026.03	2014	4,193.72	4,186.85	4,200.59
		2	664.72	658.88	670.56		270.16	265.34	274.98
		3	343.58	338.92	348.24		185.26	181.44	189.08
		4	175.62	172.18	179.06		140.66	137.75	143.57
		5	48.28	46.42	50.14		121.86	119.05	124.67
		6	22.58	21.39	23.77		86.50	83.65	89.35
		7	13.90	13.09	14.71		50.84	49.03	52.65

Table E.3: Mean and confidence interval of number of calls detected in 1 to 11 DASARs, in 2013 and 2014, from 50 resamples with singletons excluded.

Site	Year	Nr DASARs	Mean	Lower CI	Upper CI	Year	Mean	Lower CI	Upper CI
		1	–	–	–		–	–	–
		2	283.72	279.99	287.45		186.16	182.93	189.39
		3	201.70	198.06	205.34		127.74	125.28	130.20
2	2013	4	159.52	155.98	163.06	2014	102.60	99.93	105.27
		5	124.20	121.12	127.28		70.96	68.63	73.29
		6	86.10	83.46	88.74		49.34	47.28	51.40
		7	8.76	7.94	9.58		8.20	7.38	9.02
		1	–	–	–		–	–	–
		2	572.12	566.72	577.52		283.10	278.58	287.62
		3	312.86	308.27	317.45		190.54	187.53	193.55
3	2013	4	237.74	233.83	241.65	2014	151.72	148.92	154.52
		5	107.22	104.65	109.79		134.88	131.93	137.83
		6	30.24	28.69	31.79		128.00	125.19	130.81
		7	27.82	26.61	29.03		109.76	106.63	112.89
		1	–	–	–		–	–	–
		2	1,269.08	1,261.36	1,276.80		838.80	833.08	844.52
		3	457.42	451.94	462.90		293.88	289.19	298.57
4	2013	4	306.42	302.09	310.75	2014	198.56	195.16	201.96
		5	227.66	223.68	231.64		137.98	134.71	141.25
		6	184.32	180.55	188.09		103.76	101.04	106.48
		7	155.70	152.12	159.28		81.46	78.76	84.16
		8	131.82	129.12	134.52		64.34	61.90	66.78
		9	96.58	94.12	99.04		52.44	50.37	54.51
		10	12.42	11.40	13.44		45.16	43.55	46.77
		11	6.58	5.85	7.31		20.62	19.21	22.03
		1	–	–	–		–	–	–
		2	667.68	662.99	672.37		278.42	275.41	281.43
		3	343.82	340.17	347.47		182.68	179.16	186.20
5	2013	4	171.68	168.43	174.93	2014	140.76	138.02	143.50
		5	48.32	46.39	50.25		119.52	116.89	122.15
		6	23.28	21.84	24.72		87.88	85.16	90.60
		7	13.22	12.08	14.36		51.74	49.40	54.08

Table E.4: Mean and confidence interval of number of calls detected in 1 to 11 DASARs, in 2013 and 2014, from 50 resamples with a proportion of singletons included.

Site	Year	Nr DASARs	Mean	Lower CI	Upper CI	Year	Mean	Lower CI	Upper CI
		1	722.94	716.82	729.06		424.88	420.54	429.22
		2	279.64	274.95	284.33		185.76	181.88	189.64
		3	203.56	199.93	207.19		129.96	126.37	133.55
2	2013	4	161.16	157.59	164.73	2014	104.16	101.80	106.52
		5	123.62	120.89	126.35		67.22	65.31	69.13
		6	84.84	81.72	87.96		49.24	46.98	51.50
		7	9.24	8.40	10.08		8.78	7.91	9.65
		1	1,253.54	1,245.51	1,261.57		283.74	279.47	288.01
		2	576.82	570.21	583.43		284.00	280.50	287.50
		3	312.86	308.07	317.65		194.38	190.62	198.14
3	2013	4	236.92	233.07	240.77	2014	147.68	144.60	150.76
		5	105.40	102.63	108.17		132.62	129.31	135.93
		6	30.34	28.89	31.79		128.12	125.16	131.08
		7	27.12	25.69	28.55		112.46	109.10	115.82
		1	1,834.90	1,825.19	1,844.61		677.98	671.23	684.73
		2	1,260.62	1,251.87	1,269.37		841.92	834.76	849.08
		3	456.84	451.18	462.50		296.04	292.65	299.43
4	2013	4	307.22	302.62	311.82	2014	195.26	191.57	198.95
		5	224.40	219.81	228.99		139.18	136.50	141.86
		6	183.00	179.45	186.55		102.64	99.42	105.86
		7	158.14	154.39	161.89		80.98	78.17	83.79
		8	134.84	131.67	138.01		63.44	61.20	65.68
		9	96.32	93.54	99.10		53.82	51.83	55.81
		10	11.90	10.90	12.90		42.08	39.89	44.27
		11	6.82	6.20	7.44		20.66	19.35	21.97
		1	1,640.46	1,632.86	1,648.06		370.58	365.88	375.28
		2	670.48	664.63	676.33		277.10	272.95	281.25
		3	345.48	340.11	350.85		182.32	178.92	185.72
5	2013	4	171.74	167.50	175.98	2014	140.94	137.98	143.90
		5	48.66	46.55	50.77		121.10	118.00	124.20
		6	22.64	21.50	23.78		87.04	84.04	90.04
		7	14.54	13.33	15.75		50.92	48.45	53.39

Table E.5: Summary of exponential equation fitting for all sites and years.

Site	Year	$\widehat{\beta}_0$	$\widehat{\beta}_1$	Adjusted $\hat{R}^2$	Residual standard error	F-statistic	p-value
2	2013	12.448	- 0.569	$\hat{R}^2_{adj} = 0.692$	0.681	F = 12.22	p = 0.0250 **
3	2013	13.093	- 0.660	$\hat{R}^2_{adj} = 0.946$	0.294	F = 88.48	p = 0.0007 ***
4	2013	13.290	- 0.481	$\hat{R}^2_{adj} = 0.850$	0.606	F = 52.03	p = 9.126e-05 ***
5	2013	13.529	- 0.824	$\hat{R}^2_{adj} = 0.983$	0.202	F = 291.10	p = 6.923e-05 ***
2	2014	11.891	- 0.541	$\hat{R}^2_{adj} = 0.788$	0.512	F = 19.54	p = 0.0115 **
3	2014	11.120	- 0.168	$\hat{R}^2_{adj} = 0.847$	0.132	F = 28.61	p = 0.0059 ***
4	2014	12.153	- 0.337	$\hat{R}^2_{adj} = 0.931$	0.276	F = 122.60	p = 3.943e-06 ***
5	2014	11.518	- 0.309	$\hat{R}^2_{adj} = 0.966$	0.107	F = 145.00	p = 0.0003 ***

* $p < 0.1$; ** $p < .05$; *** $p < .01$

Table E.6: Call density and sigma estimates from the automated data vs data from simulated capture histories. The automated call density estimates are the mean value of 50 resamples.

		Site 2			
Approach	Estimates	2013 data	2014 data	Simulated data [a)]	Simulated data [b)]
All calls included	Call density	625.5461 [5,058]	423.9070 [3,202]	–	–
No singletons	estimate	52.2465 [864]	31.8346 [545]	$18.6417^{(*)}$ [$347.21^{(*)}$]	–
Proportion of singletons	(calls/$100km^2$)	102.5924 [1,585]	60.5376 [970]	$80.9259^{(*)}$ [$1{,}359.8^{(*)}$]	–
No transformation [c)]	[N calls]	–	–	–	$45.2740^{(*)}$ [$1{,}277.5^{(*)}$]
All calls included		$7.630^{(X)}$	$7.312^{(X)}$	–	–
No singletons	Sigma	$9.145^{(X)}$	$9.073^{(X)}$	$9.638^{(+)}$	–
Proportion of singletons	estimate (km)	$8.767^{(X)}$	$8.591^{(X)}$	$9.322^{(+)}$	–
No transformation [c)]		–	–	–	$11.860^{(+)}$
		Site 3			
Approach	Estimates	2013 data	2014 data	Simulated data [a)]	Simulated data [b)]
All calls included	Call density	700.2639 [7,648]	302.4377 [5,739]	–	–
No singletons	estimate	41.9510 [1288]	23.2596 [998]	$21.6501^{(*)}$ [$770.57^{(*)}$]	–
Proportion of singletons	(calls/$100km^2$)	110.0455 [2543]	25.6214 [1283]	$58.1064^{(*)}$ [$2105.74^{(*)}$]	–
No transformation [c)]	[N calls]	–	–	–	$15.4172^{(*)}$ [$1913.0^{(*)}$]
All calls included		$10.615^{(X)}$	$11.497^{(X)}$	–	–
No singletons	Sigma	$12.573^{(X)}$	$14.211^{(X)}$	$14.078^{(+)}$	–
Proportion of singletons	estimate (km)	$11.863^{(X)}$	$14.274^{(X)}$	$14.021^{(+)}$	–
No transformation [c)]		–	–	–	$241.444^{(+)}$
		Site 4			
Approach	Estimates	2013 data	2014 data	Simulated data [a)]	Simulated data [b)]
All calls included	Call density	1,493.2780 [17,852]	850.4499 [11,317]	–	–
No singletons	estimate	123.7110 [2,848]	70.8910 [1,837]	$37.3398^{(*)}$ [$881.98^{(*)}$]	–
Proportion of singletons	(calls/$100km^2$)	204.2116 [4,675]	97.3585 [2,514]	$144.3252^{(*)}$ [$3501.34^{(*)}$]	–
No transformation [c)]	[N calls]	–	–	–	$129.0128^{(*)}$ [$3594.5^{(*)}$]
All calls included		$7.875^{(X)}$	$8.309^{(X)}$	–	–
No singletons	Sigma	$8.540^{(X)}$	$9.293^{(X)}$	$^{(+)}$	–
Proportion of singletons	estimate (km)	$8.495^{(X)}$	$9.258^{(X)}$	$14.021^{(+)}$	–
No transformation [c)]		–	–	–	$9.893^{(+)}$
		Site 5			
Approach	Estimates	2013 data	2014 data	Simulated data [a)]	Simulated data [b)]
All calls included	Call density	819.2810 [7,287]	508.8908 [5,049]	–	–
No singletons	estimate	54.4141 [1,268]	32.0332 [861]	$24.7818^{(*)}$ [$711.75^{(*)}$]	–
Proportion of singletons	(calls/$100km^2$)	175.1285 [2,914]	55.0158 [1,230]	$91.5510^{(*)}$ [$2167.9^{(*)}$]	–
No transformation [c)]	[N calls]	–	–	–	$34.495^{(*)}$ [$1791.333^{(*)}$]
All calls included		$9.974^{(X)}$	$8.511^{(X)}$	–	–
No singletons	Sigma	$11.520^{(X)}$	$11.810^{(X)}$	$^{(+)}$	–
Proportion of singletons	estimate (km)	$10.494^{(X)}$	$10.926^{(X)}$	$14.021^{(+)}$	–
No transformation [c)]		–	–	–	$18.993^{(+)}$

a) Simulated data with a large number of singletons.

b) Simulated data without forcing a large number of singletons.

c) Simulated data with no subset/transformation performed to it.

$^{(X)}$ Median value of 50 resamples; $^{(*)}$ Mean value of 100 simulations; $^{(+)}$ Median value of 100 simulations.

Table E.7: Confidence interval (95%) of population densities from the automated data and mean values of simulated data.

25% missing migrating whales				Simulated data [a)]	Simulated data [a)]	Simulated data [b)]
	Approach	Lower CI	Upper CI	No singletons	Proportion of singletons	No transformation [c)]
Automated data	All calls	28.8988	52.0959	–	–	2.627
	No singletons	2.1110	3.8087	1.4078	–	
	Proportion of singletons	2.9868	8.8075	–	4.9792	
35% missing migrating whales				Simulated data [a)]	Simulated data [a)]	Simulated data [b)]
	Approach	Lower CI	Upper CI	No singletons	Proportion of singletons	No transformation [c)]
Automated data	All calls	23.6045	42.8418	–	–	2.148
	No singletons	1.7352	3.1165	1.1530	–	
	Proportion of singletons	2.3966	7.3078	–	4.0823	
45% missing migrating whales				Simulated data [a)]	Simulated data [a)]	Simulated data [b)]
	Approach	Lower CI	Upper CI	No singletons	Proportion of singletons	No transformation [c)]
Automated data	All calls	18.3927	33.5180	–	–	1.6752
	No singletons	1.3496	2.4424	0.899	–	
	Proportion of singletons	1.8698	5.7073	–	3.1822	

a) Simulated data with a large number of singletons.

b) Simulated data without forcing a large number of singletons.

c) Simulated data with no subset/transformation performed to it.

Appendix F

Figures

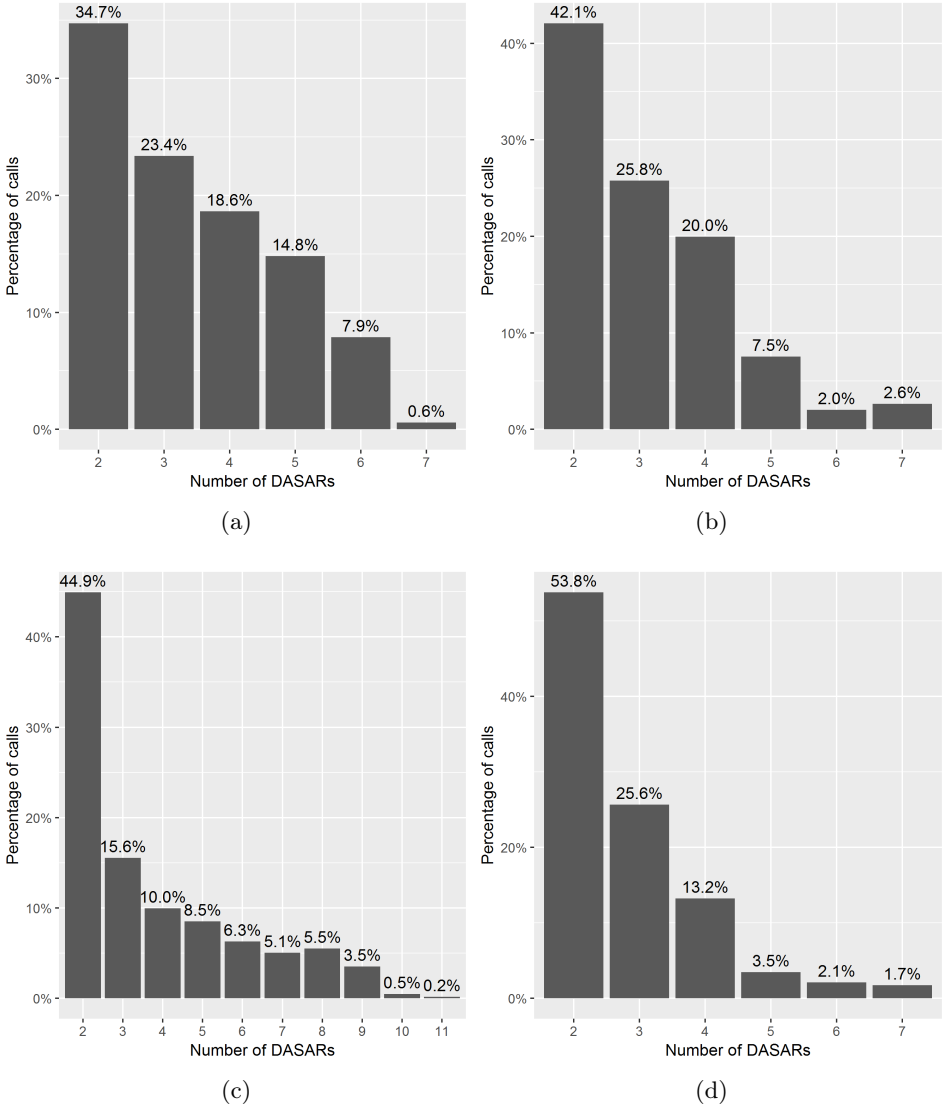

Figure F.1: Percentage of calls detected from 2 to 11 DASARs on a single resample with no singletons included. (a) Site 2, year 2013. (b) Site 3, year 2013. (c) Site 4, year 2013. (d) Site 5, year 2013.

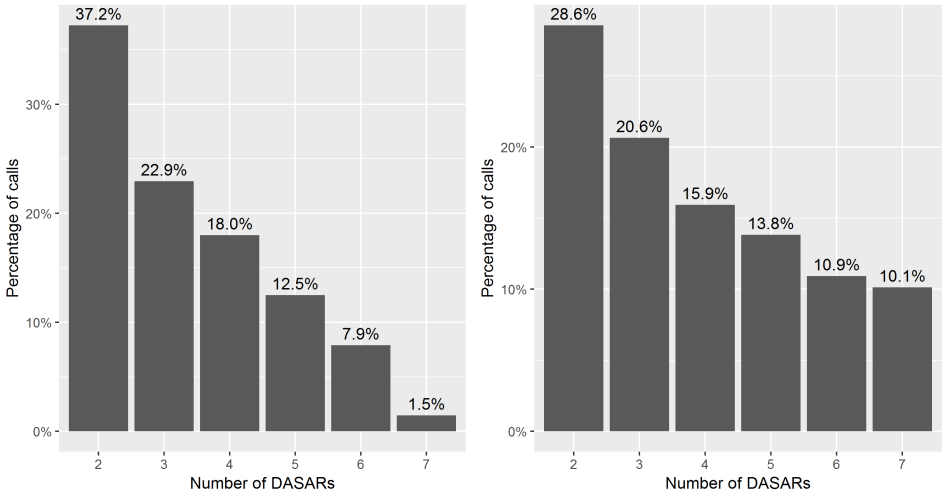

(a)

(b)

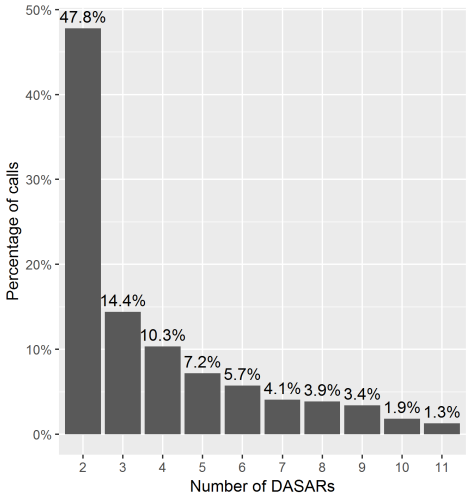

(c)

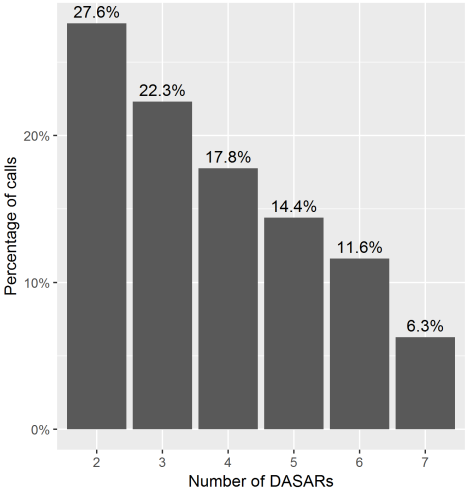

(d)

Figure F.2: Percentage of calls detected from 2 to 11 DASARs on a single resample with no singletons included. (a) Site 2, year 2014. (b) Site 3, year 2014. (c) Site 4, year 2014. (d) Site 5, year 2014.

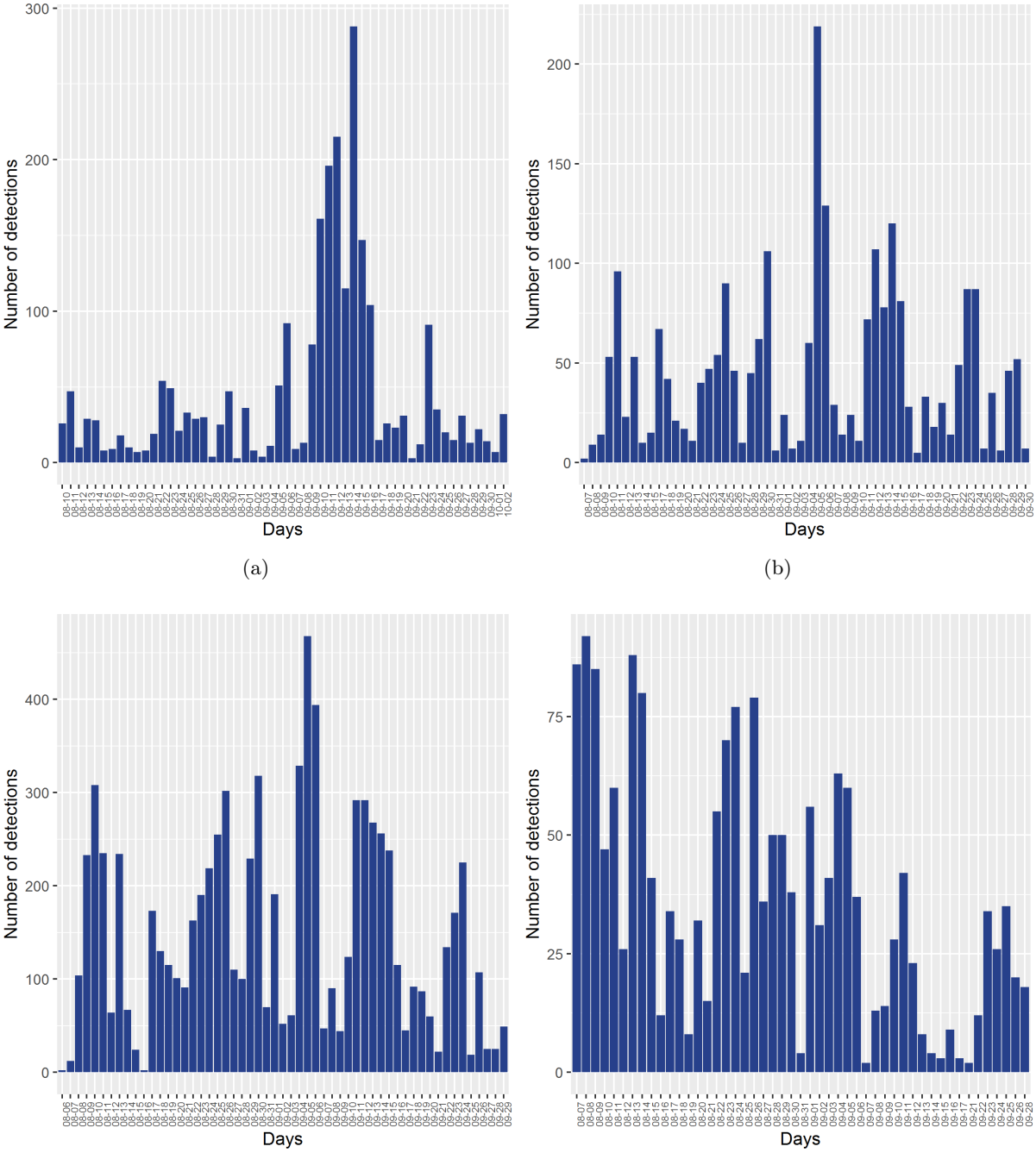

Figure F.3: Frequency of calls detected per day from one resample. (a) Site 2, year 2013: 3691 detections from a total of 1585 calls detected in 54 days. (b) Site 3, year 2013: 5290 detections from a total of 2543 calls detected in 54 days. (c) Site 4, year 2013: 12337 detections from a total of 4675 calls detected in 55 days. (d) Site 5, year 2013: 5136 detections from a total of 2914 calls detected in 49 days.

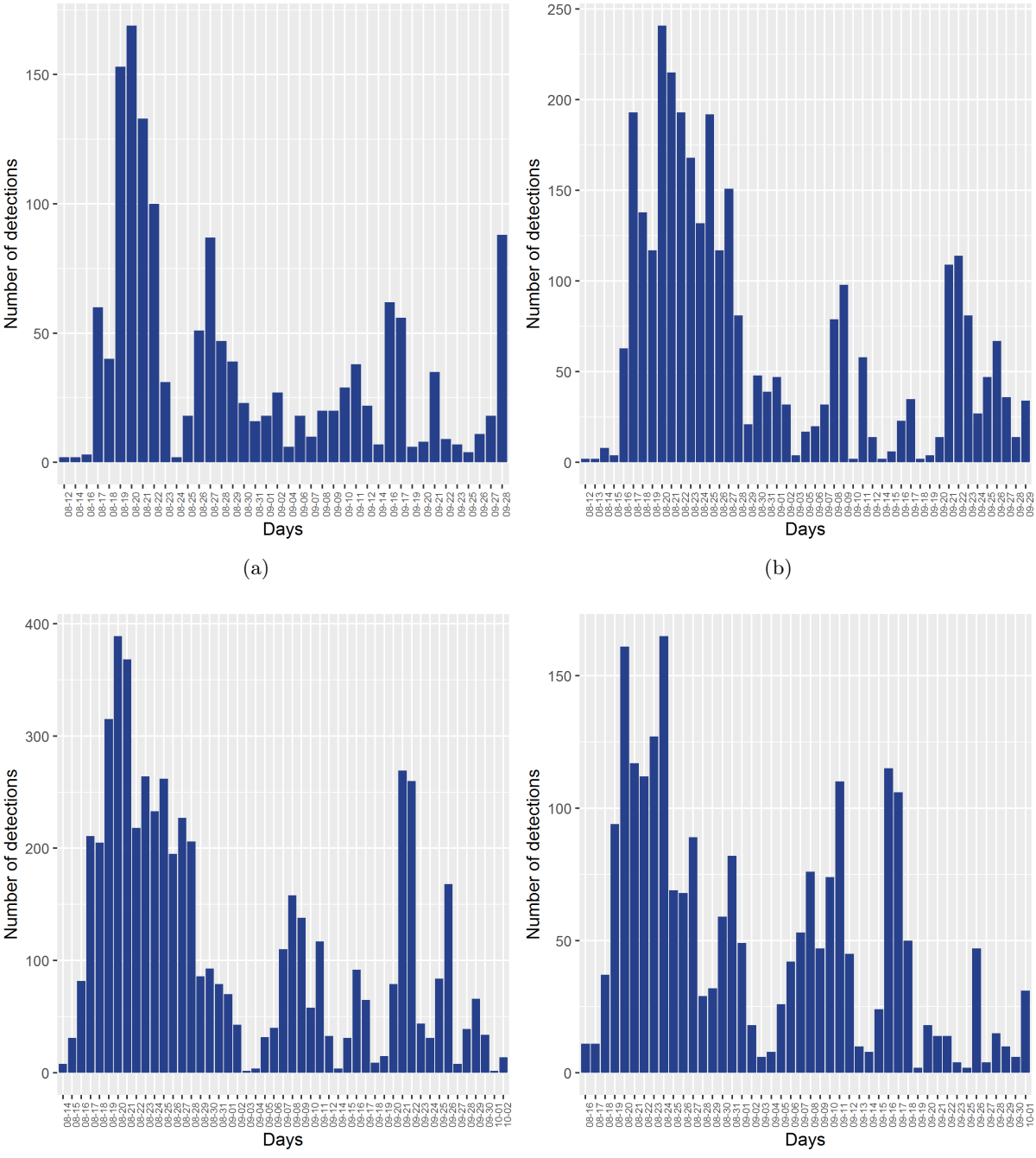

Figure F.4: Frequency of calls detected per day from one resample. (a) Site 2, year 2014: 2259 detections from a total of 970 calls detected in 40 days. (b) Site 3, year 2014: 4206 detections from a total of 1283 calls detected in 47 days. (c) Site 4, year 2014: 7609 detections from a total of 2514 calls detected in 49 days. (d) Site 5, year 2014: 3599 detections from a total of 1230 calls detected in 46 days.

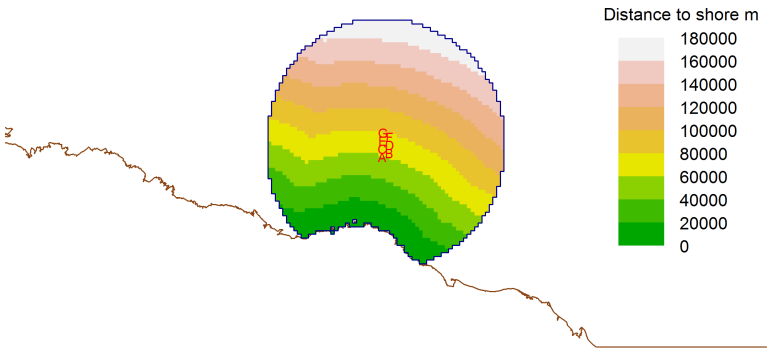

(a)

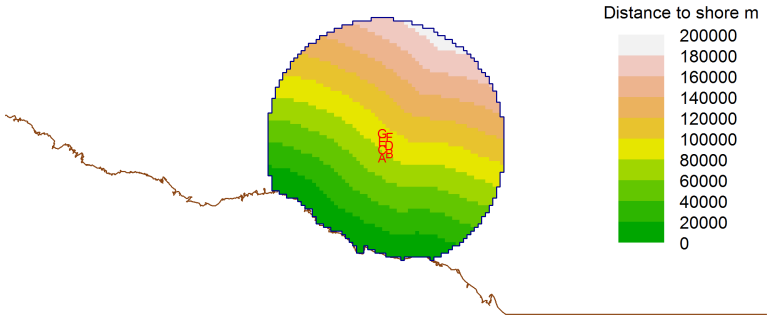

(b)

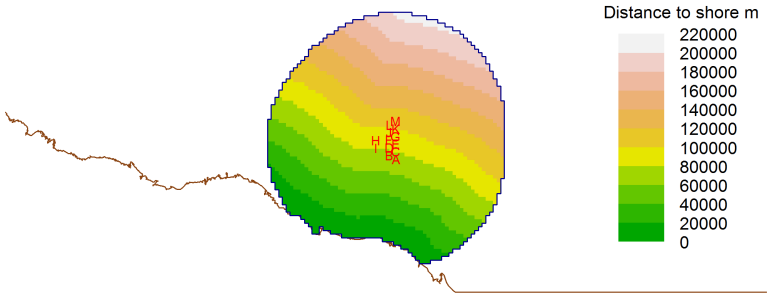

(c)

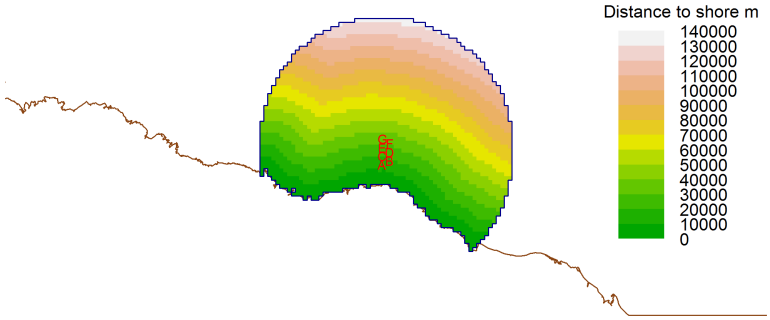

(d)

Figure F.5: Distance from the points of a habitat mask (all points inside the dark blue circle) to the coastline (brown line) with a buffer of 100 km. (a) Site 2, year 2013. (b) Site 3, year 2013. (c) Site 4, year 2013. (d) Site 5, year 2013.

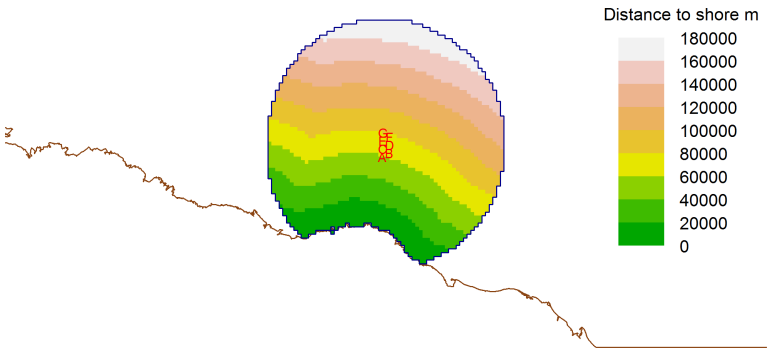

(a)

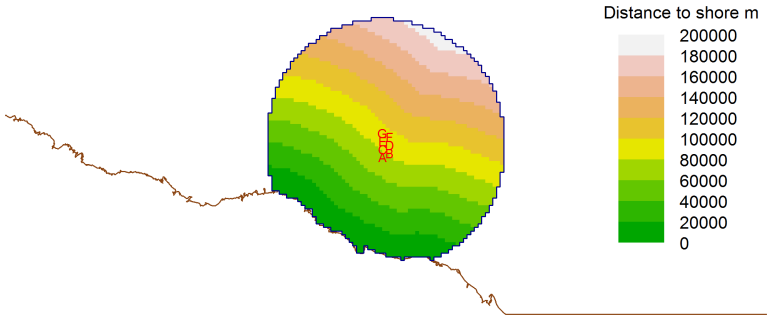

(b)

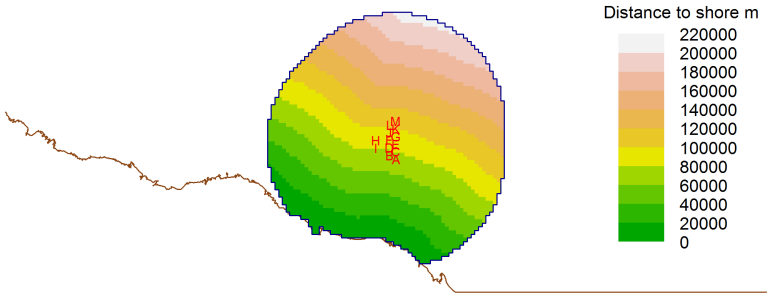

(c)

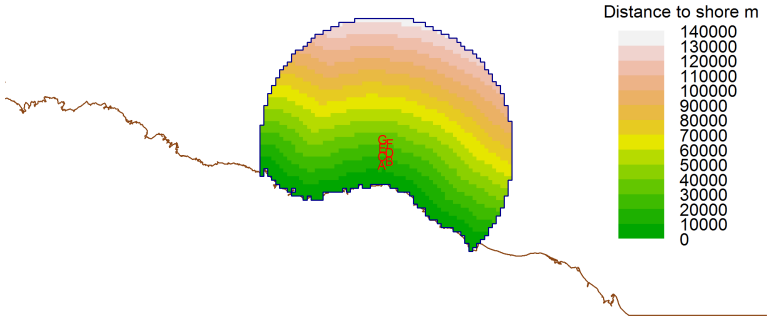

(d)

Figure F.6: Distance from the points of a habitat mask (all points inside the dark blue circle) to the coastline (brown line) with a buffer of 100 km. (a) Site 2, year 2014. (b) Site 3, year 2014. (c) Site 4, year 2014. (d) Site 5, year 2014.

Appendix G

Log-likelihood function R script

The R code for the log-likelihood formulation with truncation of singletons is as follows:

```
loglikelihood<-function(par,data.set,traps,mask,debug=FALSE){
  prop_grid<-attr(mask, 'area')# weight for each grid cell,
  #as D is homogeneous, each cell has the same weight
  # which is equal to maskarea(mask)/nrow(mask) (in ha)

  clip<-as.matrix(mask)
  nsensors<-ncol(data.set) # number of traps
  ncalls<-nrow(data.set) # number of calls
  grid<-nrow(clip) # number of points in habitat mask

  D<-par[1] # density (animals per hectare)
  g0<-par[2] # magnitude (intercept) for detection function
  sigma<-par[3] # spatial scale of detection function (in meters)

  index_traps<-1:nsensors
  index_mask<-1:grid

  P<-matrix(0,nrow=grid,ncol=nsensors) # matrix with probabilities of
  # detection that depends on k sensor and X location
  distance<-function(clip,traps){
    d<-pointDistance(c(as.numeric(traps[1]),as.numeric(traps[2])),
                     c(as.numeric(clip[1]),as.numeric(clip[2])),lonlat=FALSE)
    P<-g0*exp(-d^2/(2*sigma^2))
  }
  vecInside<-Vectorize(function(x,y) distance(clip[x,],traps[y,]))
  P<-outer(index_mask,index_traps,vecInside)
  # each row is a point in habitat mask, each column a sensor
  # P corresponds to P*(X; theta) for each X location

  P2<-invlogit(P)
  logL<-0
  for(icall in 1:ncalls){
    integration<-0
    div.p<-c()
    all.theta<-c()
    for(ipoint in index_mask){
      CurP<-P2[ipoint,]
      log.p.num<-0
      never<-0
      once<-0

      p.num<-0
      p.denom<-0
```

```
      for(isensor in index_traps){
        log.p.num<-log.p.num+data.set[icall,isensor]*log(CurP[isensor])
        +(1-data.set[icall,isensor])*log(1-CurP[isensor])
        never<-never+log(1-CurP[isensor])
        once<-once+CurP[isensor]*prod(1-CurP[-isensor])
      }
      all.theta<-c(all.theta,(1-exp(never)-once)*prop_grid)

      p.num<-p.num+exp(log.p.num)
      p.denom<-p.denom+(1-exp(never)-once)

      div.p<-c(div.p,p.num/p.denom*prop_grid)
    }
    theta<-max(all.theta)+log(sum(exp(all.theta-max(all.theta))))
    newdiv<-max(div.p)+log(sum(exp(div.p-max(div.p))))
    logL<-logL+ncalls*(log(D)+log(theta))-D*theta-log(theta)+log(newdiv)
  }
  return(-logL)
}

D<-0.5
g0<-1
sigma<-8e+03
inits<-c(D,g0,sigma)
start.time <- Sys.time()
opt<-optim(par=inits,fn=loglikelihood,data.set=data.set,
          traps=traps,mask=clippedmask,debug=TRUE)
end.time <- Sys.time()
time.taken <- end.time - start.time
time.taken # Time difference of
opt$par
```